

AFRL-PR-WP-TR-2005-2130

**AEROSPACE POWER SCHOLARLY
RESEARCH PROGRAM**

**Delivery Order 0013: Volume 1 -
Development of Performance/Design
Equations for a Direct Methanol Fuel Cell**



Sarwan S. Sandhu

**University of Dayton
Department of Chemical and Materials Engineering
1031 Irving Avenue
Dayton, OH 45469-0246**

JULY 2005

Final Report for 23 April 2001 – 23 June 2002

Approved for public release; distribution is unlimited.

STINFO FINAL REPORT

**PROPULSION DIRECTORATE
AIR FORCE MATERIEL COMMAND
AIR FORCE RESEARCH LABORATORY
WRIGHT-PATTERSON AIR FORCE BASE, OH 45433-7251**

NOTICE

Using Government drawings, specifications, or other data included in this document for any purpose other than Government procurement does not in any way obligate the U.S. Government. The fact that the Government formulated or supplied the drawings, specifications, or other data does not license the holder or any other person or corporation; or convey any rights or permission to manufacture, use, or sell any patented invention that may relate to them.

This report was cleared for public release by the Air Force Research Laboratory Wright Site Public Affairs Office (AFRL/WS) and is releasable to the National Technical Information Service (NTIS). It will be available to the general public, including foreign nationals.

PAO Case Number: AFRL/WS-05-1000, 19 April 2005

THIS TECHNICAL REPORT IS APPROVED FOR PUBLICATION.

/s/

JOSEPH P. FELLNER
Senior Chemical Engineer
Fuels Branch
AFRL/PRPA

/s/

BRIAN G. HAGER
Chief
Turbine Engine Division
AFRL/PRPA

/s/

CYNTHIA A. OBRINGER
Deputy Chief
Power Division

This report is published in the interest of scientific and technical information exchange and its publication does not constitute the Government's approval or disapproval of its ideas or findings.

REPORT DOCUMENTATION PAGE				<i>Form Approved</i> <i>OMB No. 0704-0188</i>	
<p>The public reporting burden for this collection of information is estimated to average 1 hour per response, including the time for reviewing instructions, searching existing data sources, gathering and maintaining the data needed, and completing and reviewing the collection of information. Send comments regarding this burden estimate or any other aspect of this collection of information, including suggestions for reducing this burden, to Department of Defense, Washington Headquarters Services, Directorate for Information Operations and Reports (0704-0188), 1215 Jefferson Davis Highway, Suite 1204, Arlington, VA 22202-4302. Respondents should be aware that notwithstanding any other provision of law, no person shall be subject to any penalty for failing to comply with a collection of information if it does not display a currently valid OMB control number. PLEASE DO NOT RETURN YOUR FORM TO THE ABOVE ADDRESS.</p>					
1. REPORT DATE (DD-MM-YY) July 2005		2. REPORT TYPE Final		3. DATES COVERED (From - To) 04/23/2001 – 06/23/2002	
4. TITLE AND SUBTITLE AEROSPACE POWER SCHOLARLY RESEARCH PROGRAM Delivery Order 0013: Volume 1 - Development of Performance/Design Equations for a Direct Methanol Fuel Cell				5a. CONTRACT NUMBER F33615-98-D-2891-0013	
				5b. GRANT NUMBER	
				5c. PROGRAM ELEMENT NUMBER 62203F	
6. AUTHOR(S) Sarwan S. Sandhu				5d. PROJECT NUMBER 3145	
				5e. TASK NUMBER 32	
				5f. WORK UNIT NUMBER Z2	
7. PERFORMING ORGANIZATION NAME(S) AND ADDRESS(ES) University of Dayton Department of Chemical and Materials Engineering 1031 Irving Avenue Dayton, OH 45469-0246				8. PERFORMING ORGANIZATION REPORT NUMBER UDR-TR-2002-00089	
9. SPONSORING/MONITORING AGENCY NAME(S) AND ADDRESS(ES) Propulsion Directorate Air Force Research Laboratory Air Force Materiel Command Wright-Patterson AFB, OH 45433-7251				10. SPONSORING/MONITORING AGENCY ACRONYM(S) AFRL/PRPA	
				11. SPONSORING/MONITORING AGENCY REPORT NUMBER(S) AFRL-PR-WP-TR-2005-2130	
12. DISTRIBUTION/AVAILABILITY STATEMENT Approved for public release; distribution is unlimited.					
13. SUPPLEMENTARY NOTES Report contains color.					
14. ABSTRACT This first volume, of a two volume report, consists of the development and prediction of the reversible open-circuit voltage equation for direct methanol fuel cells (DMFC). This equation, applicable when the effects of electrode poisoning and methanol crossover are not present, includes the effects of nonideal behavior of the fluid phases and differing total pressures in the anode and cathode compartments of the fuel cell. The developed equation is capable of predicting the open-circuit voltage at any desired fuel cell temperature, pressure, and methanol concentration. The optimal DMFC conditions, based on the thermodynamic development, occur when the cathode pressure is high, the anode pressure is low, the concentration of methanol is high, and the cell temperature is low. Other factors affect the actual optimal fuel cell conditions due to electrode kinetics and methanol crossover, but, the effort here delineates the true maximal thermodynamic potential available.					
15. SUBJECT TERMS direct methanol fuel cell, thermodynamics, open-circuit voltage, solid polymer electrolyte, electrochemical, modeling					
16. SECURITY CLASSIFICATION OF:			17. LIMITATION OF ABSTRACT: SAR	18. NUMBER OF PAGES 98	19a. NAME OF RESPONSIBLE PERSON (Monitor) Joseph P. Fellner 19b. TELEPHONE NUMBER (Include Area Code) (937) 255-4225
a. REPORT Unclassified	b. ABSTRACT Unclassified	c. THIS PAGE Unclassified			

Table of Contents

1	Summary	1
2	Introduction.....	1
3	Methods, Assumptions, and Procedures.....	4
4	Results and Discussion.....	5
	4.1 Development of Performance/Design Equations for a Direct Methanol Fuel Cell.....	5
	4.1.1 Equilibrium Open-Circuit Voltage Full Equation.....	5
	4.1.1.1 Simplification of the Full Equation	16
	4.1.1.2 Calculation Scheme.....	24
	4.1.1.3 Sample Calculations.....	24
	4.1.1.4 Activity and Fugacity Coefficients.....	28
	4.1.1.5 Discussion of the Computed Results.....	31
	4.1.2 Equilibrium Open-Circuit Voltage Equation Adjusted for the Case of Water Formation in the Vapor Phase by Hydrogen Ion Oxidation at the Cathode.....	32
	4.1.2.1 Sample Calculations.....	33
	4.1.2.2 Actual Procedure to Determine the Liquid Phase Mole Fractions of CH ₃ OH and H ₂ O, given the Molarity of the Solution.....	34
	4.1.2.3 An Approximate Procedure to Determine the Liquid Phase Mole Fractions of CH ₃ OH and H ₂ O, given the Molarity of the Solution.....	39
	4.2 Plotted Data.....	41
5	Conclusions.....	84

List of Figures

Figure 1. Schematic Representation of a Direct Methanol Fuel Cell (not to scale).	5
Figure 2. Set 1 - Effect of cathode pressure on the open circuit voltage for the ideal solution and gas behavior (water formation at cathode in liquid phase).	42
Figure 3. Set 1 - Effect of anode pressure on the open circuit voltage for the ideal solution and gas behavior (water formation at cathode in liquid phase).	42
Figure 4. Set 1 - Effect of temperature on the open circuit voltage for the ideal solution and gas behavior (water formation at cathode in liquid phase).	43
Figure 5. Set 1 - Effect of temperature on the open circuit voltage for the ideal solution and gas behavior (water formation at cathode in liquid phase).	43
Figure 6. Set 1 - Effect of temperature on the open circuit voltage for the ideal solution and gas behavior (water formation at cathode in liquid phase).	44
Figure 7. Set 1 - Effect of temperature on the open circuit voltage for the ideal solution and gas behavior (water formation at cathode in liquid phase).	44
Figure 8. Set 1 - Effect of temperature on the open circuit voltage for the ideal solution and gas behavior (water formation at cathode in liquid phase).	45
Figure 9. Set 1 - Effect of cathode pressure on the open circuit voltage for the nonideal solution and gas behavior (water formation at cathode in liquid phase).	45
Figure 10. Set 1 - Effect of anode pressure on the open circuit voltage for the nonideal solution and gas behavior (water formation at cathode in liquid phase).	46
Figure 11. Set 1 - Effect of temperature on the open circuit voltage for the nonideal solution and gas behavior (water formation at cathode in liquid phase).	46
Figure 12. Set 1 - Effect of temperature on the open circuit voltage for the nonideal solution and gas behavior (water formation at cathode in liquid phase).	47
Figure 13. Set 1 - Effect of temperature on the open circuit voltage for the nonideal solution and gas behavior (water formation at cathode in liquid phase).	47
Figure 14. Set 1 - Effect of temperature on the open circuit voltage for the nonideal solution and gas behavior (water formation at cathode in liquid phase).	48
Figure 15. Set 1 - Effect of temperature on the open circuit voltage for the nonideal solution and gas behavior (water formation at cathode in liquid phase).	48
Figure 16. Set 1 - Effect of cathode pressure on the open circuit voltage for the ideal solution and gas behavior (water formation at cathode in vapor phase).	49
Figure 17. Set 1 - Effect of anode pressure on the open circuit voltage for the ideal solution and gas behavior (water formation at cathode in vapor phase).	49

Figure 18. Set 1 - Effect of temperature on the open circuit voltage for the ideal solution and gas behavior (water formation at cathode in vapor phase).	50
Figure 19. Set 1 - Effect of temperature on the open circuit voltage for the ideal solution and gas behavior (water formation at cathode in vapor phase).	50
Figure 20. Set 1 - Effect of temperature on the open circuit voltage for the ideal solution and gas behavior (water formation at cathode in vapor phase).	51
Figure 21. Set 1 - Effect of temperature on the open circuit voltage for the ideal solution and gas behavior (water formation at cathode in vapor phase).	51
Figure 22. Set 1 - Effect of temperature on the open circuit voltage for the ideal solution and gas behavior (water formation at cathode in vapor phase).	52
Figure 23. Set 1 - Effect of cathode pressure on the open circuit voltage for the nonideal solution and gas behavior (water formation at cathode in vapor phase).	52
Figure 24. Set 1 - Effect of anode pressure on the open circuit voltage for the nonideal solution and gas behavior (water formation at cathode in vapor phase).	53
Figure 25. Set 1 - Effect of temperature on the open circuit voltage for the nonideal solution and gas behavior (water formation at cathode in vapor phase).	53
Figure 26. Set 1 - Effect of temperature on the open circuit voltage for the nonideal solution and gas behavior (water formation at cathode in vapor phase).	54
Figure 27. Set 1 - Effect of temperature on the open circuit voltage for the nonideal solution and gas behavior (water formation at cathode in vapor phase).	54
Figure 28. Set 1 - Effect of temperature on the open circuit voltage for the nonideal solution and gas behavior (water formation at cathode in vapor phase).	55
Figure 29. Set 1 - Effect of temperature on the open circuit voltage for the nonideal solution and gas behavior (water formation at cathode in vapor phase).	55
Figure 30. Set 1 - Effect of cathode pressure on the open circuit voltage for the ideal solution and gas behavior (water formation at cathode in liquid phase).	56
Figure 31. Set 1 - Effect of anode pressure on the open circuit voltage for the ideal solution and gas behavior (water formation at cathode in liquid phase).	56
Figure 32. Set 2 - Effect of temperature on the open circuit voltage for the ideal solution and gas behavior (water formation at cathode in liquid phase).	57
Figure 33. Set 2 - Effect of temperature on the open circuit voltage for the ideal solution and gas behavior (water formation at cathode in liquid phase).	57
Figure 34. Set 2 - Effect of temperature on the open circuit voltage for the ideal solution and gas behavior (water formation at cathode in liquid phase).	58
Figure 35. Set 2 - Effect of temperature on the open circuit voltage for the ideal solution and gas behavior (water formation at cathode in liquid phase).	58

Figure 36. Set 2 - Effect of temperature on the open circuit voltage for the ideal solution and gas behavior (water formation at cathode in liquid phase).	59
Figure 37. Set 2 - Effect of cathode pressure on the open circuit voltage for the nonideal solution and gas behavior (water formation at cathode in liquid phase).	59
Figure 38. Set 2 - Effect of anode pressure on the open circuit voltage for the nonideal solution and gas behavior (water formation at cathode in liquid phase).	60
Figure 39. Set 2 - Effect of temperature on the open circuit voltage for the nonideal solution and gas behavior (water formation at cathode in liquid phase).	60
Figure 40. Set 2 - Effect of temperature on the open circuit voltage for the nonideal solution and gas behavior (water formation at cathode in liquid phase).	61
Figure 41. Set 2 - Effect of temperature on the open circuit voltage for the nonideal solution and gas behavior (water formation at cathode in liquid phase).	61
Figure 42. Set 2 - Effect of temperature on the open circuit voltage for the nonideal solution and gas behavior (water formation at cathode in liquid phase).	62
Figure 43. Set 2 - Effect of temperature on the open circuit voltage for the nonideal solution and gas behavior (water formation at cathode in liquid phase).	62
Figure 44. Set 2 - Effect of cathode pressure on the open circuit voltage for the ideal solution and gas behavior (water formation at cathode in vapor phase).	63
Figure 45. Set 2 - Effect of anode pressure on the open circuit voltage for the ideal solution and gas behavior (water formation at cathode in vapor phase).	63
Figure 46. Set 2 - Effect of temperature on the open circuit voltage for the ideal solution and gas behavior (water formation at cathode in vapor phase).	64
Figure 47. Set 2 - Effect of temperature on the open circuit voltage for the ideal solution and gas behavior (water formation at cathode in vapor phase).	64
Figure 48. Set 2 - Effect of temperature on the open circuit voltage for the ideal solution and gas behavior (water formation at cathode in vapor phase).	65
Figure 49. Set 2 - Effect of temperature on the open circuit voltage for the ideal solution and gas behavior (water formation at cathode in vapor phase).	65
Figure 50. Set 2 - Effect of temperature on the open circuit voltage for the ideal solution and gas behavior (water formation at cathode in vapor phase).	66
Figure 51. Set 2 - Effect of cathode pressure on the open circuit voltage for the nonideal solution and gas behavior (water formation at cathode in vapor phase).	66
Figure 52. Set 2 - Effect of anode pressure on the open circuit voltage for the nonideal solution and gas behavior (water formation at cathode in vapor phase).	67

Figure 53. Set 2 - Effect of temperature on the open circuit voltage for the nonideal solution and gas behavior (water formation at cathode in vapor phase).	67
Figure 54. Set 2 - Effect of temperature on the open circuit voltage for the nonideal solution and gas behavior (water formation at cathode in vapor phase).	68
Figure 55. Set 2 - Effect of temperature on the open circuit voltage for the nonideal solution and gas behavior (water formation at cathode in vapor phase).	68
Figure 56. Set 2 - Effect of temperature on the open circuit voltage for the nonideal solution and gas behavior (water formation at cathode in vapor phase).	69
Figure 57. Set 2 - Effect of temperature on the open circuit voltage for the nonideal solution and gas behavior (water formation at cathode in vapor phase).	69
Figure 58. Set 3 - Effect of cathode pressure on the open circuit voltage for the ideal solution and gas behavior (water formation at cathode in liquid phase).	70
Figure 59. Set 3 - Effect of anode pressure on the open circuit voltage for the ideal solution and gas behavior (water formation at cathode in liquid phase).	70
Figure 60. Set 3 - Effect of temperature on the open circuit voltage for the ideal solution and gas behavior (water formation at cathode in liquid phase).	71
Figure 61. Set 3 - Effect of temperature on the open circuit voltage for the ideal solution and gas behavior (water formation at cathode in liquid phase).	71
Figure 62. Set 3 - Effect of temperature on the open circuit voltage for the ideal solution and gas behavior (water formation at cathode in liquid phase).	72
Figure 63. Set 3 - Effect of temperature on the open circuit voltage for the ideal solution and gas behavior (water formation at cathode in liquid phase).	72
Figure 64. Set 3 - Effect of temperature on the open circuit voltage for the ideal solution and gas behavior (water formation at cathode in liquid phase).	73
Figure 65. Set 3 - Effect of cathode pressure on the open circuit voltage for the nonideal solution and gas behavior (water formation at cathode in liquid phase).	73
Figure 66. Set 3 - Effect of anode pressure on the open circuit voltage for the nonideal solution and gas behavior (water formation at cathode in liquid phase).	74
Figure 67. Set 3 - Effect of temperature on the open circuit voltage for the nonideal solution and gas behavior (water formation at cathode in liquid phase).	74
Figure 68. Set 3 - Effect of temperature on the open circuit voltage for the nonideal solution and gas behavior (water formation at cathode in liquid phase).	75
Figure 69. Set 3 - Effect of temperature on the open circuit voltage for the nonideal solution and gas behavior (water formation at cathode in liquid phase).	75

Figure 70. Set 3 - Effect of temperature on the open circuit voltage for the nonideal solution and gas behavior (water formation at cathode in liquid phase).	76
Figure 71. Set 3 - Effect of temperature on the open circuit voltage for the nonideal solution and gas behavior (water formation at cathode in liquid phase).	76
Figure 72. Set 3 - Effect of cathode pressure on the open circuit voltage for the ideal solution and gas behavior (water formation at cathode in vapor phase).	77
Figure 73. Set 3 - Effect of anode pressure on the open circuit voltage for the ideal solution and gas behavior (water formation at cathode in vapor phase).	77
Figure 74. Set 3 - Effect of temperature on the open circuit voltage for the ideal solution and gas behavior (water formation at cathode in vapor phase).	78
Figure 75. Set 3 - Effect of temperature on the open circuit voltage for the ideal solution and gas behavior (water formation at cathode in vapor phase).	78
Figure 76. Set 3 - Effect of temperature on the open circuit voltage for the ideal solution and gas behavior (water formation at cathode in vapor phase).	79
Figure 77. Set 3 - Effect of temperature on the open circuit voltage for the ideal solution and gas behavior (water formation at cathode in vapor phase).	79
Figure 78. Set 3 - Effect of temperature on the open circuit voltage for the ideal solution and gas behavior (water formation at cathode in vapor phase).	80
Figure 79. Set 3 - Effect of cathode pressure on the open circuit voltage for the nonideal solution and gas behavior (water formation at cathode in vapor phase).	80
Figure 80. Set 3 - Effect of anode pressure on the open circuit voltage for the nonideal solution and gas behavior (water formation at cathode in vapor phase).	81
Figure 81. Set 3 - Effect of temperature on the open circuit voltage for the nonideal solution and gas behavior (water formation at cathode in vapor phase).	81
Figure 82. Set 3 - Effect of temperature on the open circuit voltage for the nonideal solution and gas behavior (water formation at cathode in vapor phase).	82
Figure 83. Set 3 - Effect of temperature on the open circuit voltage for the nonideal solution and gas behavior (water formation at cathode in vapor phase).	82
Figure 84. Set 3 - Effect of temperature on the open circuit voltage for the nonideal solution and gas behavior (water formation at cathode in vapor phase).	83
Figure 85. Set 3 - Effect of temperature on the open circuit voltage for the nonideal solution and gas behavior (water formation at cathode in vapor phase).	83

FOREWORD

The work documented in this report was performed by the University of Dayton between May 2001 and May 2002, for the Propulsion Directorate of the Air Force Research Laboratory, Wright-Patterson Air Force Base, Ohio. The effort was performed as Delivery Order 0013 on Contract No. F33615-98-D-2891, Aerospace Power Scholarly Research Program (SRP).

Dr. Sarwan S. Sandhu was the Delivery Order Principal Investigator. Technical discussions and support provided by Dr. Joseph P. Fellner for the execution of this delivery order are greatly appreciated. Technical assistance, including computational work, provided by the graduate students, Mr. Richard O. Crowther and Mr. Sarath C. Krishnan is sincerely acknowledged.

The author also wishes to acknowledge the assistance of Ms. Sheila Liskany, Ms. Janet Pastor, and Mr. Jeffrey Fox of the University of Dayton Research Institute, who provided the administrative support to make this work possible. Mr. Fox is the SRP Program Manager.

1 Summary

A mathematical equation has been developed to calculate the open-circuit voltage for a direct methanol fuel cell in the absence of electrode poisoning and methanol crossover by the application of thermodynamic fundamentals of the phase and electrochemical reaction equilibria. The equation accounts for the effect of nonideal behavior of fluid phases in the anode and cathode compartments of a fuel cell on the open-circuit voltage. The developed equation also accounts for the effect of different total pressures in the anode and cathode plenums on the cell voltage. For the ideal behavior of the fluid phases in the anode and cathode compartments the equation normally reduces to the Nernst equation. The developed equation is capable of predicting the open-circuit voltage at any desired fuel cell temperature.

2 Introduction

Modeling activity in conjunction with the experimental work is deemed to economically aid in the development of an optimal design of a direct methanol fuel cell (DMFC) for aerospace and ground transportation vehicle applications. To this end, research/development activity by the principal investigator (P.I.), Sarwan S. Sandhu is given below.

1. The principal investigator (P.I.) developed a theoretical scheme to predict the reversible cell voltage in the absence of electrode poisoning and methanol crossover through a polymer electrolyte membrane of a DMFC, for example, Nafion[®] perfluorosulfonic acid polymer and polybenzoxazole or polybenzimidazole based electrolyte membranes. The scheme based on the application of thermodynamic fundamentals of the phase and electrochemical reaction equilibria predicts the reversible voltage at any fuel cell temperature. The effect of nonideal behavior of fluid phases in the anodic and cathodic fluid compartments of a fuel cell on the reversible voltage is accounted for. The simulation is capable of predicting the reversible cell voltage as function of reactant feed composition and different total pressures in the anode and cathode plenums. The developed reversible voltage equation reduces to the Nernst type equation for the ideal fluid phase behavior of the fuel and oxidant feeds. The predicted reversible cell voltage can be used as an ideal standard to which the actual voltage of a direct methanol fuel cell

operating at a given set of reactant feed composition, temperature, and pressure conditions can be compared to evaluate the fuel cell performance.

A senior year undergraduate student, Mr. R. Owen Crowther, typed the entire theoretical development by the P.I. for the reversible cell voltage prediction. The P.I. guided Owen to develop a computer code to simulate the entire set of mathematical equations to generate the reversible cell voltage data as function of temperature, fuel feed composition, and anode and cathode side total pressures.

The actual theoretical development, the computer code, and the code generated numerical data in the form of tables and plots are presented in Report #1 entitled: "Fuel Cell Project: Direct Methanol Fuel Cell: Theoretical Formulation of Reversible, Open-Circuit Voltage for a Direct Methanol Fuel Cell" by Sarwan S. Sandhu, Department of Chemical & Materials Engineering, The University of Dayton, Dayton, Ohio 45469-0246.

2. The P.I. developed the first-attempt mathematical equations to predict the ionic current density and the species (H^+ , CH_3OH , H_2O) molar fluxes for their transport through a solid polymer electrolyte or polymer-ceramic material composite membrane of a DMFC at the steady state, isothermal conditions by the application of fundamentals of transport phenomena. The developed transport equations are presented in three sets. In the transport set I, the equations are based on the extension of moderately dilute solution theory. These equations involve the Fick's law type mass diffusivities that are known to be strongly dependent on the species concentrations. The transport equation sets II and III are valid for very strong solutions. The transport equation set II is based on the application of the generalized Maxwell-Stefan equations. The transport equation set III is based on the application of the Lars Onsager's irreversible thermodynamic approach to transport processes. The developed equations account for the effect of the voltage, pressure and the species concentration gradients on their transport fluxes. These equations, describing species transport fluxes through a solid polymer electrolyte membrane are to be coupled with the equations, yet to be developed, describing mass transfer through the electrode porous backing layers and species mass transport with electrochemical/chemical kinetics in the porous electrode layers. The coupled equations, describing the various phenomena occurring in a DMFC in operation, would be of immense significance in the evaluation of performance and design/development of a DMFC. The usefulness of the developed transport equations may also be seen in that they can be employed to experimentally

determine the transport properties of a membrane such as permeability of the fluid mixture and effective mass diffusivities of the species by designing appropriate fuel cell experiments.

The developed transport equations by the P.I. were typed by Mr. Sarath Krishnan, a graduate student in the chemical engineering program at the University of Dayton. Very recently, Mr. R. Owen Crowther (who is now a graduate student in our chemical engineering program) has been guided by the P.I. to simulate the first set of transport equations in the form of a computer code to generate numerical data on current density and species (H^+ , CH_3OH , H_2O) molar fluxes through a polymer electrolyte membrane of a DMFC. He is expected to start developing the computer code in the near future.

The actual theoretical development of the transport equations is presented in Report #2 entitled: "Fuel Cell Project: Direct Methanol Fuel Cell: Theoretical Formulation of Transport Fluxes of species (H^+ , CH_3OH , H_2O) through a Solid Polymer Electrolyte Membrane (PEM) of a Direct Methanol Fuel Cell," by Sarwan S. Sandhu, Department of Chemical & Materials Engineering, The University of Dayton, Dayton, Ohio 45469-0246.

3. The P.I. developed a set of first-attempt equations to predict the reversible as well as irreversible or actual power production from a continuously fed DMFC operating at steady-state conditions. This development is based on the fundamentals of classical thermodynamics and the species and overall material balances. The scheme requires the information on the reactant feed stream composition, temperature, and pressure conditions at the inlets of a DMFC, fractional conversion of methanol via electrochemical process for the production of electric power, its chemical oxidation at the catalytic surface of the cathode, and the amounts of methanol, water, and hydrogen ions transported through the solid polymer electrolyte membrane from the anode side to the cathode side of a DMFC. The development accounts for the nonideal behavior of the fluid phases.

This development is not in the typed form at the time of reporting. Mr. Sarath Krishnan, a graduate student in the chemical engineering program at the University of Dayton has gladly accepted to understand the entire scheme of equations and to present them in the form of a typed report. Also, he would develop a computer code under my direction to generate numerical data on the reversible and actual electric power production as function of input parameter values.

4. The P.I. studied and carried out partial analysis of the open literature on the research/development of direct methanol fuel cells depending on availability of time for this

equally important activity. Based on the information acquired from the literature on the direct methanol fuel cells and his knowledge of the basic and engineering sciences relevant to the research/development of a DMFC, the P.I. developed an outline of a comprehensive research/development program to develop an efficient DMFC energy conversion system. The outline has been entitled, "Direct Methanol Fuel Cell (DMFC) Research/Development - Theoretical and Experimental Integrated Approach". A copy of this outline was provided to Dr. J.P. Fellner of the Power Division of the WPAFB, Ohio.

5. The effort by Sarwan S. Sandhu (P.I.), his students and Dr. J. P. Fellner on the research/development activity has resulted in the following presentations and proceedings publications.

(a) "Direct Methanol Polymer Electrolyte Fuel Cell Modeling: Open-Circuit Voltage Equation" in the Proceedings of the 8th International Conference on Electrical and Electronic Products, Vol. 34 (2002), pp. 233-253, Product Safety Corporation, Sissonville, West Virginia; The Conference held at the Greenbrier, White Sulphur Springs, West Virginia; January 14-16, 2002.

(b) "Direct Methanol Polymer Electrolyte Fuel Cell Modeling: Reversible Open Circuit Voltage Equation and Species Flux Equations", presented at the 8th International Symposium on Polymer Electrolytes" held at the Eldorado Hotel, Santa Fe, New Mexico, May 19-24, 2002.

(c) "Direct Methanol Polymer Electrolyte Fuel Cell Modeling," presented at the 2002 AIChE North Central Regional Student Conference. "A Climate Change," Chem-E-Car Competition, University of Michigan, February 7-9, 2002.

3 Methods, Assumptions, and Procedures

Standard chemical engineering thermodynamic principles were used to develop the reversible open-circuit voltage for a direct methanol fuel cell. Open-circuit voltage equations based on gas and solution thermodynamics for ideal and non-ideal cases were derived and their effect upon open-circuit voltage was determined.

4 Results and Discussion

The results and discussion from Report #1 entitled “Theoretical Formulation of Reversible Open-Circuit Voltage for a Direct Methanol Fuel Cell” are given below.

4.1 Development of Performance/Design Equations for a Direct Methanol Fuel Cell

4.1.1 Equilibrium Open-Circuit Voltage Full Equation

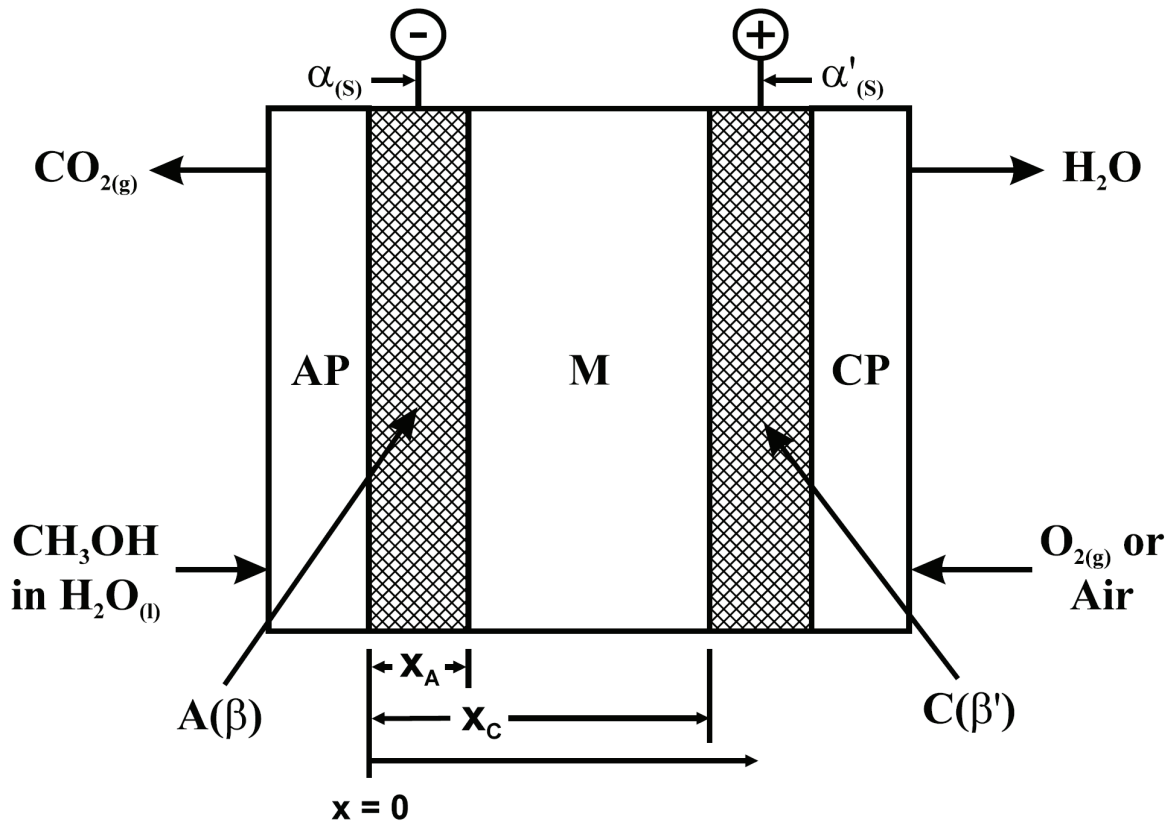


Figure 1. Schematic Representation of a Direct Methanol Fuel Cell (not to scale).

Legend

- x = distance measured from the anode toward the cathode
- AP = Anode plenum
- CP = Cathode plenum
- $A(\beta)$ = A porous, platinum-catalyzed electrode (e.g. Pt or Pt/Ru alloy), anode labeled as β phase (solid), laminated to the membrane (M)

C(β')= A porous, platinum-catalyzed electrode (e.g. Pt or Pt/Ru alloy), cathode labeled as β' phase (solid), laminated to the membrane (M)

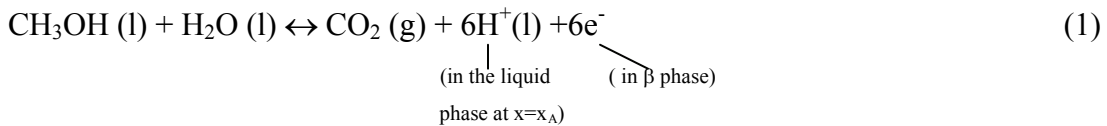
α, α' = Platinum (solid) lead wires

M= Membrane phase functioning as electrolyte medium and separator between the electrodes. This membrane phase may be consisted of a polymer electrolyte such as Dupont Nafion perfluorosulfonic acid polymer supported by porous polybenzoxazole (PBO). Or, it may be composed of a ceramic electrolyte in composite with a polymer such as PVDF (polyvinylidene fluoride) to enhance the ionic conduction by providing additional transport pathways between the ceramic electrolyte and the polymer material boundaries.

Here fuel is methanol (CH_3OH) present as mixture with water (liquid phase) at the concentration level $c_{\text{CH}_3\text{OH}, \text{AP}} \left[\frac{\text{g} - \text{molCH}_3\text{OH}}{\text{liter of solution}} \right]$ or $m_{\text{CH}_3\text{OH}, \text{AP}} \left[\frac{\text{g} - \text{molCH}_3\text{OH}}{\text{kg of solvent H}_2\text{O}} \right]$ in the anode plenum. It is assumed that the methanol concentration in the porous anode is uniform. Also, oxidant species concentration and product, water, species concentration are assumed uniform in the porous, cathode electrode. Furthermore, it is assumed that the isothermal (i.e. constant temperature T) conditions prevail in the system with the total pressures in the anode and cathode plenums at P_A^t and P_c^t , respectively.

The cell reactions are:

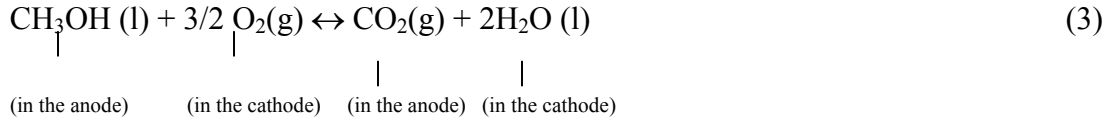
At anode:



At cathode:



The overall cell reaction:



The approach given in the Electrochemical Systems [J.S. Newman; Prentice Hall (1991 edition)] is employed here. The phase and electrochemical reaction equilibria are used. Say, the anode and cathode electric potentials are Φ^α and $\Phi^{\alpha'}$, respectively.

The difference between the electron electrochemical potentials at the cathode and anode is

$$\mu_{e^-}^{\alpha'} - \mu_{e^-}^\alpha = \left(\mu_{e^-}^{\text{chemical},\alpha'} + z_{e^-} F \Phi^{\alpha'} \right) - \left(\mu_{e^-}^{\text{chemical},\alpha} + z_{e^-} F \Phi^\alpha \right) \quad (4)$$

Because $\mu_e^{\text{chemical},\alpha'} = \mu_e^{\text{chemical},\alpha}$ for the identical platinum lead wires; therefore, Eq. (4) becomes

$$\mu_{e^-}^{\alpha'} - \mu_{e^-}^\alpha = z_{e^-} F (\Phi^{\alpha'} - \Phi^\alpha) \quad (\text{because } z_{e^-} = -1) \quad (5)$$

$$= -F (\Phi^{\alpha'} - \Phi^\alpha) \quad (5a)$$

$$= -FU$$

$$\text{Therefore, } FU = F (\Phi^{\alpha'} - \Phi^\alpha) = \mu_{e^-}^\alpha - \mu_{e^-}^{\alpha'} \quad (6)$$

where U= open-circuit (or reversible) cell potential

F= Faraday's constant =96 487 Coulomb per equivalent= magnitude of the charge on 1g-mole of electrons or protons (H^+).

$$\mu_{e^-}^\alpha = \mu_{e^-}^\beta \quad (\text{phase equilibrium with respect to electron as an electrochemical species}) \quad (7)$$

At anode, the condition is of the reaction equilibrium

$$\mu_{\text{CH}_3\text{OH}}^A + \mu_{\text{H}_2\text{O}}^A = \mu_{\text{CO}_2}^A + 6\mu_{\text{H}^+}^A + 6\mu_{e^-}^\beta \quad (8)$$

Therefore,

$$\mu_{e^-}^\beta = \left(\frac{\mu_{\text{CH}_3\text{OH}}^A + \mu_{\text{H}_2\text{O}}^A - \mu_{\text{CO}_2}^A}{6} \right) - \mu_{\text{H}^+}^A \quad (8a)$$

From Eqs. (7) and (8a), the following expression is obtained.

$$\mu_{e^-}^\alpha = \left(\frac{\mu_{\text{CH}_3\text{OH}}^A + \mu_{\text{H}_2\text{O}}^A - \mu_{\text{CO}_2}^A}{6} \right) - \mu_{\text{H}^+}^A$$

(8b)

where $\mu_{CH_3OH}^A, \mu_{H_2O}^A, \mu_{CO_2}^A$ are the chemical potentials of CH_3OH, H_2O, CO_2 in their respective phases at the anode; and $\mu_{H^+}^A$ is the electrochemical potential of H^+ in the liquid phase in the porous electrode.

$$\text{Now, } \mu_{e^-}^{\alpha'} = \mu_{e^-}^{\beta'} \quad (\text{phase equilibrium}) \quad (9)$$

At the cathode, the condition of the reaction equilibrium is

$$\begin{aligned} \frac{3}{2}\mu_{O_2}^C + 6\mu_{H^+}^C + 6\mu_{e^-}^{\beta'} &= 3\mu_{H_2O}^C \quad (10) \\ \mu_{e^-}^{\beta'} &= \frac{3\mu_{H_2O}^C - \frac{3}{2}\mu_{O_2}^C - 6\mu_{H^+}^C}{6} \end{aligned}$$

Therefore,

$$\boxed{\mu_{e^-}^{\beta'} = \left(\frac{1}{2}\mu_{H_2O}^C - \frac{1}{4}\mu_{O_2}^C\right) - \mu_{H^+}^C} \quad (11)$$

Using this result in Eq. (9), the following equation is obtained.

$$\boxed{\mu_{e^-}^{\alpha'} = \left(\frac{1}{2}\mu_{H_2O}^C - \frac{1}{4}\mu_{O_2}^C\right) - \mu_{H^+}^C} \quad (12)$$

Substitute for $\mu_{e^-}^{\alpha'}$ and $\mu_{e^-}^{\beta'}$ from Eqs. (8b) and (12), respectively, into Eq (6) to obtain Eq. (13):

$$FU = F(\Phi^{\alpha'} - \Phi^{\alpha}) = \left[\left(\frac{\mu_{CH_3OH}^A + \mu_{H_2O}^A - \mu_{CO_2}^A}{6} \right) - \mu_{H^+}^A \right] - \left[\left(\frac{1}{2}\mu_{H_2O}^C - \frac{1}{4}\mu_{O_2}^C \right) - \mu_{H^+}^C \right] \quad (13)$$

$$FU = F(\Phi^{\alpha'} - \Phi^{\alpha}) = \left(\frac{\mu_{CH_3OH}^A}{6} - \frac{\mu_{CO_2}^A}{6} + \frac{1}{4} \mu_{O_2}^C \right) + \left(\frac{\mu_{H_2O}^A}{6} - \frac{\mu_{H_2O}^C}{2} \right) + (\mu_{H^+}^C - \mu_{H^+}^A) \quad (14)$$

$$FU = F(\Phi^{\alpha'} - \Phi^{\alpha}) = \left(\frac{\mu_{CH_3OH}^A}{6} + \frac{1}{4} \mu_{O_2}^C \right) - \frac{\mu_{CO_2}^A}{6} + \frac{\mu_{H_2O(l)}^A}{6} - \frac{\mu_{H_2O(l)}^C}{2} + (\mu_{H^+}^C - \mu_{H^+}^A) \quad (15a)$$

$$FU = F(\Phi^{\alpha'} - \Phi^{\alpha}) = \frac{1}{6} \left(\mu_{CH_3OH}^A + \frac{3}{2} \mu_{O_2}^C \right) - \frac{1}{6} (\mu_{CO_2}^A - \mu_{H_2O(l)}^A + 3\mu_{H_2O(l)}^C) + (\mu_{H^+}^C - \mu_{H^+}^A)$$

$$FU = F(\Phi^{\alpha'} - \Phi^{\alpha}) = \frac{1}{6} \left[\left(\mu_{CH_3OH(l)}^A + \frac{3}{2} \mu_{O_2}^C \right) - \left\{ \mu_{CO_2}^A + (3\mu_{H_2O(l)}^C - \mu_{H_2O}^A) \right\} \right] + (\mu_{H^+}^C - \mu_{H^+}^A) \quad (16)$$

(assuming methanol and water in the liquid phases at the electrodes)

$\mu_{i(g)}$ [chemical potential of a species in a gas phase mixture at T, P] is expressed as:

$$\mu_{i(g)} = \mu_{i(g)}^{\Delta} (@ T, P^{\circ} = 1 \text{ bar-standard state pressure}) + RT \ln \left(\frac{\hat{f}_i}{P^{\circ}} \right) \quad (17)$$

where fugacity of species i in the gas mixture at (T, P^t) with composition y_i's (mole fractions) is given by

$$\hat{f}_i = \hat{\phi}_i y_i P^t \quad (17a)$$

where $\hat{\phi}_i$ = (fugacity coefficient of the component i in the gas mixture to account for the nonideal behavior of the species i in the gas mixture if the gas pressure is greater than 10 bar).

Substituting the above result into Eq. (17) leads to:

$$\mu_{i(g)} = \mu_{i(g)}^{\Delta} (@ T, P^{\circ} [\text{standard state pressure}=1 \text{ bar}] + RT \ln \left(\hat{\phi}_i y_i \frac{P^t}{P^{\circ}} \right) \quad (17b)$$

Here, $\mu_i^{\Delta} (@ T, P^{\circ} [=1 \text{ bar}])$ = chemical potential of pure species i at the temperature T

and pressure P^o=1bar where it follows ideal gas behavior;

$\hat{\phi}_i = \hat{\phi}_i(T, P^t, y_i)$ = fugacity coefficient of component i in the gas phase mixture to

account for the nonideal behavior;

y_i = mole fraction of component i in the gas mixture.

$\mu_{i(l)}$ [chemical potential of a charge neutral species in a liquid phase mixture (T,P,x_j's)], following [J.S. Newman, Electrochemical Systems (1990 edition)], is given by

$$\begin{aligned}\mu_{i(l)} &= [RT \ln \lambda_{i(l)}] - [RT \ln \lambda_{i(l)}^o] + RT \ln \lambda_{i(l)}^o \\ &= \frac{RT \ln \lambda_{i(l)}^o}{1} + RT \ln \left(\frac{\lambda_{i(l)}}{\lambda_{i(l)}^o} \right) \\ &= \mu_{i(l)} [of \text{ pure } i \text{ at } T, P^t] + RT \ln a_{r,i}\end{aligned}\quad (18)$$

where $a_{r,i}$ = relative activity of species i in the liquid – phase mixture;

$\lambda_{i(l)}$ = absolute activity of the component species i in the liquid-phase mixture;

$\lambda_{i(l)}^o$ = absolute activity of the pure species i in the liquid phase at the liquid phase mixture temperature and pressure.

According to Smith et al. [Introduction to Chemical Engineering Thermodynamics, McGraw-Hil, Inc., (1996 edition)].

$$\mu_{i(l)} = \mu_i^\Delta (@T, P^o = 1 \text{ bar}) + RT \ln \hat{a}_i \quad (19)$$

where activity of species i in the solution is given by

$$\hat{a}_i = \gamma_i x_i \left(\frac{f_i}{f_i^o} \right) = (\gamma_i x_i) \exp \left[\frac{V_i(P^t - P^o)}{RT} \right], \quad (19a)$$

where γ_i activity coefficient of species i in the liquid phase mixture; it is a function of temperature, pressure, and composition (x_i's),

f_i = fugacity of pure i in the liquid phase at the mixture temperature and pressure conditions,

f_i^o = fugacity of pure i in the liquid phase at the mixture temperature but pressure;

P^o (= 1 bar),

V_i = molar volume of pure i in the liquid phase at temperature T.

Combining Eqs. (19) and (19a) leads to:

$$\mu_{i(l)} = \left[\mu_i^\Delta (@T, P^o = 1 \text{ bar}) + V_i(P^t - P^o) \right] + RT \ln(\gamma_i x_i) \quad (19b)$$

$$= \mu_{i(0)}^o [of \text{ pure } i \text{ at } T, P] + RT \ln(\gamma_i x_i) \quad (19c)$$

On comparison of Eqs. (18) and (19c), one finds

$$a_{r,i} = \gamma_i x_i \quad (19d)$$

Equation (19b) is used for methanol and water in the liquid phase mixture to obtain:

$$\begin{aligned} \mu_{CH_3OH(l)} &= \mu_{CH_3OH(l)}^\Delta (@T, P^o = 1\text{bar}) \\ &+ V_{CH_3OH(l)}(P^t - P^o) \\ &+ RT \ln(\gamma_{CH_3OH(l)} x_{CH_3OH(l)}) \end{aligned} \quad (20a)$$

$$\begin{aligned} \mu_{H_2O(l)} &= \mu_{H_2O(l)}^\Delta (@T, P^o = 1\text{bar}) \\ &+ V_{H_2O(l)}(P^t - P^o) \\ &+ RT \ln(\gamma_{H_2O(l)} x_{H_2O(l)}) \end{aligned} \quad (20b)$$

where $V_{CH_3OH(l)}$, $V_{H_2O(l)}$ are the molar volumes of pure CH_3OH and H_2O in the liquid phase, respectively, at temperature T .

By the use of Eq. (17b), the chemical potentials of oxygen and carbon dioxide are given as:

$$\mu_{O_2(g)} = \mu_{O_2(g)}^\Delta (@T, P^o = 1\text{bar}) + RT \ln \left(\hat{\phi}_{O_2} y_{O_2} \frac{P^t}{P^o} \right) \quad (20c)$$

$$\mu_{CO_2(g)} = \mu_{CO_2(g)}^\Delta (@T, P^o = 1\text{bar}) + RT \ln \left(\hat{\phi}_{CO_2} y_{CO_2} \frac{P^t}{P^o} \right) \quad (20d)$$

Therefore, $\left\{ \mu_{CH_3OH(l)}^A + \frac{3}{2} \mu_{O_2}^C \right\} = \mu_{CH_3OH(l)}^\Delta (@T, P^o = 1\text{bar}) + V_{CH_3OH(l)}(P^{t,A} - P^o)$

$$\begin{aligned} &+ RT \ln(\gamma_{CH_3OH(l)}^A x_{CH_3OH(l)}^A) \\ &+ \frac{3}{2} \mu_{O_2}^\Delta (@T, P^o = 1\text{bar}) + RT \ln \left(\hat{\phi}_{O_2}^C y_{O_2}^C \frac{P^{t,C}}{P^o} \right) \end{aligned} \quad (20e)$$

$$\begin{aligned} &\left\{ \mu_{CO_2}^A + \left(3\mu_{H_2O(l)}^C - \mu_{H_2O(l)}^A \right) \right\} = \mu_{CO_2}^\Delta (@T, P^o = 1\text{bar}) + RT \ln \left(\hat{\phi}_{CO_2}^A y_{CO_2}^A \frac{P^{t,A}}{P^o} \right) \\ &+ 3\mu_{H_2O(l)}^\Delta (@T, P^o = 1\text{bar}) + 3V_{H_2O(l)}(P^{t,C} - P^o) + 3RT \ln(\gamma_{H_2O(l)}^C x_{H_2O(l)}^C) \\ &- \mu_{H_2O(l)}^\Delta - V_{H_2O(l)}(P^{t,A} - P^o) - RT \ln(\gamma_{H_2O(l)}^A x_{H_2O(l)}^A) \end{aligned}$$

$$\begin{aligned}
&= \mu_{CO_2}^{\Delta} + 2\mu_{H_2O(l)}^{\Delta} + V_{H_2O(l)}[(3P^{t,C} - P^{t,A}) - 2P^o] \\
&\quad + RT \ln \left[\frac{\hat{\phi}_{CO_2}^A y_{CO_2}^A \frac{P^{t,A}}{P^o}}{\gamma_{H_2O(l)}^A x_{H_2O(l)}^A} \right]
\end{aligned} \tag{20f}$$

Substituting the results from Eqs. (20e) and (20f) into Eq. (16) to obtain:

$$\begin{aligned}
FU &= F(\Phi^{\infty'} - \Phi^{\infty}) \\
&= \left(\frac{1}{6} \right) \left[\begin{aligned}
&\mu_{CH_3OH(l)}^{\Delta}(@T) + \frac{3}{2}\mu_{O_2}^{\Delta}(@T) + V_{CH_3OH(l)}(P^{t,A} - P^o) \\
&+ RT \ln \left\{ (\gamma_{CH_3OH(l)}^A x_{CH_3OH(l)}^A) (\hat{\phi}_{O_2}^C y_{O_2}^C \frac{P^{t,C}}{P^o})^{3/2} \right\} \\
&- \mu_{CO_2}^{\Delta} - 2\mu_{H_2O(l)}^{\Delta} - V_{H_2O(l)} \{ (3P^{t,C} - P^{t,A}) - 2P^o \} \\
&- RT \ln \left\{ \frac{\hat{\phi}_{CO_2}^A y_{CO_2}^A \frac{P^{t,A}}{P^o}}{\gamma_{H_2O(l)}^A x_{H_2O(l)}^A} \right\}
\end{aligned} \right] \\
&\quad + (\mu_{H^+}^C - \mu_{H^+}^A)
\end{aligned} \tag{20g}$$

$$FU = F(\Phi^{\infty'} - \Phi^{\infty})$$

$$\begin{aligned}
&= \left(\frac{1}{6} \right) + \left\{ V_{CH_3OH(l)} (P^{t,A} - P^o) - V_{H_2O(l)} (3P^{t,C} - P^{t,A} - 2P^o) \right\} \\
&+ RT \ln \left\{ \frac{\gamma_{CH_3OH(l)}^A x_{CH_3OH(l)}^A \left(\frac{\hat{\phi}_{O_2}^C y_{O_2}^C P^{t,C}}{P^o} \right)^{\frac{3}{2}}}{\frac{\hat{\phi}_{CO_2}^A y_{CO_2}^A \left(\frac{P^{t,A}}{P^o} \right)}{\gamma_{H_2O(l)}^A x_{H_2O(l)}^A}} \right\} \\
&+ (\mu_{H^+}^C - \mu_{H^+}^A)
\end{aligned} \tag{20h}$$

$$FU = F (\Phi^{\infty'} - \Phi^{\infty})$$

$$\begin{aligned}
&= \left(\frac{1}{6} \right) + \left\{ \mu_{CH_3OH(l)}^{\Delta} + \frac{3}{2} \mu_{O_2}^{\Delta} - \mu_{CO_2}^{\Delta} - 2\mu_{H_2O(l)}^{\Delta} \right\} \\
&+ \left\{ V_{CH_3OH(l)} (P^{t,A} - P^o) - V_{H_2O(l)} (3P^{t,C} - P^{t,A} - 2P^o) \right\} \\
&+ RT \ln \left\{ \left(\gamma_{CH_3OH(l)}^A \gamma_{H_2O(l)}^A x_{CH_3OH(l)}^A x_{H_2O(l)}^A \right) \left[\frac{\left(\frac{\hat{\phi}_{O_2}^C y_{O_2}^C P^{t,C}}{P^o} \right)^{\frac{3}{2}}}{\left(\frac{\hat{\phi}_{CO_2}^A y_{CO_2}^A P^{t,A}}{P^o} \right)} \right] \right\} \\
&+ (\mu_{H^+}^C - \mu_{H^+}^A)
\end{aligned} \tag{21}$$

Now, $\mu_{H^+}^C = \mu_{H^+}^{C-E-I}$ (electrochemical potential of H^+ in the polymer electrolyte at the cathode - electrolyte interface)

(22a)

$\left(\begin{array}{l} \text{condition of the phase equilibrium with regard to H}^+\text{ ions;} \\ \text{note that H}^+\text{ ion is the mobile ion in the polymer} \\ \text{electrolyte} \end{array} \right)$

$$\mu_{H^+(l)}^A = \mu_{H^+}^{A-E-I}$$

$\left(\begin{array}{l} \text{electrochemical potential of H}^+\text{ in the polymer electrolyte} \\ \text{at the anode - electrolyte interface} \end{array} \right)$

(22b)

Insert for $\mu_{H^+(l)}^C$ and $\mu_{H^+(l)}^A$ from Eqs. (22a) and (22b) into Eq. (21):

$$FU = F(\Phi^{\infty'} - \Phi^{\infty})$$

$$\begin{aligned}
 &= \left(\frac{1}{6} \right) \left[\begin{array}{l} \left\{ \mu_{CH_3OH(l)}^{\Delta} + \frac{3}{2} \mu_{O_2}^{\Delta} - \mu_{CO_2}^{\Delta} - 2 \mu_{H_2O(l)}^{\Delta} \right\} \\ + \left\{ V_{CH_3OH(l)} (P^{t,A} - P^o) - V_{H_2O(l)} (3P^{t,C} - P^{t,A} - 2P^o) \right\} \\ + RT \ln \left\{ \frac{\left(\gamma_{CH_3OH(l)}^A \gamma_{H_2O(l)}^A x_{CH_3OH(l)}^A x_{H_2O(l)}^A \right) \left(\hat{\phi}_{O_2}^C y_{O_2}^C \frac{P^{t,C}}{P^o} \right)^{3/2}}{\left(\hat{\phi}_{CO_2}^A y_{CO_2}^A \frac{P^{t,A}}{P^o} \right)} \right\} \end{array} \right] \\
 &+ \left(\mu_{H^+}^{C-E-I} - \mu_{H^+}^{A-E-I} \right)
 \end{aligned}$$

(23)

Following the approach given by J.S. Newman (Electrochemical Systems, p. 83, Prentice Hall (1991)), the electric potential (also called quasi-electrostatic potential) in the solution of the membrane phase is defined as:

$$\mu_{H^+} = RT \ln c_{H^+} + z_{H^+} F \Phi \quad (24a)$$

Then,

$$\begin{aligned}
\mu_{H^+}^{C-E-I} - \mu_{H^+}^{A-E-I} &= RT \ln \left[\frac{c_{H^+}^{C-E-I}}{c_{H^+}^{A-E-I}} \right] + z_{H^+} F(\Phi^{C-E-I} - \Phi^{A-E-I}) \\
&= RT \ln \left[\frac{c_{H^+}^{C-E-I}}{\frac{\rho_{solv}}{c_{H^+}^{A-E-I}}} \right] + z_{H^+} F(\Phi^{C-E-I} - \Phi^{A-E-I}) \\
&= RT \ln \left[\frac{m_{H^+}^{C-E-I}}{m_{H^+}^{A-E-I}} \right] + z_{H^+} F(\Phi^{C-E-I} - \Phi^{A-E-I})
\end{aligned} \tag{24b}$$

where m_{H^+} = molality of H^+ in the solution with water as solvent,

c_{H^+} = molar concentration of H^+ in the solution,

ρ_{solv} = solvent (water) density,

$z_{H^+} = +1$,

Φ = electric potential.

From Eq. (24b), the expression for $(\mu_{H^+}^{C-E-I} - \mu_{H^+}^{A-E-I})$ is inserted into Eq. (23) to obtain

$$\begin{aligned}
FU &= F(\Phi^{\infty'} - \Phi^{\infty}) \\
&= \frac{1}{6} \left[\left\{ \mu_{CH_3OH(l)}^{\Delta} + \frac{3}{2} \mu_{O_2}^{\Delta} - \mu_{CO_2}^{\Delta} - 2\mu_{H_2O(l)}^{\Delta} \right\} \right. \\
&\quad \left. + \left\{ V_{CH_3OH(l)}(P^{t,A} - P^o) - V_{H_2O(l)}(3P^{t,C} - P^{t,A} - 2P^o) \right\} \right. \\
&\quad \left. + RT \ln \left\{ \gamma_{CH_3OH(l)}^A \gamma_{H_2O(l)}^A x_{CH_3OH(l)}^A x_{H_2O(l)}^A \left(\frac{\left[\hat{\phi}_{O_2}^C y_{O_2}^C \frac{P^{t,c}}{P^o} \right]^{3/2}}{\left[\hat{\phi}_{O_2}^A y_{O_2}^A \frac{P^{t,A}}{P^o} \right]} \right) \right\} \right] \\
&\quad + RT \ln \left(\frac{m_{H^+}^{C-E-I}}{m_{H^+}^{A-E-I}} \right) + z_{H^+} F(\Phi^{C-E-I} - \Phi^{A-E-I})
\end{aligned} \tag{25}$$

4.1.1.1 Simplification of the Full Equation

Equation (25) shows that the cell potential is dependent, for the selected standard states of the species (CH_3OH , O_2 , CO_2 , H_2O) at the cell temperature T , on

- total pressures at the electrodes, the standard state pressure (P^0);
- pure molar volumes of $\text{CH}_3\text{OH}(\text{l})$, $\text{H}_2\text{O}(\text{l})$ in the liquid phase;
- mole fractions of CH_3OH , H_2O in the liquid phase mixture at the anode and the mole fractions of $\text{O}_2(\text{g})$, $y_{\text{O}_2}^{\text{C}}$, and $\text{CO}_2(\text{g})$, $y_{\text{CO}_2}^{\text{A}}$, at the cathode and anode, respectively;
- activity coefficients of $\text{CH}_3\text{OH}(\text{l})$, $\gamma_{\text{CH}_3\text{OH}(\text{l})}^{\text{A}}$, and $\text{H}_2\text{O}(\text{l})$, $\gamma_{\text{H}_2\text{O}(\text{l})}^{\text{A}}$ at the anode;
- fugacity coefficients of $\text{O}_2(\text{g})$, $\hat{\phi}_{\text{O}_2}^{\text{C}}$, and $\text{CO}_2(\text{g})$, $\hat{\phi}_{\text{CO}_2}^{\text{A}}$, in the gas phase at the cathode and anode, respectively;
- the hydrogen ion concentrations, $m_{\text{H}^+}^{\text{C-E-I}}$, $m_{\text{H}^+}^{\text{A-E-I}}$, in the membrane at the cathode and anode interfaces and on the electric potential difference $(\Phi^{\text{C-E-I}} - \Phi^{\text{A-E-I}})$ in the electrolyte membrane between its interfaces with cathode and anode.

Simplifications of Eq. (25):

- (1) If the potential variation across the membrane is ignored, especially for the case of no poison reaction such as the parasitic oxidation of methanol at the cathode, i.e.

$(\Phi^{\text{C-E-I}} - \Phi^{\text{A-E-I}}) = 0$ in Eq. (25), the open-circuit potential should then be given

by

$$\begin{aligned}
 \text{FU} &= F(\Phi^{\infty'} - \Phi^{\infty}) \\
 &= \frac{1}{6} \left[\begin{aligned} &\left\{ \mu_{\text{CH}_3\text{OH}(\text{l})}^{\Delta} + \frac{3}{2} \mu_{\text{O}_2}^{\Delta} - \mu_{\text{CO}_2}^{\Delta} - 2\mu_{\text{H}_2\text{O}(\text{l})}^{\Delta} \right\} \\ &+ \left\{ V_{\text{CH}_3\text{OH}(\text{l})} (P^{t,\text{A}} - P^0) - V_{\text{H}_2\text{O}(\text{l})} (3P^{t,\text{C}} - P^{t,\text{A}} - 2P^0) \right\} \\ &+ RT \ln \left\{ \left(\gamma_{\text{CH}_3\text{OH}(\text{l})}^{\text{A}} \gamma_{\text{H}_2\text{O}(\text{l})}^{\text{A}} x_{\text{CH}_3\text{OH}(\text{l})}^{\text{A}} x_{\text{H}_2\text{O}(\text{l})}^{\text{A}} \right) \left(\frac{\left[\hat{\phi}_{\text{O}_2}^{\text{C}} y_{\text{O}_2}^{\text{C}} \frac{P^{t,\text{C}}}{P^0} \right]^{3/2}}{\left[\hat{\phi}_{\text{CO}_2}^{\text{A}} y_{\text{CO}_2}^{\text{A}} \frac{P^{t,\text{A}}}{P^0} \right]} \right) \right\} \end{aligned} \right] \\
 &\quad + RT \ln \left(\frac{m_{\text{H}^+}^{\text{C-E-I}}}{m_{\text{H}^+}^{\text{A-E-I}}} \right)
 \end{aligned} \tag{26}$$

Comment: Determination of the cell potential using this equation requires information on $\frac{m_{H^+}^{C-E-I}}{m_{H^+}^{A-E-I}}$ in addition to other parameters. These can be determined if one has the thermodynamic information of the partition or distribution coefficient defined as

$$K_{H^+} = \frac{m_{H^+}^M}{m_{H^+} \text{ (in aqueous solution)}} \quad (26a)$$

(obtained from the phase equilibrium data)

In case one cannot evaluate the last term in Eq. (26), one may assume the last term in this equation to be negligible. This is equivalent to the assumption that $\bar{V}m_{H^+}$ in the membrane = 0 under the cell open-circuit conditions. This equation is then reduced to:

$$\begin{aligned} FU &= F(\Phi^\infty - \Phi^\circ) \\ &= \frac{1}{6} \left[\begin{aligned} &\left\{ \mu_{CH_3OH(l)}^\Delta + \frac{3}{2} \mu_{O_2}^\Delta - \mu_{CO_2}^\Delta - 2\mu_{H_2O(l)}^\Delta \right\} \\ &+ \left\{ V_{CH_3OH(l)}(P^{t,A} - P^\circ) - V_{H_2O(l)}(3P^{t,C} - P^{t,A} - 2P^\circ) \right\} \\ &+ RT \ln \left\{ \left(\gamma_{CH_3OH(l)}^A \gamma_{H_2O(l)}^A x_{CH_3OH(l)}^A x_{H_2O(l)}^A \right) \left(\frac{\left[\hat{\phi}_{O_2}^C y_{O_2}^C \frac{P^{t,C}}{P^\circ} \right]^{3/2}}{\left[\hat{\phi}_{CO_2}^A y_{CO_2}^A \frac{P^{t,A}}{P^\circ} \right]} \right) \right\} \end{aligned} \right] \quad (27) \end{aligned}$$

- The activity and fugacity coefficients of the species can be determined using the methods given in the standard thermodynamic books:

Smith, et al., Introduction to Chemical Engineering Thermodynamics, Chapters 10-14; The McGraw-Hill Companies, Inc., 5th Edition (1996);

Tester, J.W., and M. Modell, Thermodynamics and Its Applications, Chapters 9, 11, 12, 15; Prentice Hall; 1997 edition.

J.S. Newman, Electrochemical Systems, Chapter 4 (for ionic activity coefficients), Prentice Hall (1991 edition).

- Standard state chemical potential data at a reference temperature and methods to obtain them at any other desired cell temperature are also provided in the standard thermodynamic books. Also, the other property values such as V_i [pure component molar volume] can be obtained from the references given above.

- For the case of dilute solution of $CH_3OH(l)$ in $H_2O(l)$ (e.g., $c_{CH_3OH(l)} < 0.1 \frac{mol}{l}$) and

total anode and cathode pressures being ≤ 10 bars, one may assume that the liquid and gas phases to follow ideal solution and ideal gas behavior, respectively. With this

assumption, $\gamma_{CH_3OH(l)}^A = \gamma_{H_2O(l)}^A = 1$; $\hat{\phi}_{O_2}^C = \hat{\phi}_{O_2}^A = 1$ equation (27) becomes

$$FU = \frac{1}{6} \left[\begin{aligned} & \left\{ \mu_{CH_3OH(l)}^\Delta + \frac{3}{2} \mu_{O_2(g)}^\Delta - \mu_{CO_2(g)}^\Delta - 2\mu_{H_2O(l)}^\Delta \right\} \\ & + \left\{ V_{CH_3OH(l)} (P^{t,A} - P^\circ) - V_{H_2O(l)} (3P^{t,C} - P^{t,A} - 2P^\circ) \right\} \\ & + RT \ln \left(x_{CH_3OH(l)}^A x_{H_2O(l)}^A \right) \left(\frac{\left[y_{O_2}^C \frac{P^{t,C}}{P^\circ} \right]^{3/2}}{\left[y_{CO_2}^A \frac{P^{t,A}}{P^\circ} \right]} \right) \right] \end{aligned} \right] \quad (28)$$

- The pure component molar volumes $V_{CH_3OH(l)}$ and $V_{H_2O(l)}$ can be determined using the methods given in Thermodynamics by Smith et al. (pp. 94-96).
- The total pressures in the anode and cathode plenums may be expressed as:

$$P^{t,A} = P_{CO_2(g)}^A + P_{CH_3OH(g)}^A + P_{H_2O(g)}^A, \quad (29a)$$

the partial pressures of CH_3OH , $P_{CH_3OH(g)}^A$, H_2O , $P_{H_2O(g)}^A$ may be obtained from the following equation:

$$P_{i(g)} = y_{i(g)} P^t = x_{i(l)} P_i^{sat} \quad (29b)$$

(Raoult's law for the ideal solution and ideal vapor mixture behavior)

where $y_{i(g)}$ = mole fraction of species i in the gas phase,

$x_{i(l)}$ = mole fraction of species i in the liquid phase,

P_i^{sat} = saturated vapor pressure of pure i at the cell temperature can be estimated from an empirical equation such as the Antoine equation.

From Eq. (29a),

$$1 = y_{CO_2(g)}^A + \left(\frac{P_{CH_3OH(g)}^A}{P^{t,A}} \right) + \left(\frac{P_{H_2O(g)}^A}{P^{t,A}} \right) \quad (29c)$$

Calculate $y_{CO_2(g)}^A$ from Eq. (29c) and use in Eq. (28).

$$\text{Also, } P^{t,C} = P_{H_2O(g)}^C + P_{O_2(g)}^C \text{ (for the case of pure oxygen as the oxidant)} \quad (29d)$$

or

$$= P_{H_2O(g)}^C + P_{O_2(g)}^C + P_{N_2(g)}^C \text{ (for the case of air as the oxidant)} \quad (29e)$$

From Eq. (29d),

$$1 = \left(\frac{P_{H_2O(g)}^C}{P^{t,C}} \right) + y_{O_2(g)}^C \quad (29f)$$

From Eq. (29e),

$$1 = \left[\frac{P_{H_2O(g)}^C}{P^{t,C}} \right] + \left(\frac{P_{O_2(g)}^C}{P^{t,C}} \right) + \frac{P_{N_2(g)}^C}{P^{t,C}} \quad (30)$$

In the gas phase,

$$\left[\frac{P_{N_2(g)}^{(C)}}{P_{O_2(g)}^{(C)}} \right] = \frac{3.76}{1} \quad (\text{for the large excess air condition}) \quad (31)$$

(air composition)

Therefore, $P_{N_2(g)}^{(C)} = 3.76 P_{O_2(g)}^C \quad (32)$

Therefore, $\left[\frac{P_{N_2(g)}^{(C)}}{P^{t,C}} \right] = \frac{3.76 P_{O_2(g)}^C}{P^{t,C}} \quad (33)$

Using the result from Eq. (33) in Eq. (30), the following results:

$$1 = \frac{P_{H_2O(g)}^C}{P^{t,C}} + 4.76 \left(\frac{P_{O_2(g)}^C}{P^{t,C}} \right)$$

$$1 = \left[\frac{P_{H_2O(g)}^C}{P^{t,C}} \right] + 4.76 y_{O_2(g)}^C$$

Hence, for the air feed to the cathode:

$$y_{O_2(g)}^C = \frac{1}{4.76} \left[1 - \frac{P_{H_2O(g)}^C}{P^{t,C}} \right] \quad (34)$$

or

$$\boxed{\left[y_{O_2(g)}^C P^{t,C} \right] = \frac{\left[P^{t,C} - P_{H_2O(g)}^C \right]}{4.76}}$$

Also,
$$1 = \left[\frac{P_{H_2O(g)}^C}{P^{t,C}} \right] + y_{O_2(g)}^C + y_{N_2(g)}^C \quad (35)$$

- The evaluation of the standard-state chemical potentials $\mu_i^{\Delta,s}$ of the species at any temperature T other than their values given at a reference temperature such as 25°C, i.e., $T_0 = 298.15K$, can be carried out by the thermodynamic equations developed below:

The change in chemical potential of a pure species is given by

$$d\mu_i = V_i dP - S_i dT \quad (36)$$

[Ref. Smith et al. Introduction to Chemical Engineering Thermodynamics, p. 181 (1996 edition).]

If the standard state of a species i is chosen at the pressure of $P = P^0 = 1\text{bar}$; then, Eq. (36) is written for a selected standard state of a species at the constant pressure of $P = P^0$ as

$$d\mu_i^\Delta = -S_i^\Delta dT \quad (37)$$

The change in the chemical potential μ_i^Δ at the reference pressure P^0 for the change in temperature from T_0 (reference temperature) to any temperature T is obtained by the integration of Eq. (37):

$$\int_{\mu_i^\Delta = \mu_{i,T_0}^\Delta}^{\mu_i^\Delta = \mu_i^\Delta} d\mu_i^\Delta = - \int_{T_0}^T S_i^\Delta dT \quad (38)$$

↓

$$\mu_i^\Delta - \mu_{i,T_0}^\Delta = - \int_{T_0}^T S_i^\Delta dT \quad (39)$$

↓

$$\mu_i^\Delta = \mu_{i,T_0}^\Delta - \int_{T_0}^T S_i^\Delta dT \quad (40)$$

↓

$$= \Delta G_{i,f,T_0}^\Delta - \int_{T_0}^T S_i^\Delta dT \quad (\text{at } P^0=1 \text{ bar}) \quad (41)$$

For a pure chemical species *i*, change in entropy per mole for a change in its thermodynamic state is given by:

$$dS_i = C_{pi} T \frac{dT}{T} - \left(\frac{\partial V_i}{\partial T} \right)_P dP \quad (42)$$

(p. 184 in Ref. Smith et al. Thermodynamics (1996

edition))

where C_{pi} = heat capacity per mole of species *i*,

V_i = molar volume of species *i* (@T,P).

For a selected standard state of a pure species *i* at the reference pressure of P° (=1 bar), Eq. (42) is reduced to

$$dS_i^\Delta = C_{pi}^\Delta \frac{dT}{T} \quad (43a)$$

Integrating Eq. (43a),

$$\int_{S_{i,T_o}^\Delta}^{S_i^\Delta} dS_i^\Delta = \int_{T_o}^T C_{pi}^\Delta \frac{dT}{T}$$

$$\downarrow$$

$$S_i^\Delta = S_{i,T_o}^\Delta + \int_{T_o}^T C_{pi}^\Delta \frac{dT}{T} \quad (43b)$$

where S_{i,T_o}^Δ = entropy per mole of pure (standard state) species *i* at the reference pressure P° (=1 bar) and the reference temperature T_o (= 298.15K or 25 °C),

C_{pi}^Δ = heat capacity of pure species *i*.

Insert S_i^Δ from Eq. (43b) into Eq. (41) to obtain:

$$\mu_i^\Delta = \Delta G_{i,f,T_o}^\Delta - \int_{T_o}^T \left[S_{i,T_o}^\Delta + \int_{T_o}^T C_{pi}^\Delta \frac{dT}{T} \right] dT$$

$$\downarrow$$

$$\mu_i^\Delta = \Delta G_{i,f,T_o}^\Delta - \int_{T_o}^T S_{i,T_o}^\Delta dT - \int_{T_o}^T \left[\int_{T_o}^T C_{pi}^\Delta \frac{dT}{T} \right] dT$$

$$\downarrow$$

$$\mu_i^\Delta = \Delta G_{i,f,T_o}^\Delta - S_{i,T_o}^\Delta (T - T_o) - \int_{T_o}^T \left[\int_{T_o}^T C_{pi}^\Delta \frac{dT}{T} \right] dT \quad (44)$$

where $\Delta G_{i,f,T_o}^\Delta$ = Gibbs free energy of formation of species i in the selected standard state (from its elemental species in the pure state at the standard state pressure of $P^\circ = 1$ bar, and the reference temperature of $T_o (=298.15 \text{ K})$,
 S_{i,T_o}^Δ = entropy per mole of species i in the standard state at the reference temperature of $T_o (=298.15 \text{ K})$,
 C_{pi}^Δ = constant pressure heat capacity of pure species i in the selected standard state.

The value of S_{i,T_o}^Δ is to be computed from the following equation:

$$S_{i,T_o}^\Delta = \frac{\Delta H_{i,f,T_o}^\Delta - \Delta G_{i,f,T_o}^\Delta}{T_o} + \sum_j \nu_j S_{j,T_o}^\Delta \quad (45)$$

where data on $\Delta H_{i,f,T_o}^\Delta$ (enthalpy of formation) and $\Delta G_{i,f,T_o}^\Delta$ (Gibbs free energy of formation) at the reference temperature of $T_o = 298.15 \text{ K}$ are usually provided in the thermodynamic literature (e.g. Smith et al., *Introduction to Chemical Engineering Thermodynamics* (1996 edition)). ν_j is the number of moles of an elemental species j involved in forming 1 g-mole of a chemical compound i and S_{j,T_o}^Δ is the standard state entropy per mole of the elemental species, j, at the reference temperature of $T_o (=298.15 \text{ K})$. Data on the standard state entropies of elemental species, S_{j,T_o}^Δ , are also provided in the literature (e.g. R.C. West (editor), *Handbook of Chemistry and Physics*, CRC Press, Cleveland, Ohio.)

The standard state heat capacity of a species i in the gas phase at temperature T is given

$$\text{as: } C_{pi}^{ig} = R \left[A + BT + CT^2 + \frac{D}{T^2} \right] \quad (46)$$

where $R = 8.314 \text{ J mol}^{-1}\text{K}^{-1}$ (the universal gas constant)

T = temperature in [K]

A,B,C,D = heat capacity coefficients for the species i in the ideal gas standard state (values given on p. 638 in the reference given above).

The standard heat capacity of species i in the pure liquid phase at temperature T is given

$$\text{by: } C_{pi}^{(l)} = R [A + BT + CT^2] \quad (47)$$

where values of the heat capacity coefficients A,B, and C for the pure chemical species in the liquid phase are given on p. 639 in the reference by Smith et al.

The molar volume of a chemical species i in the liquid phase at the mixture liquid phase

temperature and pressure may be computed from the following scheme:

The Rackett equation can be used to obtain the molar volume of a pure liquid in the saturated state, $V_{i(l)}^{sat}$, at the temperature T of the fuel cell system:

$$V_{i(l)}^{sat} = V_{ci} Z_{ci}^{(1-T_r)^{0.2857}} \quad (48)$$

where $T_r = \frac{T(K)}{T_{ci}(K)}$ (reduced temperature)

V_{ci}, Z_{ci}, T_{ci} = critical molar volume, compressibility factor, and temperature of the species i. The species critical property data are given for some chemical species in Appendix B in the reference by Smith et al (1996 edition [pp. 634-636]). Also, one determines the saturated vapor pressure of the pure liquid phase species i at the system temperature T using the following

Antoine equation: $\log_{10} P_i^{sat} = A - \frac{B}{T + C}$ (49)

where P_i^{sat} = vapor pressure of pure i in the liquid phase at the temperature T (in °C)

A,B,C = the Antoine equation constants; values of which are given in the Ref. R.M.

Felder and R.W. Rousseau, Elementary Principles of Chemical Processes, pp. 640-641, John Wiley & Sons, Inc. (2000, third edition).

Then, one determines the reduced density, ρ_r^{sat} at $P_{r,i}^{sat} = \frac{P_i^{sat}}{P_{ci}}$ using the generalized density correlation for liquids given on page 95 in the Ref. by Smith et al. Also, at the system pressure and temperature, using $P_r = \frac{P}{P_{ci}}$ and $T_r = \frac{T}{T_{ci}}$, one determines ρ_r . Then, the required molar volume $V_{i(l)}$ of a pure species in the liquid phase is computed from the following equation:

$$V_{i(l)}(@T, P) = \rho_r^{sat} \frac{V_{i(l)}^{sat}}{\rho_r} \quad (50)$$

Comments:

- The Rackett equation is accurate within 5% [See the Ref. by Smith et al.].
- Because the effect of pressure on the liquid phase molar volume is small for pressures < 15 bar; then, one may assume $V_{i(l)}[@T, P] \approx V_{i(l)}^{sat}(@T)$ for pure species i.

4.1.1.2 Calculation Scheme

A. For $\text{CH}_3\text{OH}(\text{l})$ in $\text{H}_2\text{O}(\text{l})$ feed composition at a temperature T , calculate the reversible or open-circuit cell voltage, U for

$$\left. \begin{array}{l} P^{t,C} = 1, 3, 5, 7 \text{ bar;} \\ P^{t,A} = 1, 3, 5, 7 \text{ ba} \end{array} \right\} \text{for } P^{t,C} \text{ and } P^{t,A}$$

to be of equal and different values. Repeat such calculations for temperatures of 25, 50, 60 and 80°C for each fuel feed composition.

B. For the case of fuel feed composition of ≤ 1 molar $\text{CH}_3\text{OH}(\text{l})$ in water(l), one may use Eq. 28 and for the case of fuel composition of > 1 molar $\text{CH}_3\text{O}(\text{l})$ in water(l), one should use Eq. (27). In case the total pressures in the anode and cathode plenums are less than 10 bar, one may set $\hat{\phi}_{\text{CO}_2}^A = \phi_{\text{O}_2}^C = 1$, i.e., the gas phase is assumed to follow ideal behavior.

4.1.1.3 Sample Calculations

[Note: This computation is only for the illustration of the calculation steps.]

(1)

- Cell temperature, $T = 25^\circ\text{C} = 298.15\text{K}$
Fuel feed: 1 molar CH_3OH in $\text{H}_2\text{O}(\text{l})$ at $P^{t,A} = 1 \text{ bar}$.
- Air feed: $P^{t,C} = 1 \text{ bar}$.

$P^0 = 1 \text{ bar}$ – standard-state pressure.

From the thermodynamic tables, @ $T = 25^\circ\text{C} = 298.15\text{K}$:

$$\begin{aligned} \mu_{\text{CH}_3\text{OH}(\text{l})}^\Delta &= \Delta G_{\text{f,CH}_3\text{OH}(\text{l})}^\Delta \\ \mu_{\text{CH}_3\text{OH}(\text{l})}^\Delta &= \frac{-166270\text{J}}{\text{mol}} \quad ; \quad \mu_{\text{O}_2(\text{g})}^\Delta = 0.0 \frac{\text{J}}{\text{mol}} \end{aligned}$$

$$\mu_{\text{CO}_2(\text{g})}^\Delta = -394359 \frac{\text{J}}{\text{mol}} \quad ; \quad \mu_{\text{H}_2\text{O}(\text{l})}^\Delta = -237129 \frac{\text{J}}{\text{mol}}$$

$$R = 8.314 \text{ J/mol-K}$$

In one molar methanol solution of the anode feed, $n_{CH_3OH(l)} = \frac{1 \text{ g-mol}}{l}$; and

$$n_{H_2O(l)} = \frac{\left(1 \text{ liter} * \rho_{solu} \left[\frac{gm}{l} \right] \right) - \left[1 \text{ g-mol} * M_{CH_3OH} \left[\frac{gm}{g-mol} \right] \right]}{M_{H_2O}} \quad (51)$$

(where ρ_{solu} = density of the solution)

$$x_{CH_3OH(l)}^A = \left[\frac{n_{CH_3OH(l)}}{n_{CH_3OH(l)} + n_{H_2O(l)}} \right] \quad (51a)$$

$$x_{H_2O(l)}^A = 1 - x_{CH_3OH(l)}^A \quad (51b)$$

$$\rho_{water(l) \text{ pure}} \text{ at } 25^\circ\text{C} = \left[\frac{1 \text{ kg}}{0.001003 \text{ m}^3} \right] \left[\frac{1 \text{ m}^3}{1000 \text{ l}} \right] = 0.997 \left[\frac{\text{kg}}{\text{l}} \right]$$

(from steam tables p. 662-Felder and Rousseau)

$$n_{H_2O(l)} \text{ (estimated)} = \left[\left(0.997 \frac{\text{kg}}{\text{l}} \right) (1 \text{ l}) \left(\frac{1000 \text{ gm}}{1 \text{ kg}} \right) \left(\frac{1 \text{ g-mol}}{18 \text{ gm}} \right) \right] = 55.4 \text{ g-moles}$$

(See Sections C and D for the exact and approximate procedures to compute the liquid phase mole fractions, pp. 40 - 49)

$$x_{CH_3OH}^A = \left[\frac{1 \text{ g-mol}}{(1 + 55.4) \text{ g-mol}} \right] = 0.017731 \quad (51c)$$

$$x_{H_2O(l)}^A = 1 - x_{CH_3OH(l)}^A = 0.982269 \quad (51d)$$

$$y_{CO_2(g)}^A = ?$$

From Eq. (29c)

$$1 = y_{CO_2(g)}^A + \left(\frac{P_{CH_3OH(g)}^A}{P^{t,A}} \right) + \left(\frac{P_{H_2O(g)}^A}{P^{t,A}} \right) \quad (52)$$

From Eq. (29b),

$$P_{CH_3OH(g)}^A = x_{CH_3OH(l)}^A P_{CH_3OH}^{sat} \quad (52a)$$

$$P_{H_2O(g)}^A = x_{H_2O(l)}^A P_{H_2O}^{sat} \quad (52b)$$

at 25°C from the Antoine Eq. (49)

$$\log_{10} P_{CH_3OH}^{sat} = 7.87863 - \frac{1473.11}{25 + 230} \quad (\text{vapor pressure in mm Hg}) \quad (52c)$$

$$= 2.101728$$

(A,B,C data from Felder and Rosseau)

$$\log_{10} P_{H_2O}^{sat} = 8.10765 - \frac{1750.286}{25 + 235} \quad (\text{vapor pressure in mm Hg})$$

$$= 1.375781$$

$$P_{CH_3OH}^{sat} = 126.4 \text{ mm Hg}; \quad P_{H_2O}^{sat} = 23.76 \text{ mm Hg}$$

$$P_{CH_3OH}^{sat} = (126.4 \text{ mm Hg}) \left(\frac{1.01325 \text{ bar}}{760 \text{ mm Hg}} \right) = 0.1685 \text{ bar}$$

$$P_{H_2O}^{sat} = (23.76 \text{ mm Hg}) \left(\frac{1.01325 \text{ bar}}{760 \text{ mm Hg}} \right) = 0.0317 \text{ bar}$$

All the parametric information into Eqs. (52a) and (52b):

$$P_{CH_3OH(g)}^A = 0.017731 * 0.1685 \text{ bar} = 0.00299 \text{ bar}$$

$$P_{H_2O(g)}^A = 0.982269 * (0.0317 \text{ bar}) = 0.03114 \text{ bar}$$

Substitute the data above into Eq. (52) with $P^{t,A} = P^o = 1 \text{ bar}$

$$1 = y_{CO_2(g)}^A + (0.00299) + (0.03114)$$

$$y_{CO_2(g)}^A = 0.9659 \quad (52e)$$

Now, $y_{O_2(g)}^C = ?$

From Eq. (34a),

$$y_{O_2(g)}^C = \frac{1}{4.76} \left[1 - \frac{P_{H_2O(g)}^C}{P^{t,C}} \right] \quad (52f)$$

Using Eq. (29b):

$$P_{H_2O(g)}^C = x_{H_2O(l)}^C P_{H_2O}^{sat} \quad @ 25^\circ\text{C} \quad (52g)$$

$$P_{H_2O(g)}^C = 0.0317 \text{ bar} \quad (52h)$$

From (52f), (52h), with $P^{t,C} = 1 \text{ bar}$:

$$y_{O_2(g)}^C = \left(\frac{1}{4.76} \right) [1 - 0.0317] = 0.203 \quad (52i)$$

Insert all the parametric data into Eq. (28) to obtain:

$$FU = \frac{1}{6} \left[\begin{array}{l} \left(-166270 + \frac{3}{2}(0) - (-394359) - 2(-237129); \frac{J}{mol - CH_3OH} \right) \\ + \left[V_{CH_3OH(l)}(1-1, bar) - V_{H_2O(l)}(3*1-1-2, bar) \right] \\ + \left(\frac{8.314J}{mol - K} \right) (298.15K) \ln \left((.017731)(.982269) \left(\frac{\left[\frac{0.203 \frac{1bar}{1bar} \right]^{\frac{3}{2}}}{\left[\frac{0.9659 \frac{1bar}{1bar}} \right]} \right) \right) \end{array} \right]$$

Term I

Term II

Term III

$$FU = \left(\frac{1}{6} \right) \left[(702347) + 0 + (-15,882.934) \right] \quad \left[\frac{J}{mol} \right]$$

Term I Term II Term III

$$F = 96487 \frac{Coulomb}{equiv} = 96487 \frac{Coulomb}{1 \text{ mol of unity charged particles}}$$

$$U = \frac{1}{6} \left[\frac{702347}{96487} + \left(\frac{0}{96487} \right) + \left(\frac{-15882.934}{96487} \right) \right] \left[\frac{\frac{J}{mol}}{C} \right]$$

Note: [J = Coulomb·Volt]

$$\begin{aligned}
 U &= \frac{1}{6} [7.2792 + 0 + (-.1646)] \text{ Volt} \\
 &= [1.2132 + 0 + (-0.02743)] \text{ Volt} \\
 &\quad \begin{array}{ccc} \uparrow & \uparrow & \uparrow \\ \boxed{\text{I}} & \boxed{\text{II}} & \boxed{\text{III}} \end{array} \\
 &\quad \boxed{=1.1858 \text{ Volt}} \qquad (53)
 \end{aligned}$$

- Cell open-circuit potential for
 - $P^{t,A} = P^{t,C} = 1$ bar, air as oxidant,
 - Fuel composition: 1 molar CH_3OH (in water (l)),
 - Cell temperature $T=25^\circ\text{C}$

$$\begin{aligned}
 \left[\frac{\text{Term(III)}}{U} \right] &= \left| \frac{-0.023}{1} \right| \\
 &= \boxed{2.3\%} \leftarrow \boxed{<3\%}
 \end{aligned}$$

- Then, @ $T=60^\circ\text{C}$; $P^{t,A} = P^{t,C} = 1$ bar; 1 molar feed of $\text{CH}_3\text{OH(l)}$ in $\text{H}_2\text{O(l)}$, air: oxidant
 - ↳ First calculate μ_i^\wedge 's at $T=60^\circ\text{C}$;
Then, calculate U

Here, activity coefficient values would be needed! (one should make calculations)!

4.1.1.4 Activity and Fugacity Coefficients

The local-composition models, though limited in flexibility in the fitting of experimental data, are adequate for most engineering purposes. These can be generalized to multicomponent systems and require only the parameters needed to describe the constituent binary systems.

Here, the Wilson equation for a multicomponent, liquid phase has been used and is given by

$$\frac{G^E}{RT} = -\sum_i \left[x_i \ln \left(\sum_j x_j \Lambda_{ij} \right) \right], \qquad (54)$$

$$\ln \gamma_i = 1 - \ln \left(\sum_j x_j \Lambda_{ij} \right) - \sum_k \frac{x_k \Lambda_{ki}}{\sum_j x_j \Lambda_{kj}}, \quad (55)$$

where $G^E = G - G^{\text{ideal solution}} = \text{excess Gibbs free energy per g-mole of the liquid phase at the liquid phase at the liquid phase temperature, pressure, and composition conditions; } x_i \text{ (or } x_j\text{), mole fraction of a component in the liquid phase; } \gamma_i \text{, the activity coefficient of a chemical species } i \text{ in the liquid phase. In the above equations all summations are over all chemical species. For each } ij \text{ pair, there are two interaction parameters such as } \Lambda_{ij} \text{ and } \Lambda_{ji} \text{, because } \Lambda_{ij} \neq \Lambda_{ji} \text{. For } i = j \text{, } \Lambda_{ij} = 1 \text{. The temperature dependence of the parameters, } \Lambda_{ij} \text{, is computed from the following equation:}$

$$\Lambda_{ij} = \frac{V_j}{V_i} \exp \left(\frac{-a_{ij}}{RT} \right), \quad (i \neq j), \quad (56)$$

where V_j and V_i are the molar volumes at temperature T of pure liquids j and i , and a_{ij} is a constant independent of composition and temperature. Values of V_i and a_{ij} of some binary systems, including $\text{CH}_3\text{OH} / \text{water}$, are given in Smith et al., Introduction to Chemical Engineering Thermodynamics, p. 467, The McGraw-Hill Co. (1996).

Fugacity coefficient of a component k in a multicomponent gas phase is computed from the following general equation:

$$\ln \hat{\phi}_k = \left(\frac{P}{RT} \right) \left[B_{kk} + \frac{1}{2} \sum_i \sum_j y_i y_j (2\delta_{ik} - \delta_{ij}) \right], \quad (57)$$

the dummy indices i and j run over all species in the gas phase mixture, and

$$\delta_{ik} = 2B_{ik} - B_{ii} - B_{kk}, \quad (58a)$$

$$\delta_{ij} = 2B_{ij} - B_{ii} - B_{jj}, \quad (58b)$$

with $\delta_{ii} = \delta_{kk} = 0$, etc., and $\delta_{ki} = \delta_{ik}$, etc.

Values of the virial coefficients of pure chemical species B_{ii} , B_{jj} , etc., can be calculated from the following generalized correlations:

$$B_{ij} \left(\frac{P_c}{RT_c} \right) = B^0 + \omega B^1 \quad (59)$$

The second virial coefficients are functions of temperature only. Similarly B^0 and B^1 are functions of reduced temperature, T_r only.

$$B^0 = 0.083 - \frac{0.422}{T_r^{1.6}} \quad (60)$$

$$B^1 = 0.139 - \frac{0.172}{T_r^{4.2}} \quad (61)$$

The cross coefficients B_{ik} , B_{ij} , etc., are computed from the following equations:

$$B_{ij} = \frac{RT_{cij}}{P_{cij}} (B^0 + \omega_{ij} B^1) \quad (62)$$

where B^0 and B^1 are the same functions as given in Eqs. (60) and (61). The combining rules are used to compute ω_{ij} , T_{cij} , P_{cij} as follows:

$$\omega_{ij} = \frac{\omega_i + \omega_j}{2} \quad (63a)$$

$$T_{cij} = (T_{ci} T_{cj})^{\frac{1}{2}} (1 - k_{ij}) \quad (63b)$$

$$Z_{cij} = \frac{Z_{ci} + Z_{cj}}{2} \quad (63c)$$

$$V_{cij} = \left(\frac{V_{ci}^{1/3} + V_{cj}^{1/3}}{2} \right)^3 \quad (63d)$$

$$P_{cij} = \frac{Z_{cij} RT_{cij}}{V_{cij}} \quad (63e)$$

In Eq. (63b), k_{ij} is an empirical interaction parameter associated with an i-j molecular pair.

When $i=j$ (i.e. a pure chemical species) and for species that are chemically similar $k_{ij} = 0$. In the absence of data, k_{ij} is set = 0.

The reduced temperature, $T_{rij} \equiv \frac{T}{T_{cij}}$, for a given i-j pair, is used for the computation

of B^0 and B^1 from Eqs. (60) and (61) for application in Eq. (62). For more information on the subject, Molecular Thermodynamics of Fluid-Phase Equilibria by Prausnitz et al. (1999) may be consulted.

In the above equations ω_i and T_{ci} , Z_{ci} , and V_{ci} are the acentric factor and critical temperature, compressibility factor and volume of a species i respectively. Values of these parameters are given in the Ref. by Smith et al. (1996), pp. 635, 636.

4.1.1.5 Discussion of the Computed Results

Set 1 – Methanol Concentration Range: 0.01-0.50 M (Figs. 2 through 15).

Figures 2 and 3, and 9 and 10 show the effect of pressure on the cell voltage at the cell temperature of 25 °C at three molar concentrations of methanol in water as the fuel for the ideal and nonideal liquid-phase solution and gas behavior, respectively. It is quite apparent that for each fuel concentration the open-circuit voltage increases with an increase in the cathode pressure over the range of 1-10 bar, whereas it decreases with an increase in the anode pressure over the same pressure range. Figures 2 and 9 show the effect of accounting for the nonideal behavior of liquid and gas phase on the open-circuit voltage as function of cathode pressure and fuel concentration. There is a slight increase in open-circuit voltage in the case of accounting for the nonidealities of liquid and gas phases. Similar effect of the nonideal behavior of liquid and gas phases is shown by Figs. 3 and 10 at each anodic pressure and fuel molar concentration.

Figures 4 through 8 show the effect of temperature on the open-circuit voltage for the ideal liquid-phase solution and gas phase behavior. The voltage decreases with an increase in the cell temperature at a set of fuel concentration, cathodic, and anodic pressure values. Similar trend is seen in Figs. 11 through 15 for the nonideal liquid-phase solution and gas phase behavior.

The overall conclusion from the computed data is that a set of higher cathode and lower anode pressures, higher methanol concentrations in the fuel, and lower fuel cell temperature results in a higher open-circuit voltage. For example, at the cathode pressure of 10 bar, anode pressure of 1 bar, methanol concentration of 0.5 M in the liquid fuel and temperature of 25 °C with air as the oxidant in the cathodic chamber; the open-circuit voltage is more than 1.200 volt shown in Fig. 13; in comparison with less than 1.145 volt at the cathode pressure of 1 bar, anode pressure of 10 bar, 0.01 M methanol concentration, and temperature of 60 °C as shown in Fig. 8.

Figures 16 through 29 show the computed results for the assumption of water formation at cathode in vapor phase for the Set 1 – Methanol concentration range: 0.01 – 0.50 M. Some effect of this assumption is shown by the data in Figs. 25 through 29 relative to the data in Figs. 11 through 15 for the situation of water formation at cathode in the liquid phase. However, one observes the similarity in the trends of the plotted data for these two situations.

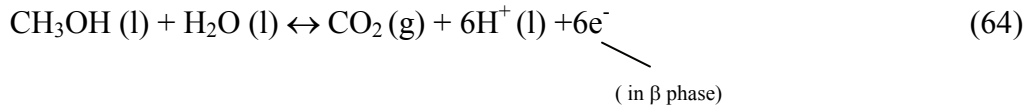
Sets 2 and 3 computed data are for methanol concentration ranges of 0.5 - 1.0 and 1.0 - 2.0 M. Trends of the plotted data for these sets are similar to Set 1 data.

4.1.2 Equilibrium Open-Circuit Voltage Equation Adjusted for the Case of Water Formation in the Vapor Phase by Hydrogen Ion Oxidation at the Cathode

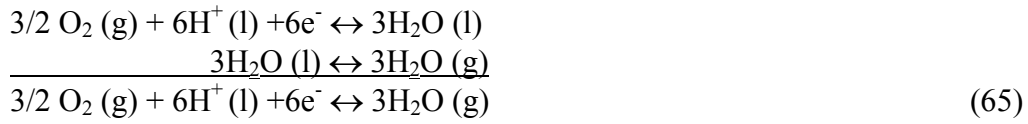
(see sketch on page 5)

The cell reactions are written as:

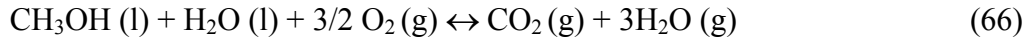
At anode:



At cathode:



The overall cell reaction is



The cell potential equation is

$$\text{FU} = \frac{1}{6} \left[\begin{aligned} &\left(\mu_{\text{CH}_3\text{OH(l)}}^\Delta - \mu_{\text{CO}_2}^\Delta + \frac{3}{2} \mu_{\text{O}_2}^\Delta + \mu_{\text{H}_2\text{O(l)}}^\Delta - 3\mu_{\text{H}_2\text{O(g)}}^\Delta \right) \\ &+ \left(V_{\text{CH}_3\text{OH(l)}} + V_{\text{H}_2\text{O(l)}} \right) \left(P^{t,A} - P^o \right) \\ &+ \text{RTln} \left\{ \left(\gamma_{\text{CH}_3\text{OH(l)}}^A \gamma_{\text{H}_2\text{O(l)}}^A x_{\text{CH}_3\text{OH(l)}}^A x_{\text{H}_2\text{O(l)}}^A \right) \frac{\left(\phi_{\text{O}_2}^C y_{\text{O}_2}^C \frac{P^{t,C}}{P^o} \right)^{3/2}}{\left(\phi_{\text{CO}_2}^A y_{\text{CO}_2}^A \frac{P^{t,A}}{P^o} \right) \left(\phi_{\text{H}_2\text{O}}^C y_{\text{H}_2\text{O}}^C \frac{P^{t,C}}{P^o} \right)^3} \right\} \end{aligned} \right] \quad (67)$$

For the ideal liquid phase and gas phase behavior,

$$\text{FU} = \frac{1}{6} \left[\begin{aligned} & \left(\mu_{\text{CH}_3\text{OH}(l)}^\Delta - \mu_{\text{CO}_2}^\Delta + \frac{3}{2} \mu_{\text{O}_2}^\Delta + \mu_{\text{H}_2\text{O}(l)}^\Delta - 3\mu_{\text{H}_2\text{O}(g)}^\Delta \right) \\ & + (V_{\text{CH}_3\text{OH}(l)}^\Delta + V_{\text{H}_2\text{O}(l)}^\Delta) (P^{t,A} - P^\circ) \\ & + \text{RTln} \left\{ \left(x_{\text{CH}_3\text{OH}(l)}^A x_{\text{H}_2\text{O}(l)}^A \right) \frac{\left(y_{\text{O}_2}^C \frac{P^{t,C}}{P^\circ} \right)^{3/2}}{\left(y_{\text{CO}_2}^A \frac{P^{t,A}}{P^\circ} \right) \left(y_{\text{H}_2\text{O}}^C \frac{P^{t,C}}{P^\circ} \right)^3} \right\} \end{aligned} \right] \quad (68)$$

Standard-state potential U^θ from Eq. (68):

$$U^\theta = \frac{\mu_{\text{CH}_3\text{OH}(l)}^\Delta - \mu_{\text{CO}_2(g)}^\Delta + \frac{3}{2} \mu_{\text{O}_2(g)}^\Delta + \mu_{\text{H}_2\text{O}(l)}^\Delta - 3\mu_{\text{H}_2\text{O}(g)}^\Delta}{6F} \quad (69)$$

Using the thermodynamic equations given in the document A., Eq. (69) has been reduced to

$$U^\theta \cong \left(\frac{\mu_{\text{CH}_3\text{OH}(l),T_o}^\Delta - \mu_{\text{CO}_2(g),T_o}^\Delta + \frac{3}{2} \mu_{\text{O}_2(g),T_o}^\Delta + \mu_{\text{H}_2\text{O}(l),T_o}^\Delta - 3\mu_{\text{H}_2\text{O}(g),T_o}^\Delta}{6F} \right) \\ + (T - T_o) \left(\frac{-S_{\text{CH}_3\text{OH}(l),T_o}^\Delta + S_{\text{CO}_2(g),T_o}^\Delta - \frac{3}{2} S_{\text{O}_2(g),T_o}^\Delta - S_{\text{H}_2\text{O}(l),T_o}^\Delta + 3S_{\text{H}_2\text{O}(g),T_o}^\Delta}{6F} \right) \quad (70)$$

(\cong , approximate because heat capacity correction terms have been neglected). $T_o = 298.15$ K, the reference state temperature.

4.1.2.1 Sample Calculations

Using the thermodynamic data, the following approximate equations for U^θ have been obtained:

$$U^\theta \cong 1.2132 - 0.0014(T - T_o), \quad [\text{volt}] \quad (\text{water produced at the cathode in liquid phase}) \quad (71a)$$

$$U^\theta \cong 1.1689 + 0.00048(T - T_o), \quad [\text{volt}] \quad (\text{water produced at the cathode in gas phase}) \quad (71b)$$

Temperature [K]	U^θ from Eq. (71a) [volt]	U^θ from Eq. (71b) [volt]
323.15	1.1781	1.1809
353.15	1.1362	1.1953

Comment: Note the effect of temperature on approx. U^θ . If the water produced at the cathode is taken to be in the liquid phase, U^θ decreases with an increase in temperature. However, it increases with an increase in temperature if the water produced at the cathode is taken to be in the gas phase.

4.1.2.2 Actual Procedure to Determine the Liquid Phase Mole Fractions of CH₃OH and H₂O, given the Molarity of the Solution

In general, the liquid phase mixture containing n_{CH_3OH} moles of methanol and n_{H_2O} moles of water at given pressure and temperature values has the volume given as:

$$n_{CH_3OH} \bar{V}_{CH_3OH} + n_{H_2O} \bar{V}_{H_2O} = V_{solution}^t \quad (72)$$

where \bar{V}_{CH_3OH} and \bar{V}_{H_2O} are the partial molar volumes of methanol and water in the liquid mixture; expressed as liter per g-mol of a species. By definition, methanol molarity is,

$$c_M = \left[\frac{n_{CH_3OH}}{V_{solution}^t} \right] [\text{mol of CH}_3\text{OH per liter of solution}] \quad (73a)$$

Also,

$$c_W = \left[\frac{n_{H_2O}}{V_{solution}^t} \right] \quad (73b)$$

Mole fractions of methanol and water are then given as

$$x_{CH_3OH} = \frac{n_{CH_3OH}}{n_{CH_3OH} + n_{H_2O}} = \frac{c_M}{c_M + c_W} \quad (73c)$$

$$x_{H_2O} = \frac{n_{H_2O}}{n_{CH_3OH} + n_{H_2O}} = \frac{c_W}{c_M + c_W} \quad (73d)$$

$$\text{where } x_{CH_3OH} + x_{H_2O} = 1.0 \quad (73e)$$

Equation is written as

$$\left(\frac{n_{CH_3OH}}{V_{solution}^t} \right) \bar{V}_{CH_3OH} + \left(\frac{n_{H_2O}}{V_{solution}^t} \right) \bar{V}_{H_2O} = 1 \quad (74)$$

$$c_M \bar{V}_{CH_3OH} + c_W \bar{V}_{H_2O} = 1 \quad (74a)$$

If the molarity of the solution with respect to methanol has been fixed, then one should determine c_W , molar concentration of water in the liquid mixture to calculate the mole fraction of methanol, x_{CH_3OH} , from Eq. (73c). This can be done with the help of Eq. (74a) if one has the values of partial molar volumes of the species at the desired temperature and pressure conditions. The partial molar volumes are functions of the species mole fractions at the given temperature and pressure conditions. These should either be determined experimentally (using the definition of a species partial molar volume) or from the literature data – in the graphical or mathematical equation form. If one likes to use the data on the species (CH₃OH, H₂O) partial molar volumes as given in the graphical form in Fig. 10.3 of the reference: J.M. Smith, H.C. Van Ness, M.M. Abbott, Introduction to Chemical Engineering Thermodynamics, p. 327, the McGraw-Hill Companies, Inc. (1996, 5th edition); one should use the following procedure:

First assume that the mixture follows the ideal solution behavior, then $\bar{V}_{CH_3OH} = V_{CH_3OH}$, $\bar{V}_{H_2O} = V_{H_2O}$; i.e. partial molar volumes are equal to the pure component molar volumes at the temperature and pressure conditions of the desired solution. Equation (74a) is written as:

$$c_M V_{CH_3OH} + c_W V_{H_2O} = 1 \quad (74b)$$

For a fixed c_M value, values of pure component volumes V_{CH_3OH} and V_{H_2O} at the solution temperature and pressure are inserted in Eq. (74b) to obtain the value of c_W . The mole fraction of methanol, x_{CH_3OH} , should then be computed from Eq. (73c). At this composition the partial molar volumes are obtained from Fig 10.3 and c_W is now computed from Eq. (74a) for the fixed c_M value. Calculation of x_{CH_3OH} is repeated. The most recently calculated value of x_{CH_3OH} is compared with its previous value. If these values agree within a preset tolerance; then, the most recently calculated values of c_W and x_{CH_3OH} for a fixed c_M value at the desired temperature and

pressure conditions are correct. If the most recent and previous value of x_{CH_3OH} do not agree within the set tolerance, the procedure is repeated until the tolerance condition is satisfied.

Example 1. What is the mole fraction of methanol in the 1 molar solution of methanol in water at 25 °C and 1 atm.

Solution:

$c_M = 1 \text{ mol/liter}$ of methanol in the methanol-water liquid at 25 °C, 1 atm.

At 25°, 1 atm, the pure component molar volumes are

$V_{CH_3OH} = 0.040727 \text{ liter/mol}$; $V_{H_2O} = 0.018068 \text{ liter/mol}$.

From Eq. (74b):

$$c_W = \frac{1 - c_M V_{CH_3OH}}{V_{H_2O}} = \frac{1 - (1)(0.040727)}{0.018068} = 53.092 \frac{\text{mol of water}}{\text{liter}} \quad (75)$$

$$x_{CH_3OH} = \frac{c_M}{c_M + c_W} = \frac{1}{1 + 53.092} = 0.01849 \quad (76)$$

From Fig. 10.3 in the reference by Smith et al., at $x_{CH_3OH} = 0.018149$;

$\bar{V}_{CH_3OH} \cong \bar{V}_{CH_3OH}^\infty = 0.0375 \text{ liter/mole}$ and $\bar{V}_{H_2O} \cong V_{H_2O} = 0.01843 \text{ liter/mole}$

From Eq. (74a):

$$c_W = \frac{1 - c_M \bar{V}_{CH_3OH}}{\bar{V}_{H_2O}} = \frac{1 - (1)(0.0375)}{0.018068} = 53.271 \frac{\text{mol of water}}{\text{liter}} \quad (77)$$

$$x_{CH_3OH} = \frac{1}{1 + 53.271} = 0.01843 \quad (78)$$

This value differs from that in Eq. (76) by

$$\frac{|0.01843 - 0.01849|}{0.01843} \times 100 \cong 0.326\% \text{ [i.e. } < 1\% \text{ (set tolerance)]}$$

Repeat the procedure.

At $x_{CH_3OH} = 0.01843$, \bar{V}_{CH_3OH} and \bar{V}_{H_2O} are obtained from Fig. 10.3. They are about the same as given above. So, $x_{CH_3OH} = 0.01843$ as in Eq. (78). Thus, no further trial is needed.

$$x_{CH_3OH} = 0.01843 \cong 0.018, \quad x_{H_2O} = 1 - 0.01843 = 0.98157 \cong 0.982$$

On the question of effect of pressure on the species partial molar volumes in the liquid phase mixture of methanol and water, one may ignore the effect of pressure on the molar

volumes over the pressure range: 1 – 10 bar. This is supported by the information given on page 185 of the reference by Smith et al. For example, molar volumes of pure liquid water at 25 °C are 18.071 and 18.070 cm³/mol at pressure of 1 and 10 bar, respectively. As to the effect of temperature on the partial molar volume of a species (CH₃OH, H₂O) in the liquid mixture, one may obtain the parameter $\bar{\beta}_i$, from the experimental data on the partial molar volumes as a function of temperature at fixed pressure and composition conditions, defined below:

$$\bar{\beta}_i = \frac{1}{\bar{V}_i} \left(\frac{\partial \bar{V}_i}{\partial T} \right)_{P, x_i} \quad [K^{-1}] \quad (79)$$

where \bar{V}_i = partial molar volume of species i in the liquid mixture of given composition, temperature and pressure conditions.

Data on $\bar{\beta}_i$ versus temperature should be generated as function of temperature for each fixed set of composition and pressure conditions. For dilute solutions of methanol in water (i.e. for $c_M \leq 1 \text{ mol/liter}$), $\bar{\beta}_W$ for water may be approximated by the pure water expansion

$$\text{coefficient, } \beta_W = \frac{1}{V_W} \left(\frac{\partial V_W}{\partial T} \right)_P .$$

The experimentally developed information on $\bar{\beta}_i$ can then be used to obtain a value of \bar{V}_i at the desired temperature of the liquid mixture of interest provided a value of \bar{V}_i at a nearby temperature is known. Note that the partial molar volumes of the species are required in Eq. (74a) to relate the species molar concentrations and mole fractions in the liquid phase mixture. Example 2: Find the partial molar volume of water at 50 °C for 0.1 molar solution of methanol in water at pressure of 1 bar.

Solution:

This solution is very dilute with regard to methanol. At 25 °C,

$$\bar{V}_{H_2O, 25} \cong V_{H_2O, 25} = 18.068 \text{ cm}^3 \text{ mol}^{-1} \quad (80)$$

From Eq. (79),

$$\bar{\beta}_W = \frac{1}{\bar{V}_{H_2O}} \left(\frac{\partial \bar{V}_{H_2O}}{\partial T} \right)_{P, x_i} \quad (81)$$

$$\partial \bar{V}_{H_2O} = (\bar{\beta}_W \bar{V}_{H_2O}) dT \quad (82)$$

$$\int_{\bar{V}_{H_2O,T_0}}^{\bar{V}_{H_2O,T}} \partial \bar{V}_{H_2O} = \int_{T_0}^T (\bar{\beta}_w \bar{V}_{H_2O}) dT \quad (83)$$

$$(\bar{V}_{H_2O,T} - \bar{V}_{H_2O,T_0}) = \int_{T_0}^T (\bar{\beta}_w \bar{V}_{H_2O}) dT$$

$$\bar{V}_{H_2O,T} = \bar{V}_{H_2O,T_0} + \int_{T_0}^T (\bar{\beta}_w \bar{V}_{H_2O}) dT \quad (\text{at given composition and pressure conditions}) \quad (84)$$

If mathematical expressions for $\bar{\beta}_w$ and \bar{V}_{H_2O} are available as functions of temperature, the integration can be carried out analytically or graphically. If such information is not available; then, $\bar{\beta}_w$ and \bar{V}_{H_2O} may be approximated by the pure water expansivity, β_w , and pure water liquid volume, V_{H_2O} . This approximation is valid particularly in the dilute solution of methanol in water of 0.1 molar concentration. For such a situation, Eq. (84) becomes

$$\bar{V}_{H_2O,T} = \bar{V}_{H_2O,T_0} + \int_{T_0}^T (\beta_w V_{H_2O}) dT \quad (85)$$

One may use the arithmetic average of the $(\beta_w V_{H_2O})$ values at the two temperatures in the integration on the right side of Eq. (85) and approximate the integral as given below:

$$\bar{V}_{H_2O,T} = \bar{V}_{H_2O,T_0} + (\beta_w V_{H_2O})(T - T_0) \quad (86)$$

$$\text{where } (\beta_w V_{H_2O}) = \frac{(\beta_w V_{H_2O}|_{25^\circ\text{C}}) + (\beta_w V_{H_2O}|_{50^\circ\text{C}})}{2} \quad (87)$$

$$= \frac{[(256 \times 10^{-6})(18.071)] + [(456 \times 10^{-6})(18.234)]}{2}, \quad [cm^3 mol^{-1} K^{-1}]$$

$$= 0.006470 \quad [cm^3 mol^{-1} K^{-1}] \quad (88)$$

$$\text{Hence, } \bar{V}_{H_2O,50} = \bar{V}_{H_2O,25} + (0.00647 \text{ cm}^3 \text{ mol}^{-1} \text{ K}^{-1})([50 + 273.15] - [25 + 273.15] \text{ K})$$

$$= 18.068 + (0.00647)(25) = 18.230 \text{ cm}^3 \text{ mol}^{-1} \quad (89)$$

Note that this volume differs from the given value of $V_{H_2O,50} = 18.234 \text{ cm}^3 \text{ mol}^{-1}$

by $\frac{|18.234 - 18.230|}{18.234} \times 100 = 0.022\%$ which is less than 0.1 %.

4.1.2.3 An Approximate Procedure to Determine the Liquid Phase Mole Fractions of CH_3OH and H_2O , given the Molarity of the Solution

If the solution density ρ_{solu} as $[\text{gm} \cdot \text{cm}^{-3}]$ is available as a function of the molarity of methanol in water, c_M [g-mol CH_3OH per liter of the solution] at a given set of temperature and pressure conditions; then, molar concentration of water in the solution can be computed from

$$c_W \left[\frac{\text{g-mol } H_2O}{l} \right] = \frac{\left[\rho_{solu} \left(\frac{\text{gms}}{\text{cm}^3} \right) \left(\frac{1000 \text{cm}^3}{\text{liter}} \right) \right] - \left[\left(c_M \frac{\text{g-mol } CH_3OH}{\text{liter}} \right) \left(M_{CH_3OH} \frac{\text{gm } CH_3OH}{\text{g-mol } CH_3OH} \right) \right]}{M_{H_2O} \left[\frac{\text{gm } H_2O}{\text{g-mol } H_2O} \right]} \quad (90)$$

$$\text{Then, } x_{CH_3OH} = \frac{c_M}{c_M + c_W} \quad (90a)$$

$$\text{and } x_{H_2O} = 1 - x_{CH_3OH} \quad (90b)$$

In the event that neither the partial molar volumes of the species nor the solution density as a function of composition is available; then, the pure component methanol molar volume at the solution temperature and pressure is used to approximate the volume occupied by methanol in the solution as given below:

Volume occupied by methanol in the solution of c_M (mol/liter), molar concentration of methanol in water, is

$$v_M = c_M \left(\frac{\text{mol } CH_3OH}{\text{liter of solution}} \right) \left(\frac{V_{CH_3OH, \text{liter of pure } CH_3OH}}{\text{mol } CH_3OH} \right)$$

$$v_M = c_M V_{CH_3OH} [\text{liter of } CH_3OH / \text{liter of solution}] \quad (91a)$$

Therefore, volume occupied by water in solution is approximated by:

$$v_{water} = (1 - v_M) [\text{liter of water / liter of solution}] \quad (91b)$$

Now, moles of water present in 1 liter of the solution are approximated by:

$$c_W = \frac{\left[(1 - v_M), \frac{\text{liter of water}}{\text{liter of solution}} \right]}{\left[V_W, \frac{\text{liter of water}}{\text{mol } H_2O} \right]} = \left(\frac{1 - v_M}{V_W} \right) \left[\frac{\text{mol } H_2O}{\text{liter of solution}} \right] \quad (91c)$$

where $V_W =$ pure component water molar volume at the solution temperature and pressure conditions.

Then, the mole fraction of methanol in water is approximated by:

$$x_{CH_3OH} = \frac{c_M}{c_M + c_W} = \frac{1}{1 + \left(\frac{c_W}{c_M} \right)} \quad (91d)$$

Using Eqs. (91a) and (91b),

$$\left(\frac{c_W}{c_M} \right) = \frac{1}{c_M} \left(\frac{1 - v_M}{V_W} \right) = \frac{1}{c_M} \left(\frac{1 - c_M V_{CH_3OH}}{V_W} \right) = \left(\frac{1}{c_M V_{H_2O}} - \frac{V_{CH_3OH}}{V_{H_2O}} \right) \quad (91e)$$

From Eqs. (6d) and (6e):

$$\begin{aligned} x_{CH_3OH} &= \frac{1}{1 + \left(\frac{1}{c_M V_{H_2O}} - \frac{V_{CH_3OH}}{V_{H_2O}} \right)} \\ &= \frac{c_M V_{H_2O}}{c_M V_{H_2O} + 1 - c_M V_{CH_3OH}} = \frac{c_M V_{H_2O}}{1 + c_M (V_{H_2O} - V_{CH_3OH})} \end{aligned} \quad (91f)$$

where $c_M = \left[\frac{\text{mol of } CH_3OH}{\text{liter of solution}} \right]$, $V_{CH_3OH} = \left[\frac{\text{liter of pure } CH_3OH}{g - \text{mol of } CH_3OH} \right]$,

$$V_{H_2O} = \left[\frac{\text{liter of pure } H_2O}{g - \text{mol of } H_2O} \right].$$

Equation (91f) is the approximate formula to calculate x_{CH_3OH} .

Comparison of the actual procedure (Section C) with the approximate Eq. (91f) to compute x_{CH_3OH} given the molar concentration of methanol in water:

$$c_M = \frac{1 \text{ mol of } CH_3OH}{1 \text{ liter of solution}} \text{ at } 25 \text{ }^\circ\text{C, } 1 \text{ atm.}$$

$$V_{CH_3OH} = 0.040727[\text{liter/mol}]; V_{H_2O} = 0.018068[\text{liter/mol}].$$

From Eq. (91f)

$$x_{CH_3OH,appr} = \frac{(1)(0.018068)}{1 + (1)(0.018068 - 0.040727)} = 0.01849$$

Difference:

$$\left| \frac{x_{CH_3OH,exact} - x_{CH_3OH,appr}}{x_{CH_3OH,exact}} \right| \times 100 \cong 0.33\% \text{ (i.e. less than 0.5 \%)}$$

So, for practical purpose, one may use Eq. (91f) to compute mole fraction of CH₃OH in solution instead of the exact procedure, requiring more work.

4.2 Plotted Data

The equilibrium cell voltage as a function of cell temperature, pressure, and reactant concentration is given Figures 2-85 and starts on the next page.

Set 1 – Concentration of methanol range from 0.01 to 0.50 M.

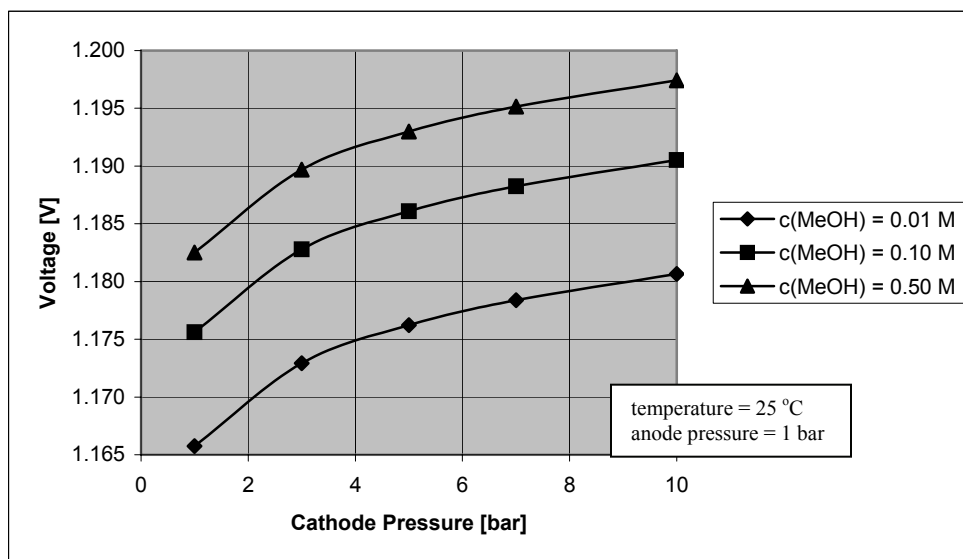


Figure 2. Set 1 - Effect of cathode pressure on the open circuit voltage for the ideal solution and gas behavior (water formation at cathode in liquid phase).

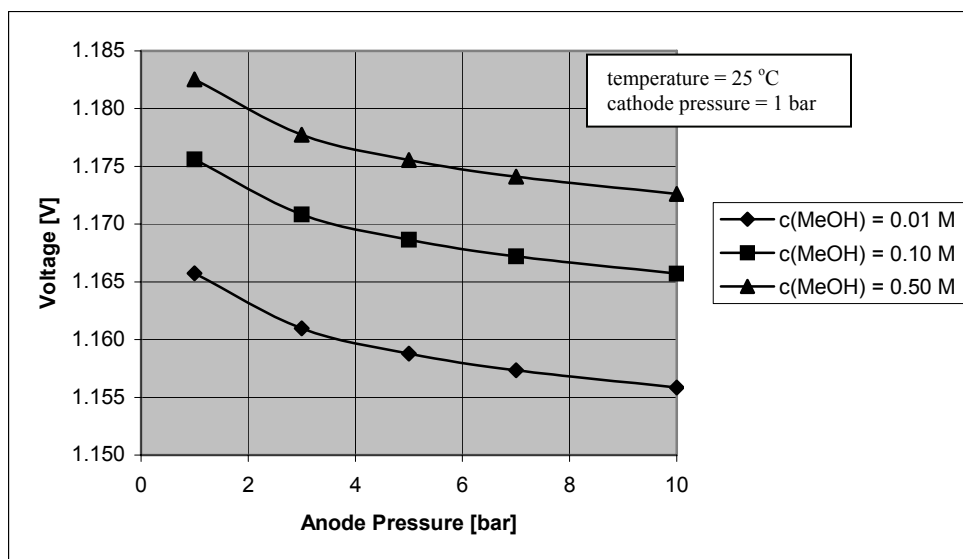


Figure 3. Set 1 - Effect of anode pressure on the open circuit voltage for the ideal solution and gas behavior (water formation at cathode in liquid phase).

Set 1 – Concentration of methanol range from 0.01 to 0.50 M.

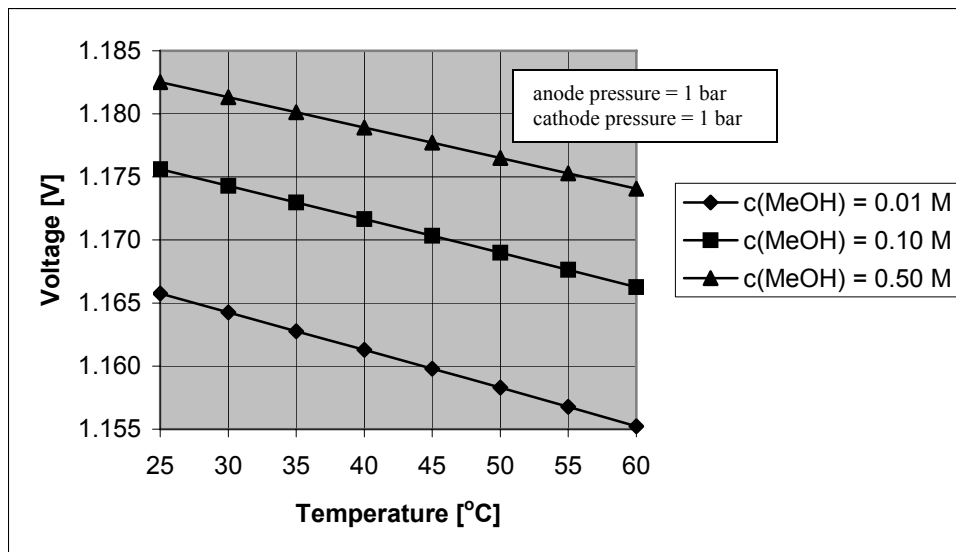


Figure 4. Set 1 - Effect of temperature on the open circuit voltage for the ideal solution and gas behavior (water formation at cathode in liquid phase).

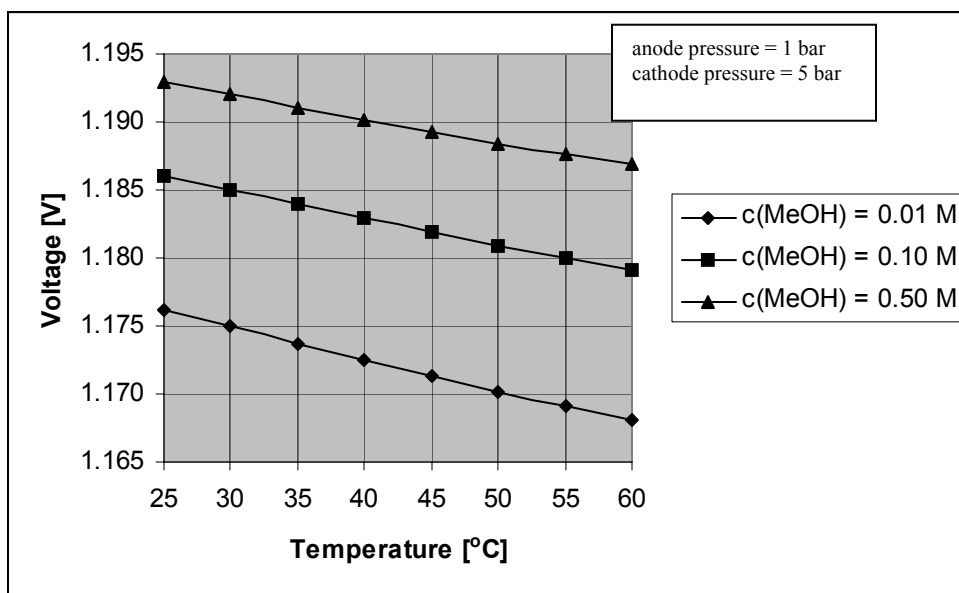


Figure 5. Set 1 - Effect of temperature on the open circuit voltage for the ideal solution and gas behavior (water formation at cathode in liquid phase).

Set 1 – Concentration of methanol range from 0.01 to 0.50 M.

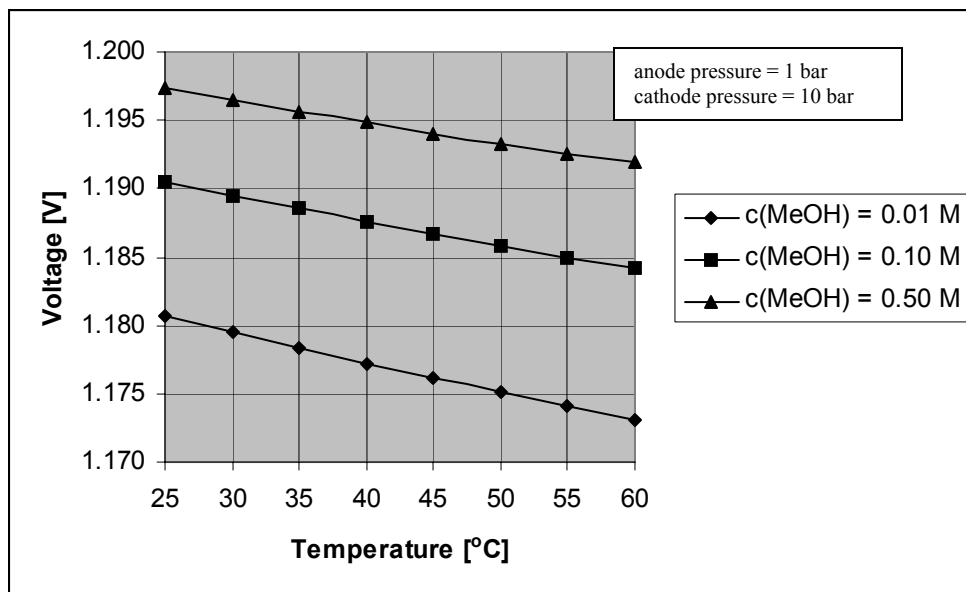


Figure 6. Set 1 - Effect of temperature on the open circuit voltage for the ideal solution and gas behavior (water formation at cathode in liquid phase).

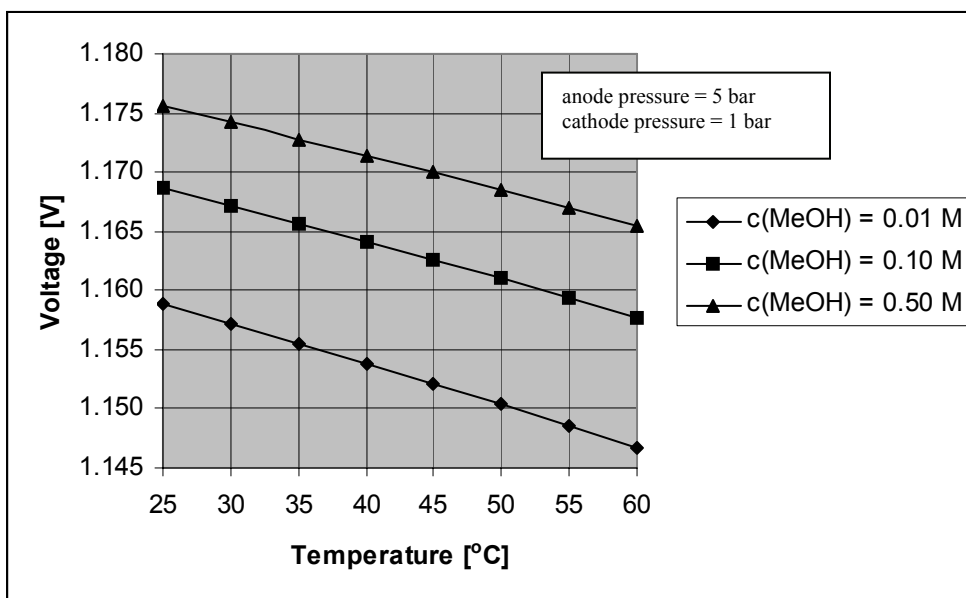


Figure 7. Set 1 - Effect of temperature on the open circuit voltage for the ideal solution and gas behavior (water formation at cathode in liquid phase).

Set 1 – Concentration of methanol range from 0.01 to 0.50 M.

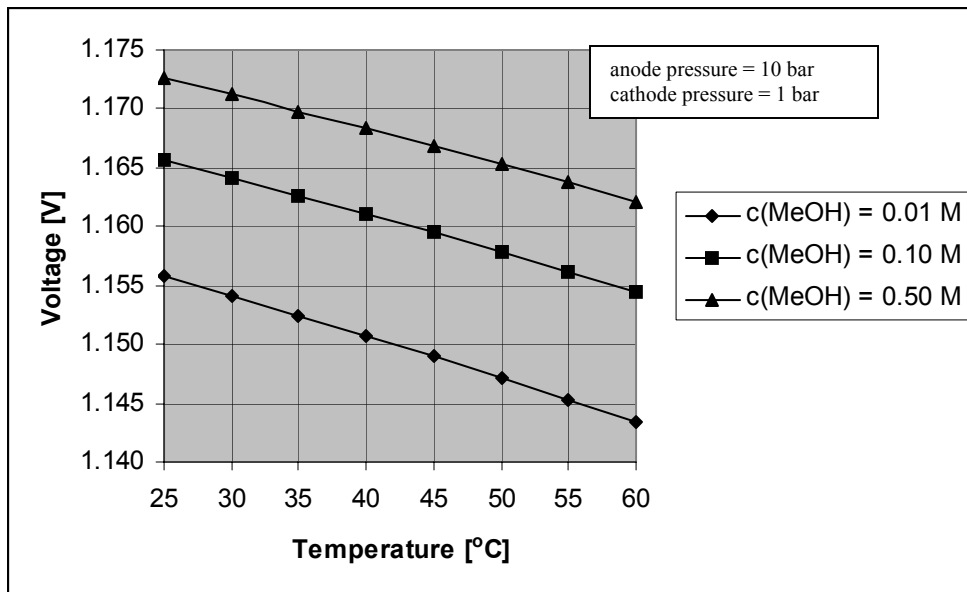


Figure 8. Set 1 - Effect of temperature on the open circuit voltage for the ideal solution and gas behavior (water formation at cathode in liquid phase).

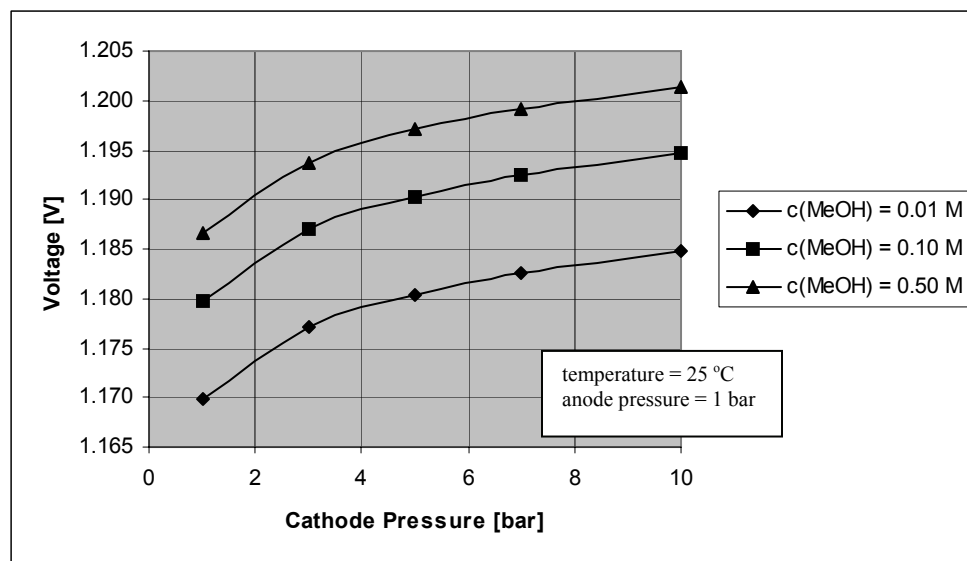


Figure 9. Set 1 - Effect of cathode pressure on the open circuit voltage for the nonideal solution and gas behavior (water formation at cathode in liquid phase).

Set 1 – Concentration of methanol range from 0.01 to 0.50 M.

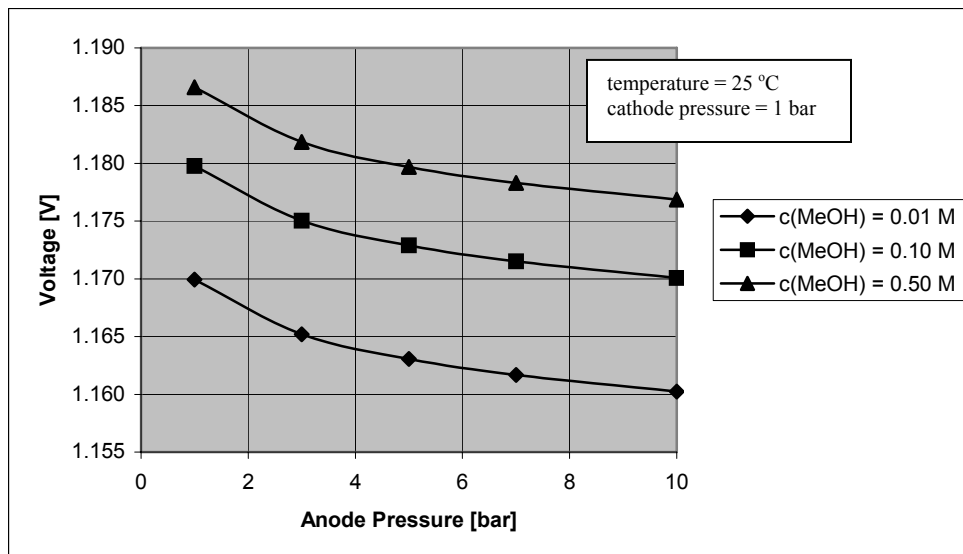


Figure 10. Set 1 - Effect of anode pressure on the open circuit voltage for the nonideal solution and gas behavior (water formation at cathode in liquid phase).

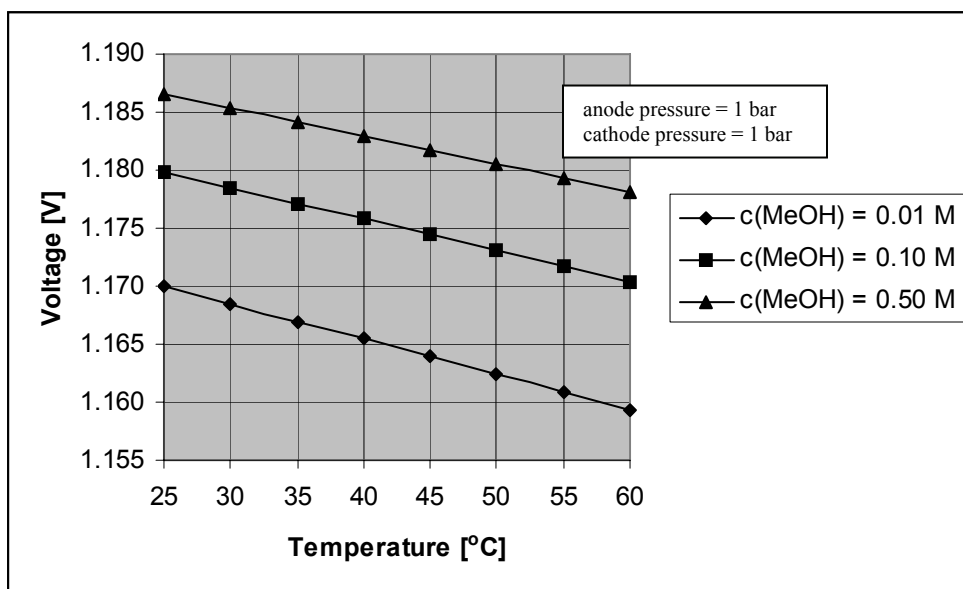


Figure 11. Set 1 - Effect of temperature on the open circuit voltage for the nonideal solution and gas behavior (water formation at cathode in liquid phase).

Set 1 – Concentration of methanol range from 0.01 to 0.50 M.

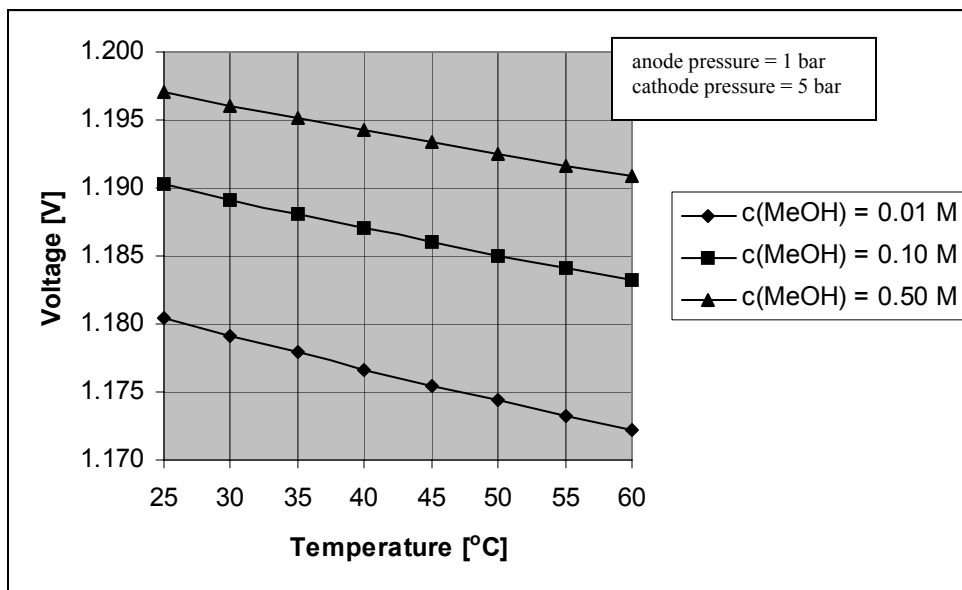


Figure 12. Set 1 - Effect of temperature on the open circuit voltage for the nonideal solution and gas behavior (water formation at cathode in liquid phase).

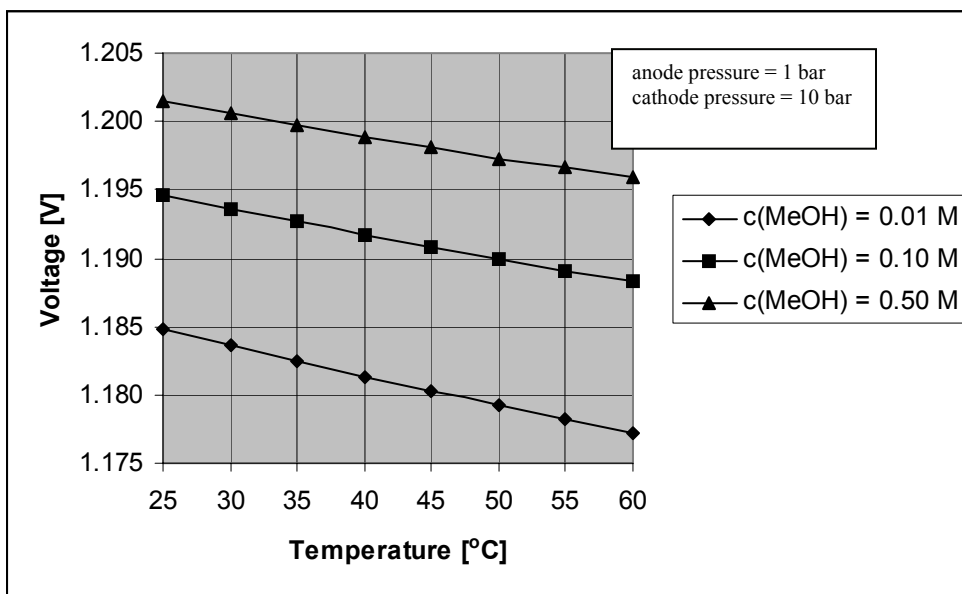


Figure 13. Set 1 - Effect of temperature on the open circuit voltage for the nonideal solution and gas behavior (water formation at cathode in liquid phase).

Set 1 – Concentration of methanol range from 0.01 to 0.50 M.

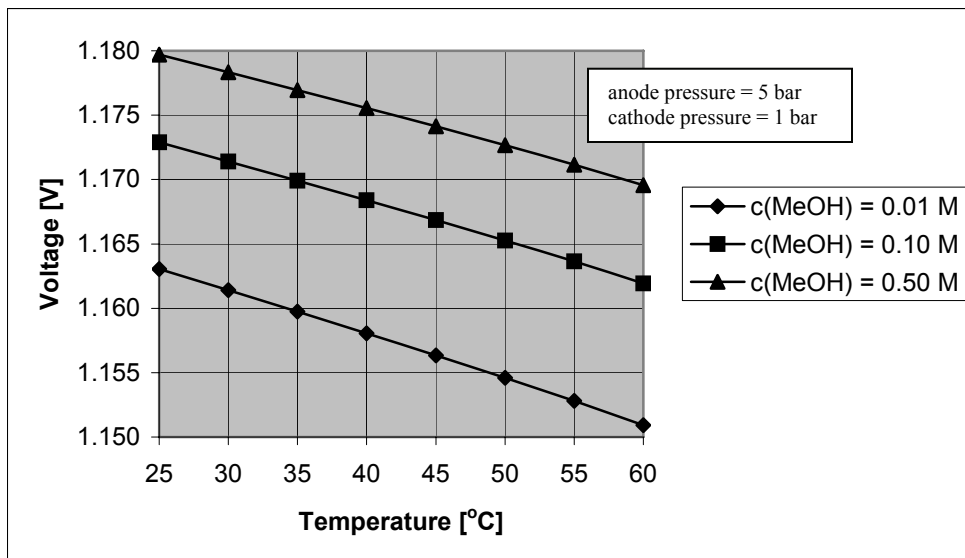


Figure 14. Set 1 - Effect of temperature on the open circuit voltage for the nonideal solution and gas behavior (water formation at cathode in liquid phase).

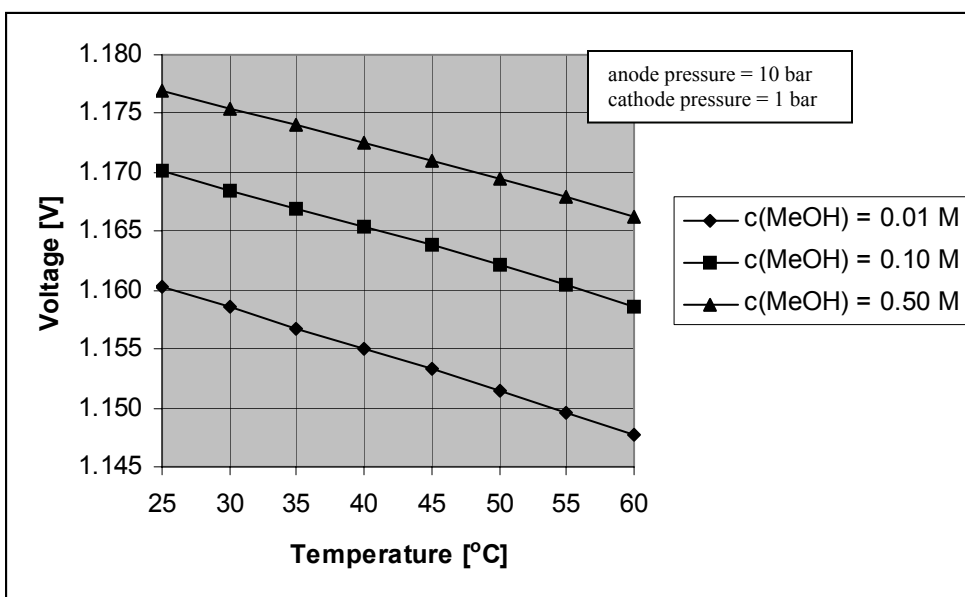


Figure 15. Set 1 - Effect of temperature on the open circuit voltage for the nonideal solution and gas behavior (water formation at cathode in liquid phase).

Set 1 – Concentration of methanol range from 0.01 to 0.50 M.

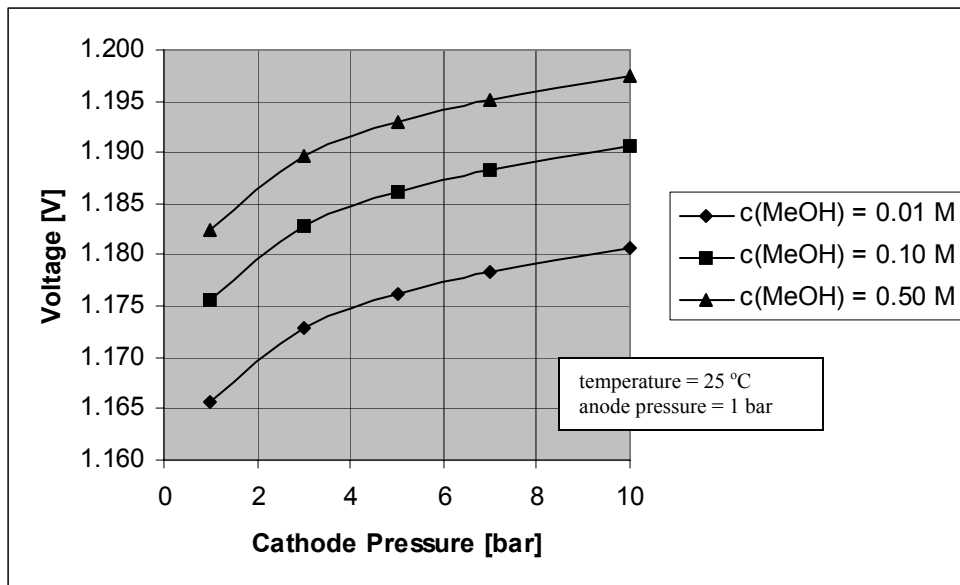


Figure 16. Set 1 - Effect of cathode pressure on the open circuit voltage for the ideal solution and gas behavior (water formation at cathode in vapor phase).

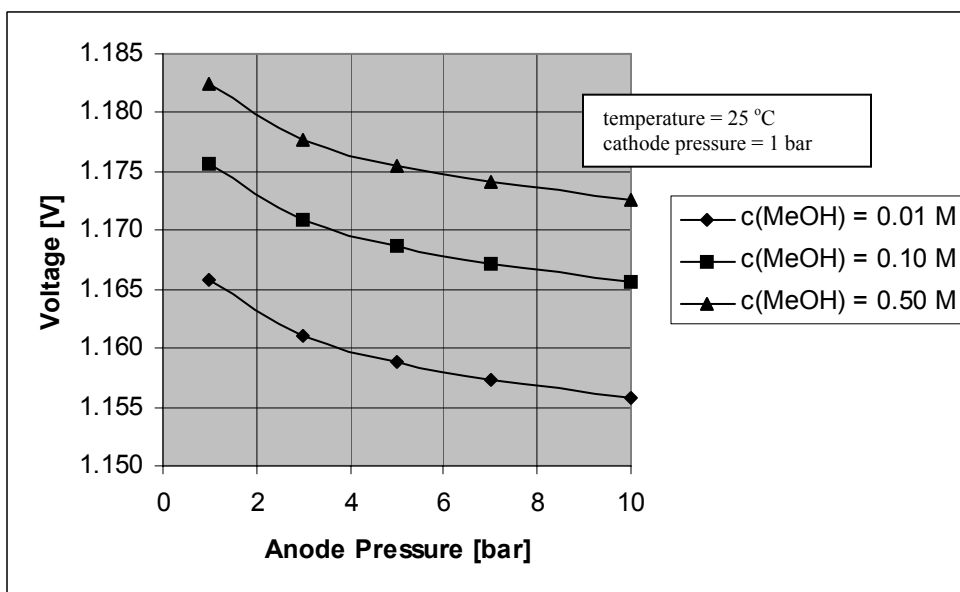


Figure 17. Set 1 - Effect of anode pressure on the open circuit voltage for the ideal solution and gas behavior (water formation at cathode in vapor phase).

Set 1 – Concentration of methanol range from 0.01 to 0.50 M.

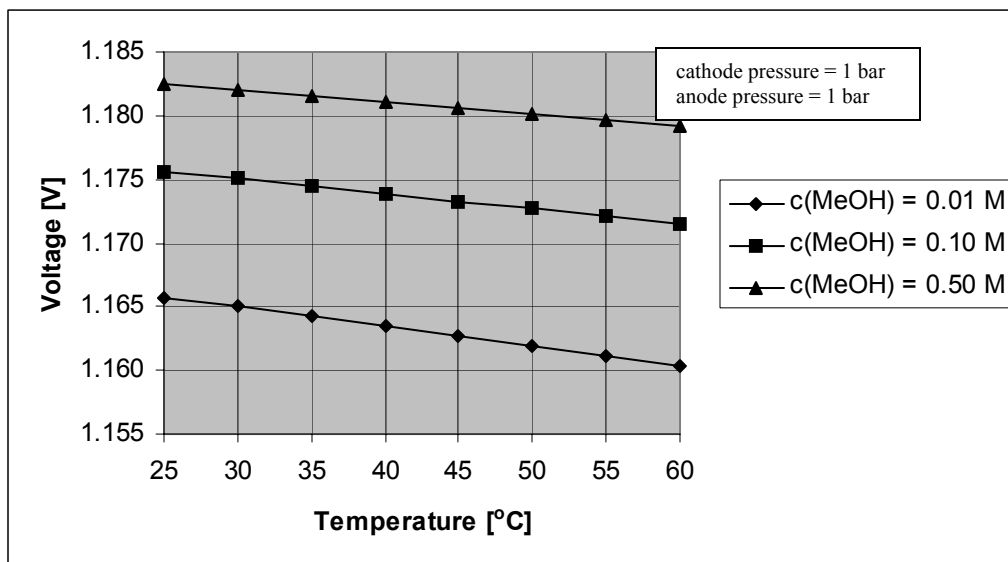


Figure 18. Set 1 - Effect of temperature on the open circuit voltage for the ideal solution and gas behavior (water formation at cathode in vapor phase).

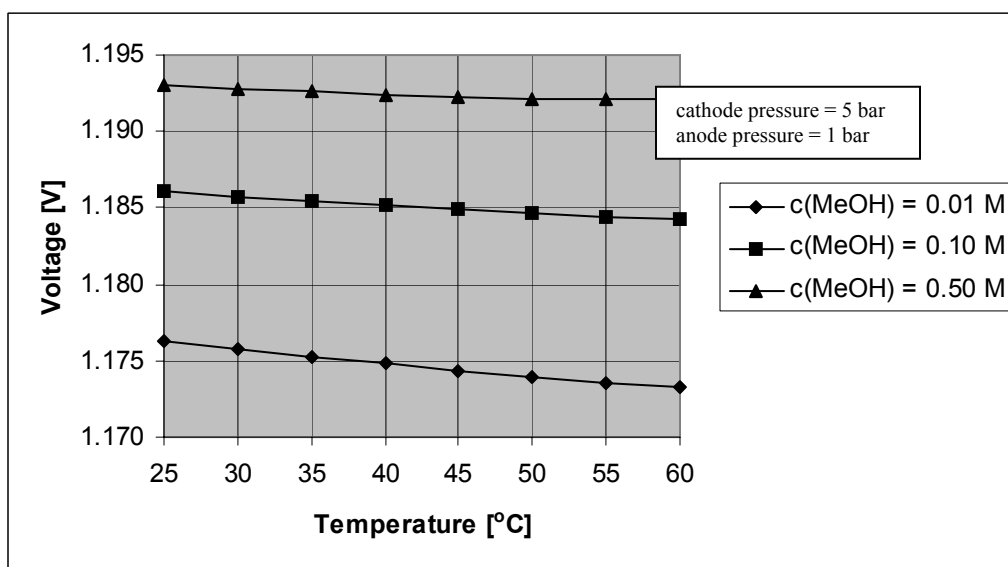


Figure 19. Set 1 - Effect of temperature on the open circuit voltage for the ideal solution and gas behavior (water formation at cathode in vapor phase).

Set 1 – Concentration of methanol range from 0.01 to 0.50 M.

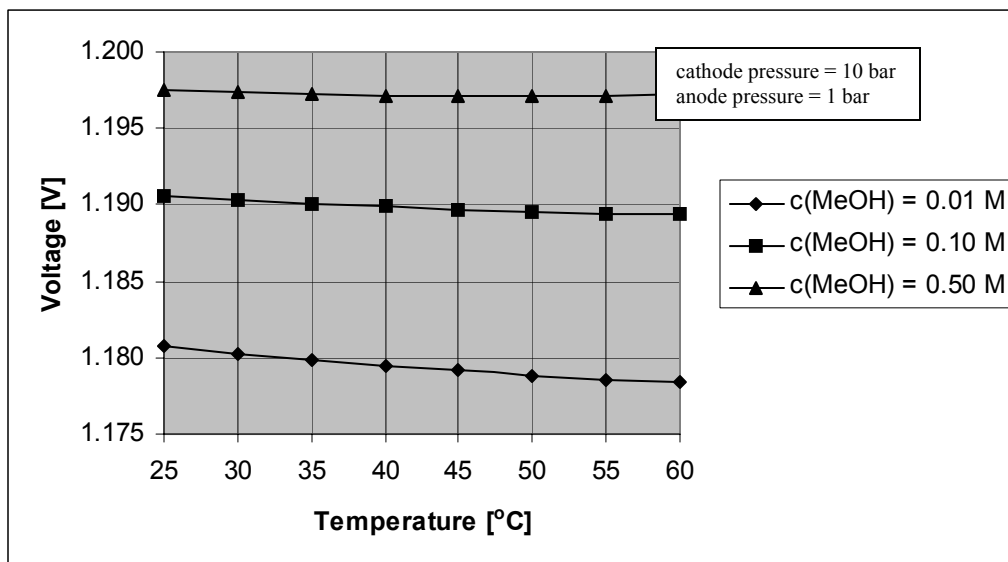


Figure 20. Set 1 - Effect of temperature on the open circuit voltage for the ideal solution and gas behavior (water formation at cathode in vapor phase).

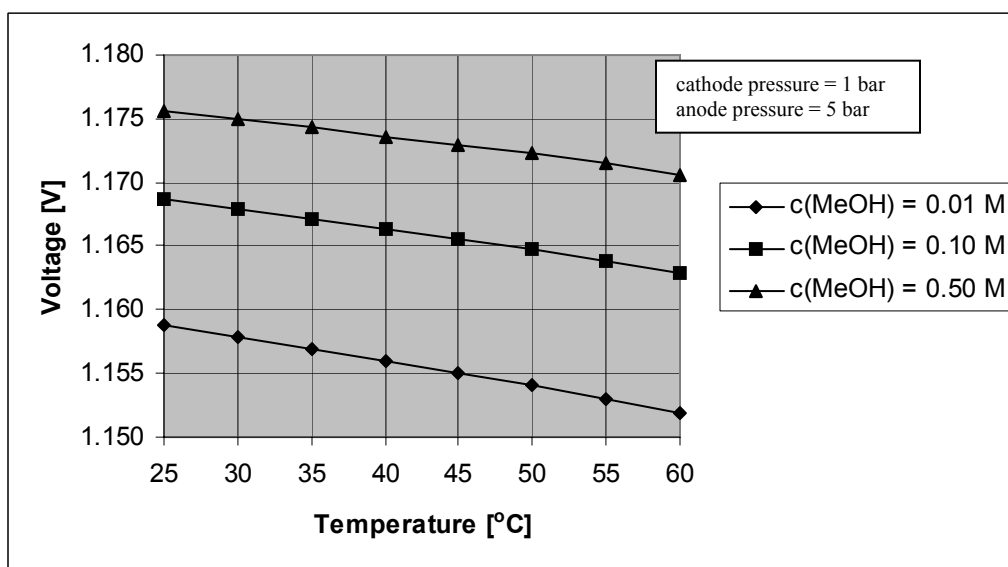


Figure 21. Set 1 - Effect of temperature on the open circuit voltage for the ideal solution and gas behavior (water formation at cathode in vapor phase).

Set 1 – Concentration of methanol range from 0.01 to 0.50 M.

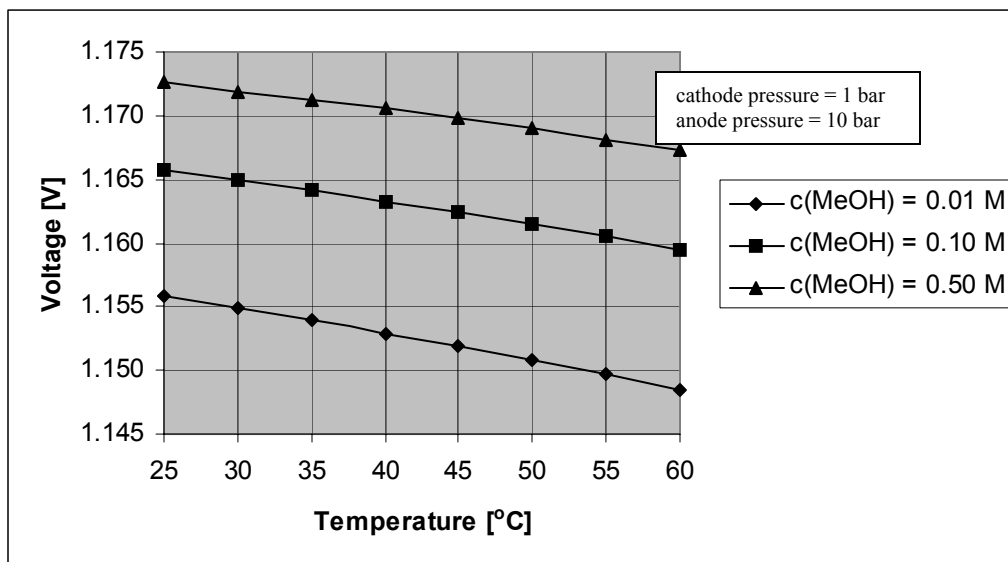


Figure 22. Set 1 - Effect of temperature on the open circuit voltage for the ideal solution and gas behavior (water formation at cathode in vapor phase).

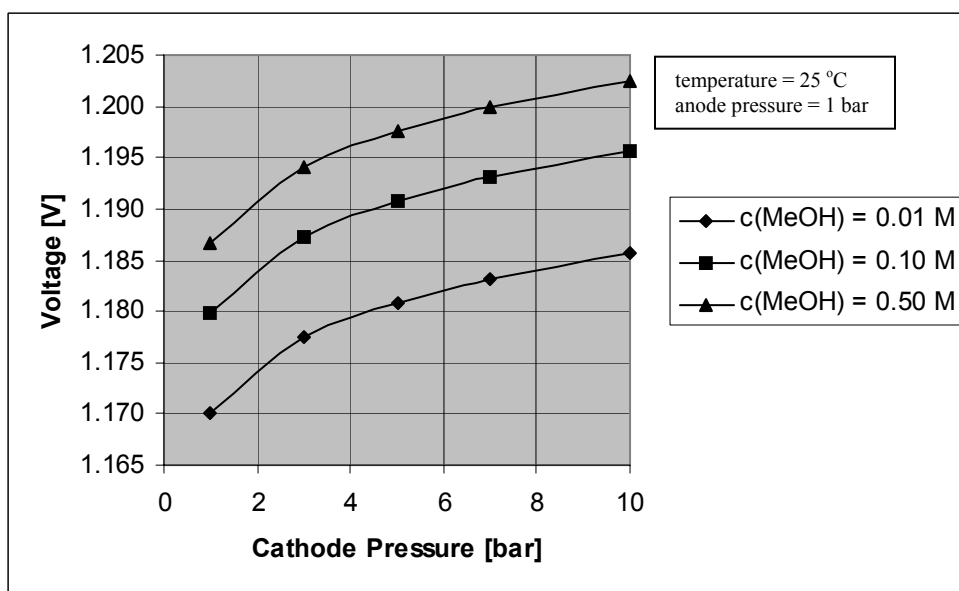


Figure 23. Set 1 - Effect of cathode pressure on the open circuit voltage for the nonideal solution and gas behavior (water formation at cathode in vapor phase).

Set 1 – Concentration of methanol range from 0.01 to 0.50 M.

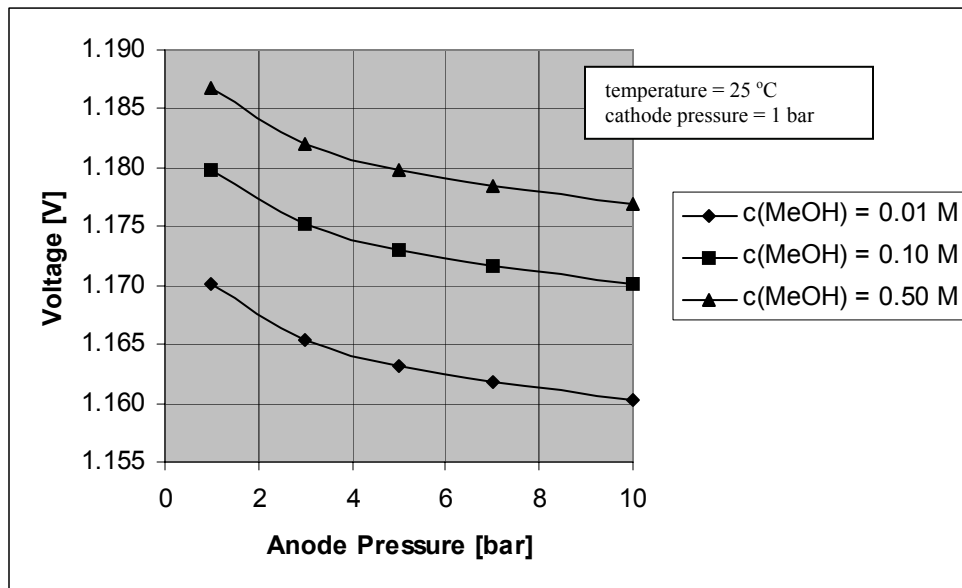


Figure 24. Set 1 - Effect of anode pressure on the open circuit voltage for the nonideal solution and gas behavior (water formation at cathode in vapor phase).

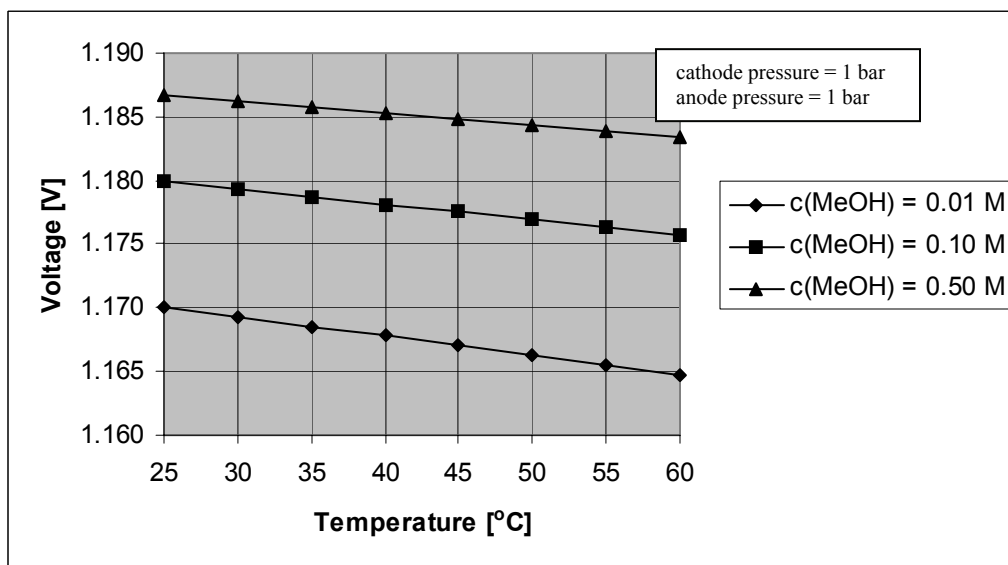


Figure 25. Set 1 - Effect of temperature on the open circuit voltage for the nonideal solution and gas behavior (water formation at cathode in vapor phase).

Set 1 – Concentration of methanol range from 0.01 to 0.50 M.

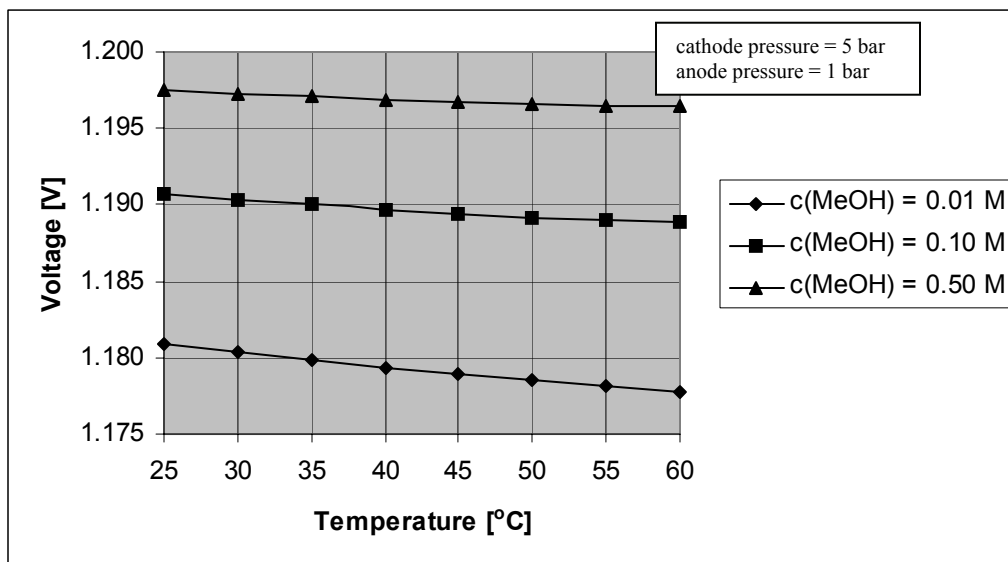


Figure 26. Set 1 - Effect of temperature on the open circuit voltage for the nonideal solution and gas behavior (water formation at cathode in vapor phase).

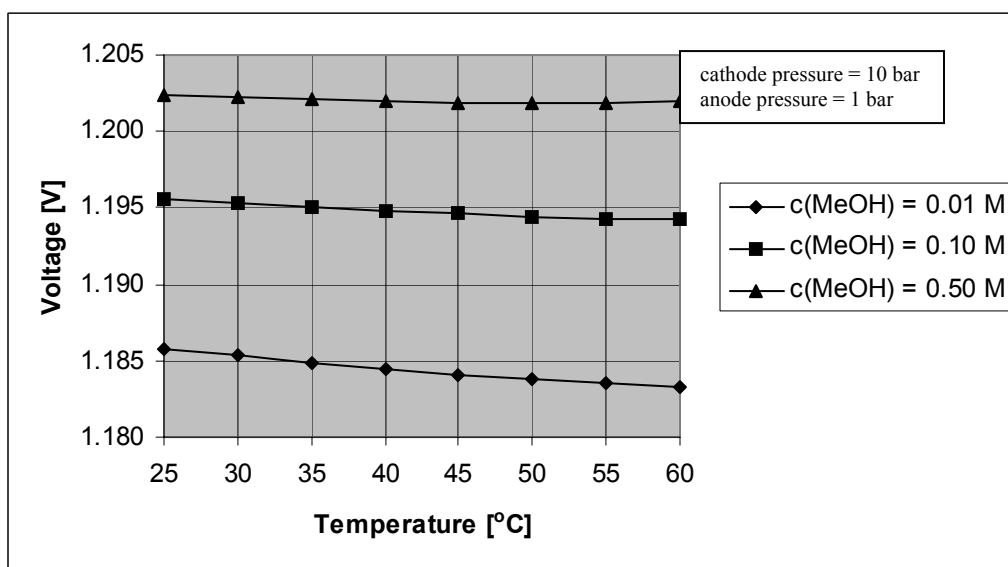


Figure 27. Set 1 - Effect of temperature on the open circuit voltage for the nonideal solution and gas behavior (water formation at cathode in vapor phase).

Set 1 – Concentration of methanol range from 0.01 to 0.50 M.

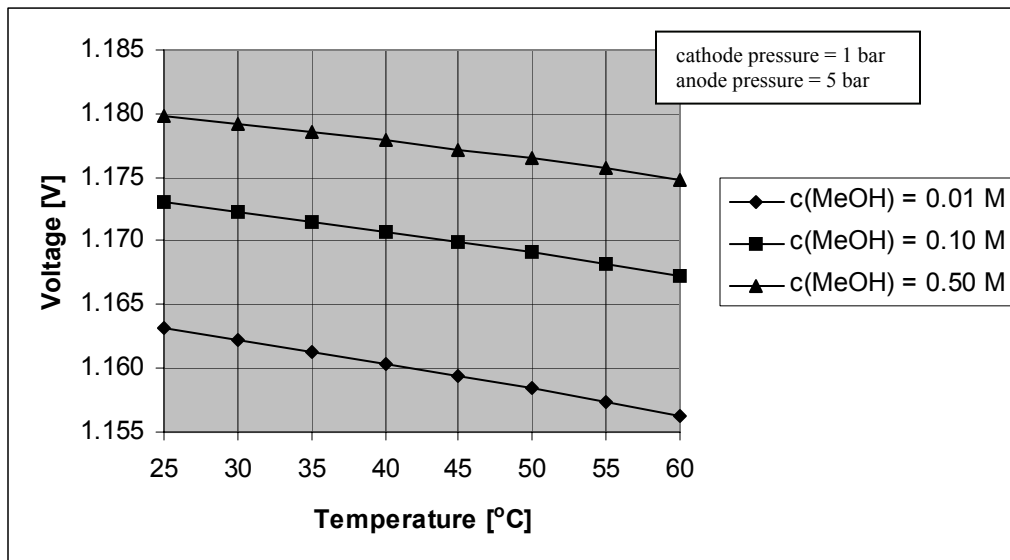


Figure 28. Set 1 - Effect of temperature on the open circuit voltage for the nonideal solution and gas behavior (water formation at cathode in vapor phase).

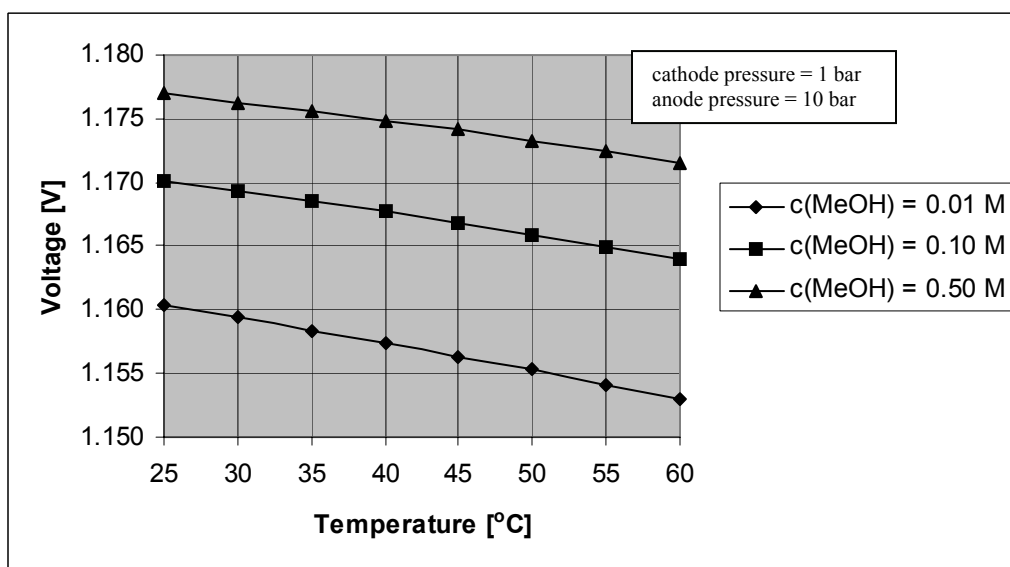


Figure 29. Set 1 - Effect of temperature on the open circuit voltage for the nonideal solution and gas behavior (water formation at cathode in vapor phase).

Set 1 – Concentration of methanol range from 0.01 to 0.50 M.

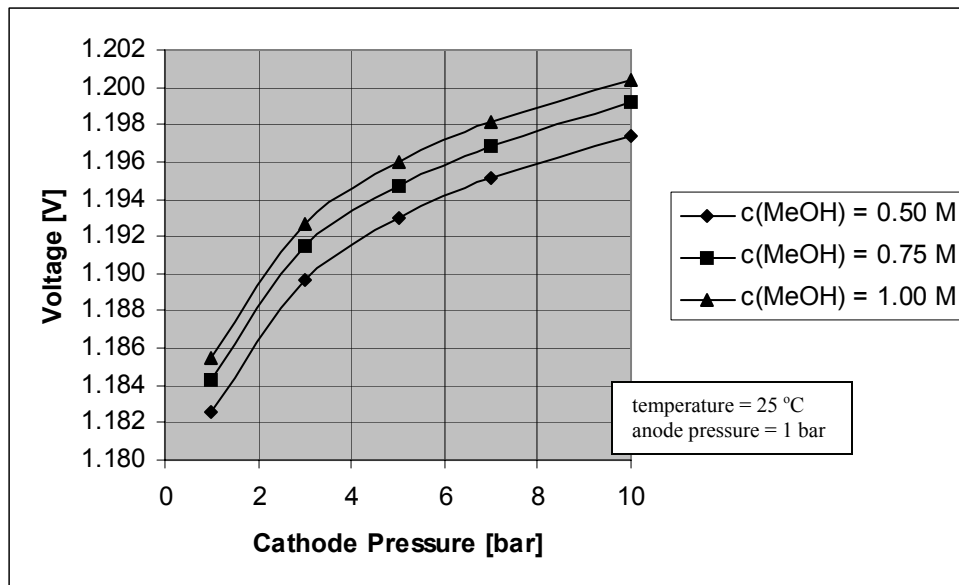


Figure 30. Set 1 - Effect of cathode pressure on the open circuit voltage for the ideal solution and gas behavior (water formation at cathode in liquid phase).

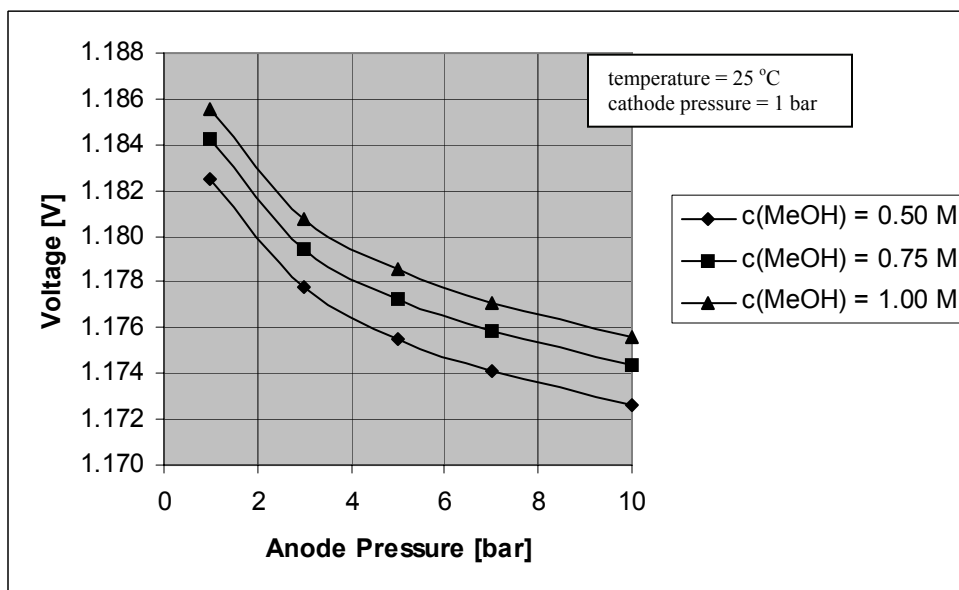


Figure 31. Set 1 - Effect of anode pressure on the open circuit voltage for the ideal solution and gas behavior (water formation at cathode in liquid phase).

Set 2 – Concentration of methanol range from 0.50 to 1.00 M

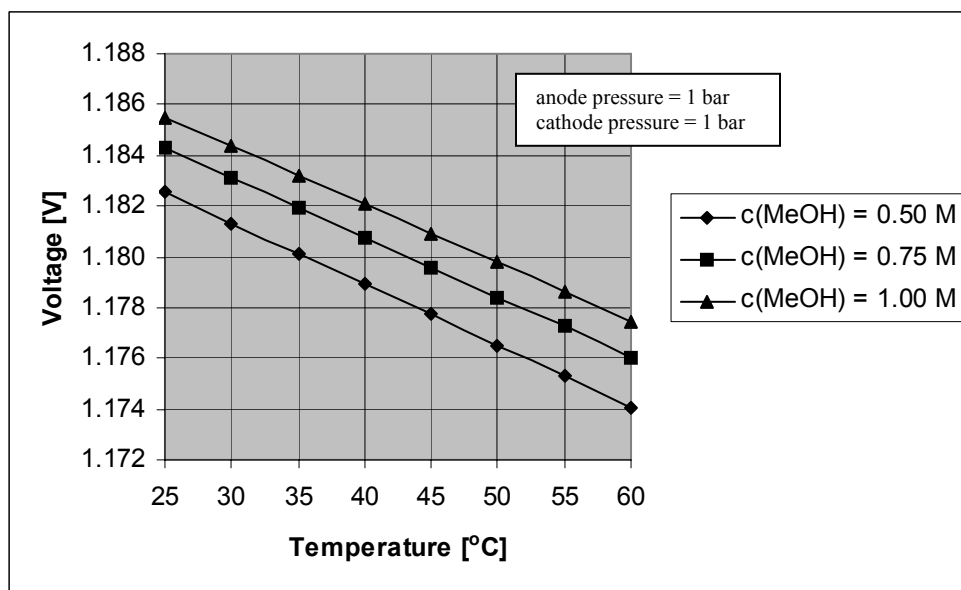


Figure 32. Set 2 - Effect of temperature on the open circuit voltage for the ideal solution and gas behavior (water formation at cathode in liquid phase).

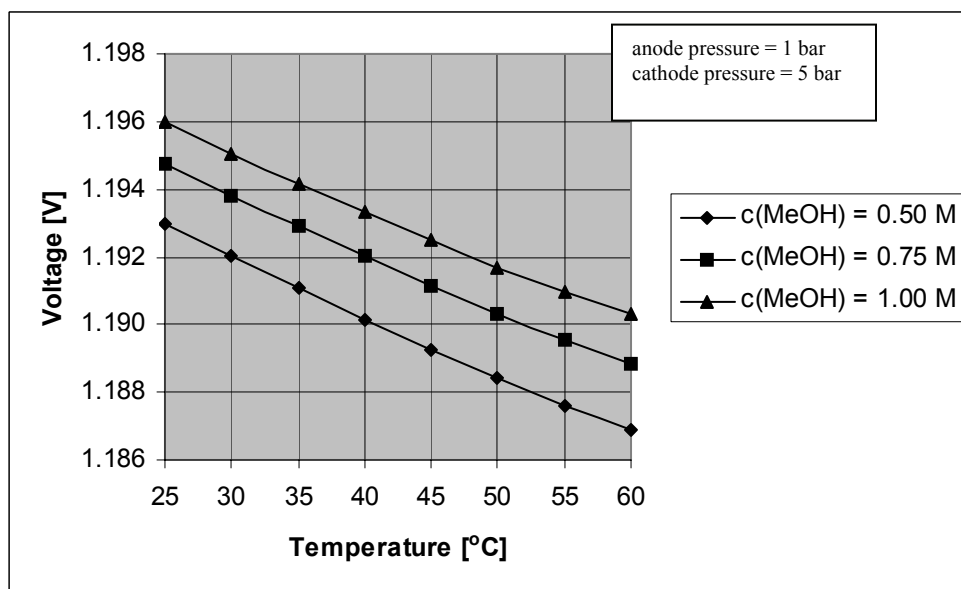


Figure 33. Set 2 - Effect of temperature on the open circuit voltage for the ideal solution and gas behavior (water formation at cathode in liquid phase).

Set 2 – Concentration of methanol range from 0.50 to 1.00 M

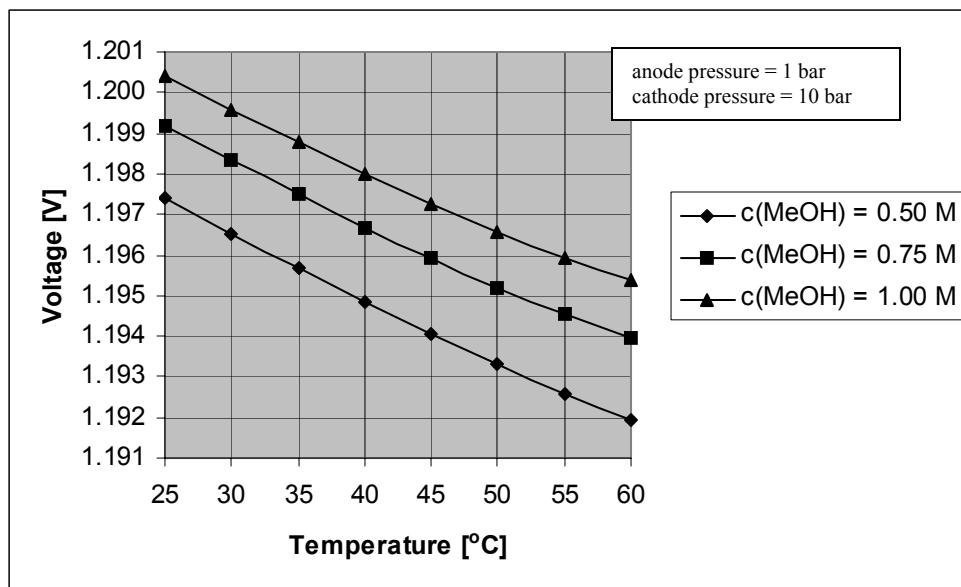


Figure 34. Set 2 - Effect of temperature on the open circuit voltage for the ideal solution and gas behavior (water formation at cathode in liquid phase).

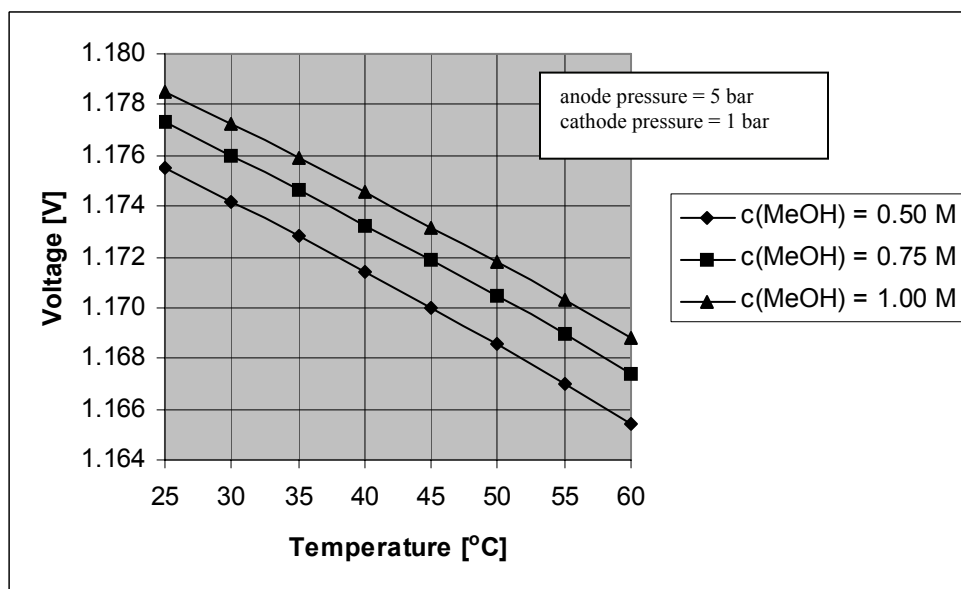


Figure 35. Set 2 - Effect of temperature on the open circuit voltage for the ideal solution and gas behavior (water formation at cathode in liquid phase).

Set 2 – Concentration of methanol range from 0.50 to 1.00 M

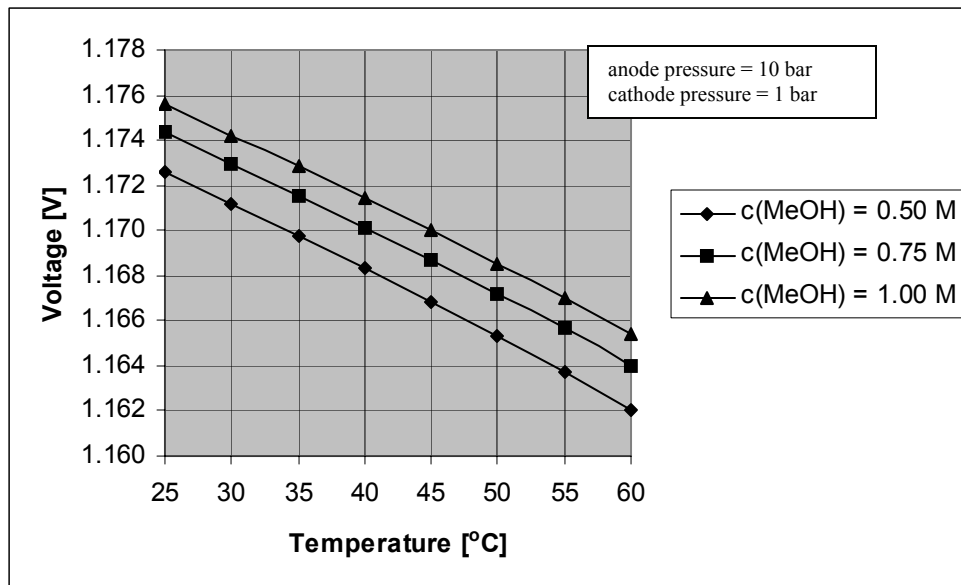


Figure 36. Set 2 - Effect of temperature on the open circuit voltage for the ideal solution and gas behavior (water formation at cathode in liquid phase).

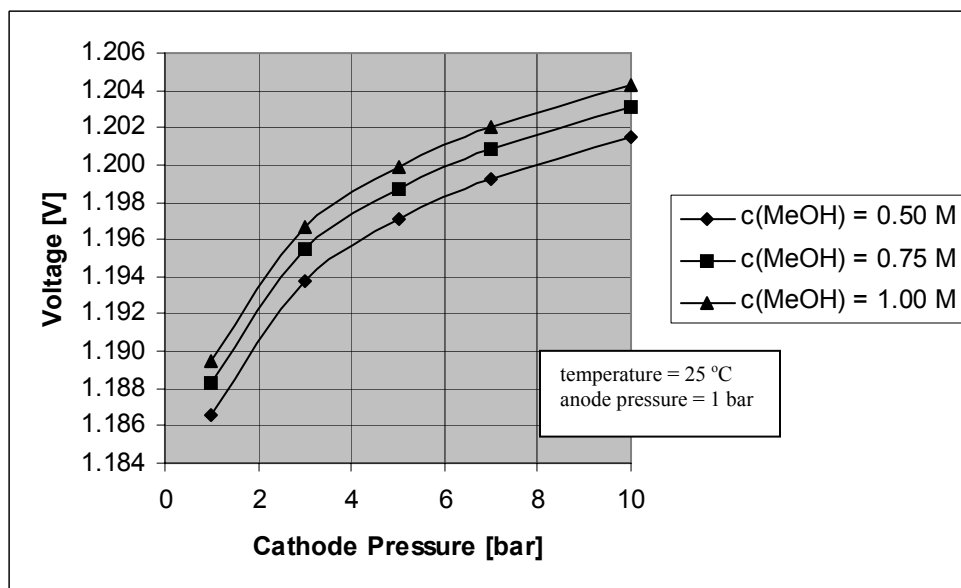


Figure 37. Set 2 - Effect of cathode pressure on the open circuit voltage for the nonideal solution and gas behavior (water formation at cathode in liquid phase).

Set 2 – Concentration of methanol range from 0.50 to 1.00 M

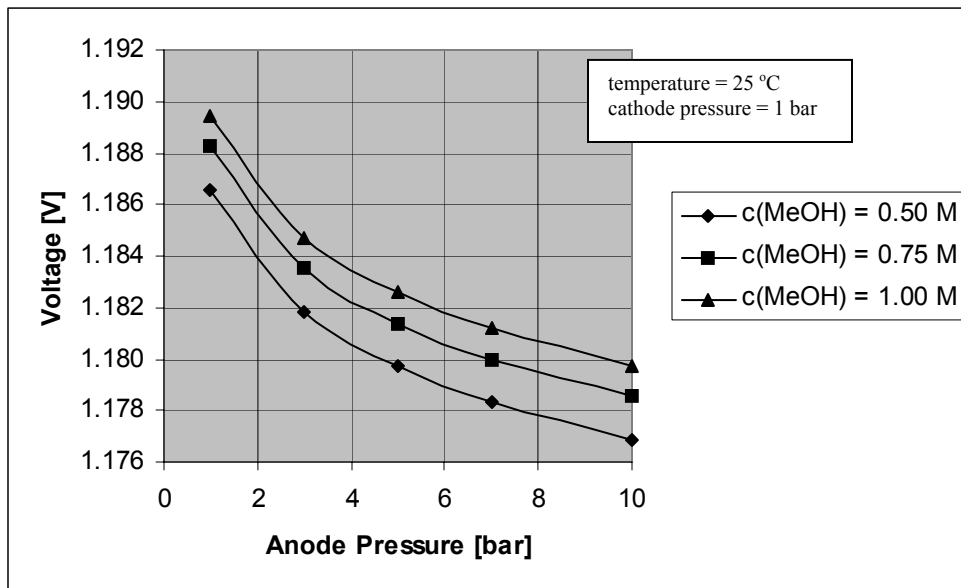


Figure 38. Set 2 - Effect of anode pressure on the open circuit voltage for the nonideal solution and gas behavior (water formation at cathode in liquid phase).

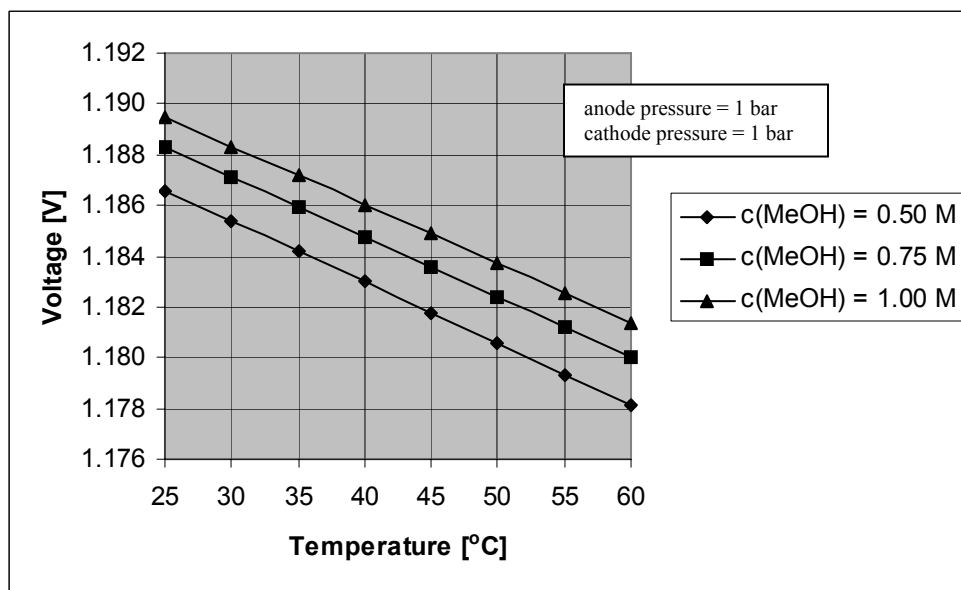


Figure 39. Set 2 - Effect of temperature on the open circuit voltage for the nonideal solution and gas behavior (water formation at cathode in liquid phase).

Set 2 – Concentration of methanol range from 0.50 to 1.00 M

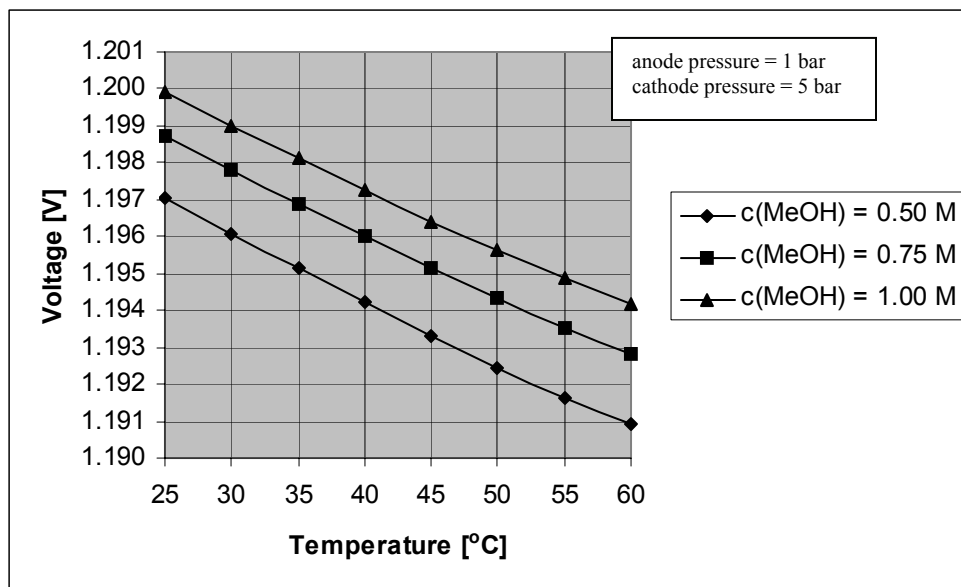


Figure 40. Set 2 - Effect of temperature on the open circuit voltage for the nonideal solution and gas behavior (water formation at cathode in liquid phase).

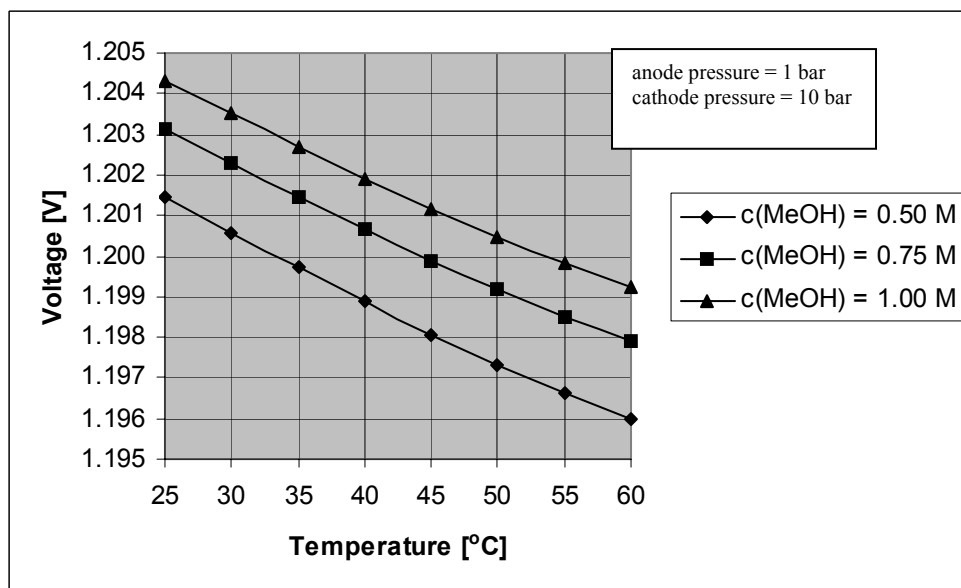


Figure 41. Set 2 - Effect of temperature on the open circuit voltage for the nonideal solution and gas behavior (water formation at cathode in liquid phase).

Set 2 – Concentration of methanol range from 0.50 to 1.00 M

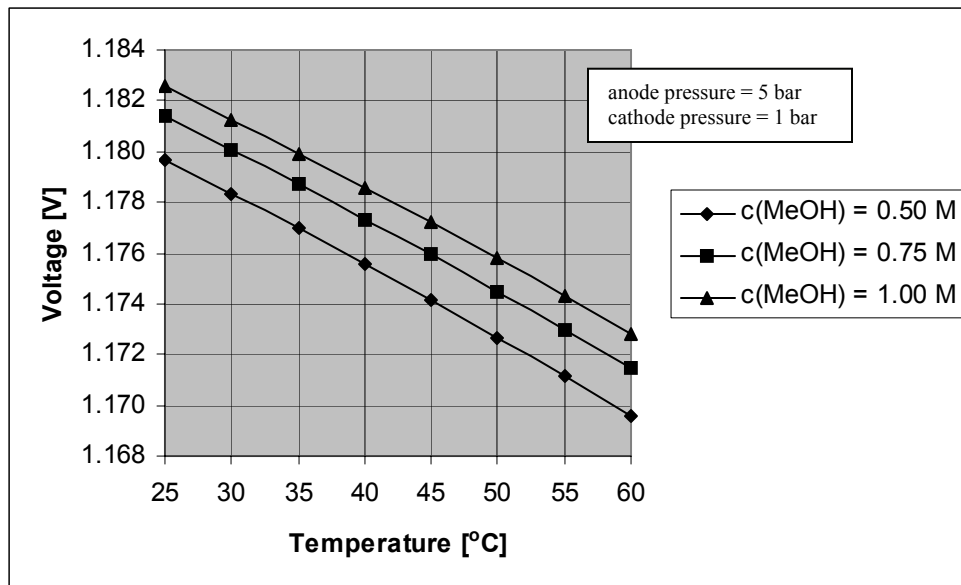


Figure 42. Set 2 - Effect of temperature on the open circuit voltage for the nonideal solution and gas behavior (water formation at cathode in liquid phase).

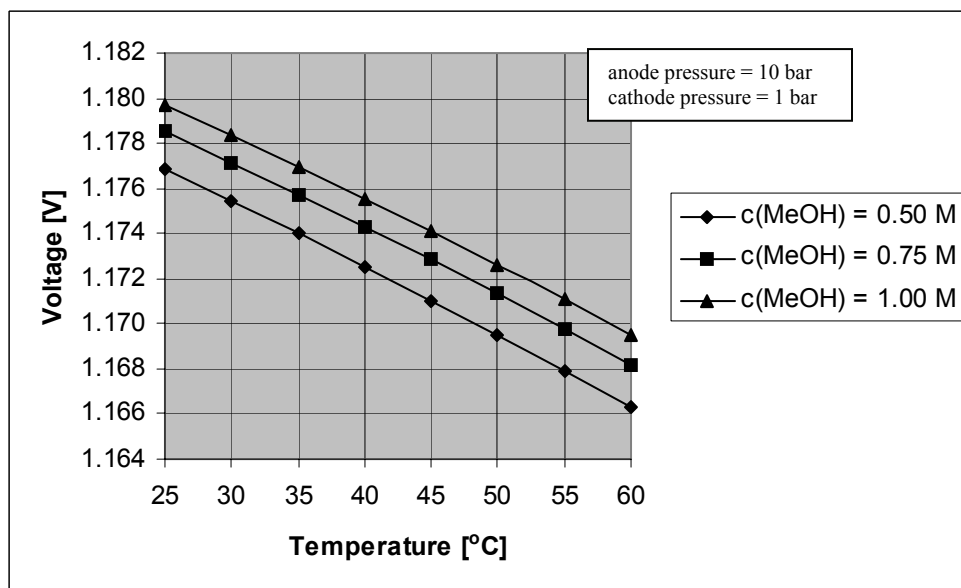


Figure 43. Set 2 - Effect of temperature on the open circuit voltage for the nonideal solution and gas behavior (water formation at cathode in liquid phase).

Set 2 – Concentration of methanol range from 0.50 to 1.00 M

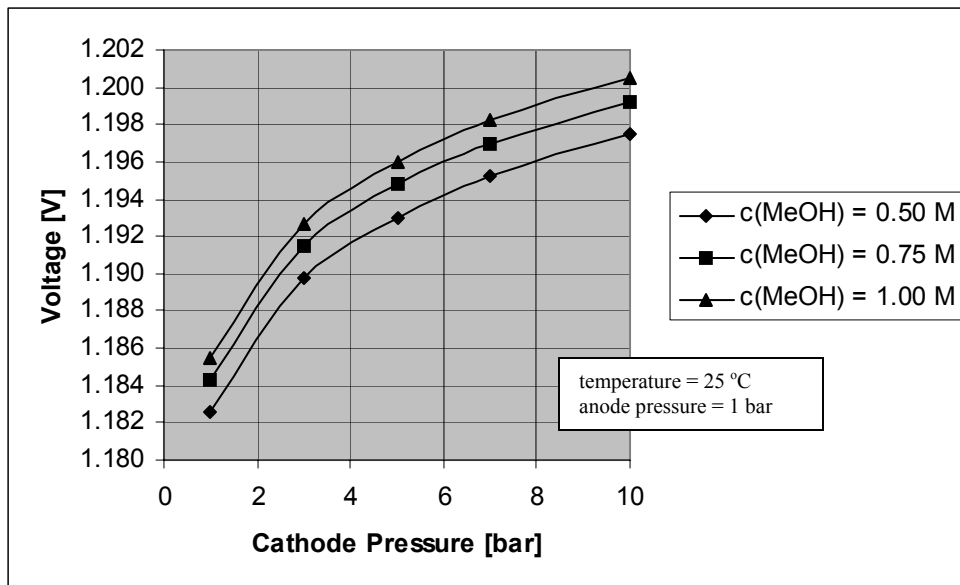


Figure 44. Set 2 - Effect of cathode pressure on the open circuit voltage for the ideal solution and gas behavior (water formation at cathode in vapor phase).

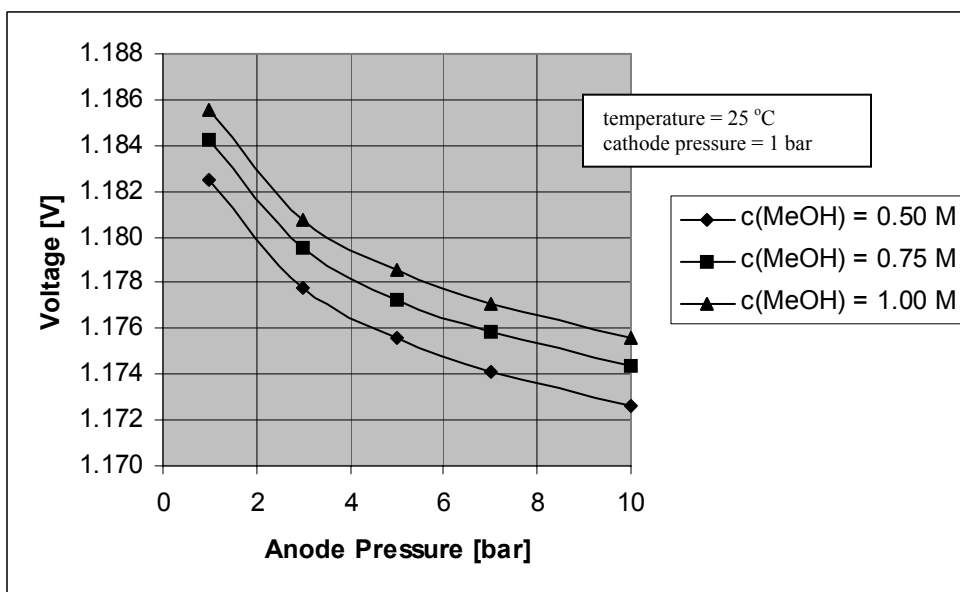


Figure 45. Set 2 - Effect of anode pressure on the open circuit voltage for the ideal solution and gas behavior (water formation at cathode in vapor phase).

Set 2 – Concentration of methanol range from 0.50 to 1.00 M

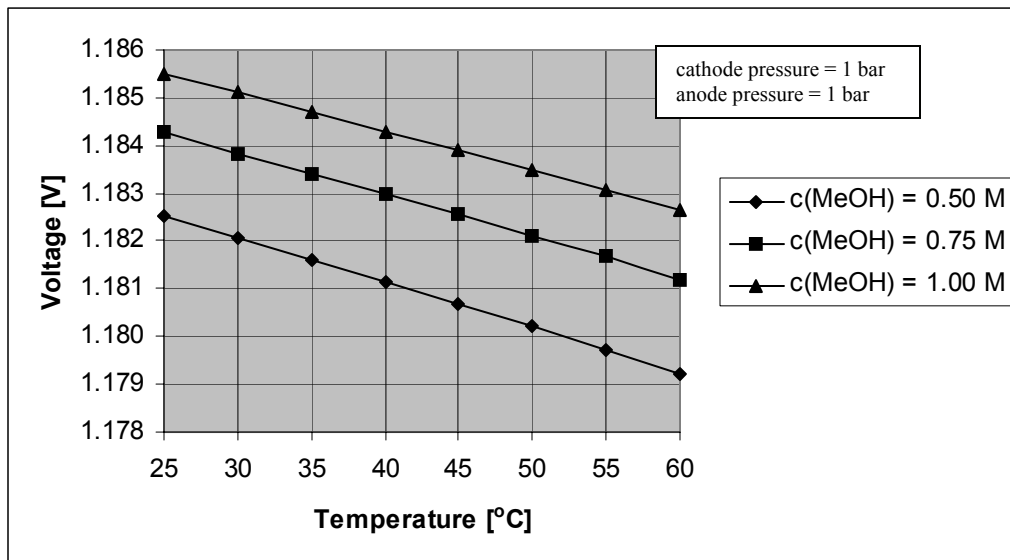


Figure 46. Set 2 - Effect of temperature on the open circuit voltage for the ideal solution and gas behavior (water formation at cathode in vapor phase).

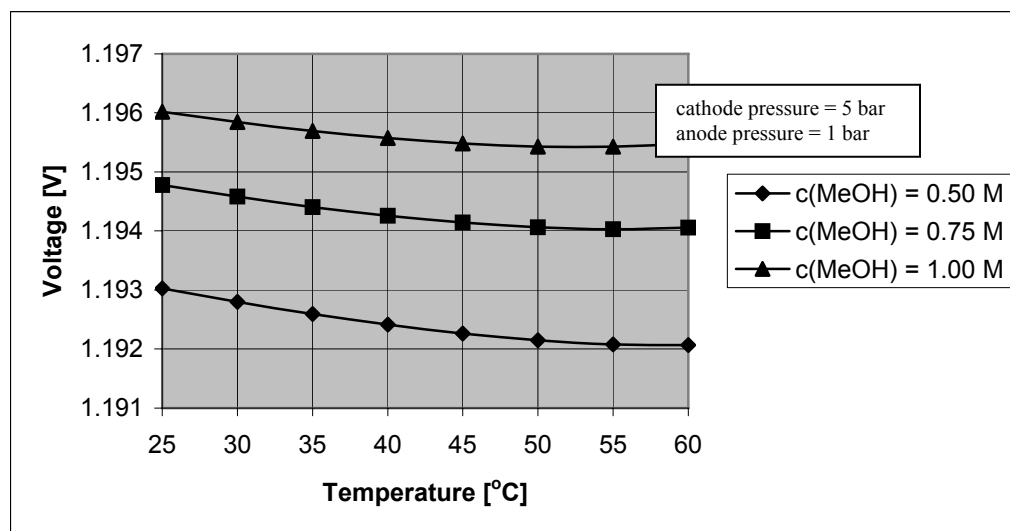


Figure 47. Set 2 - Effect of temperature on the open circuit voltage for the ideal solution and gas behavior (water formation at cathode in vapor phase).

Set 2 – Concentration of methanol range from 0.50 to 1.00 M

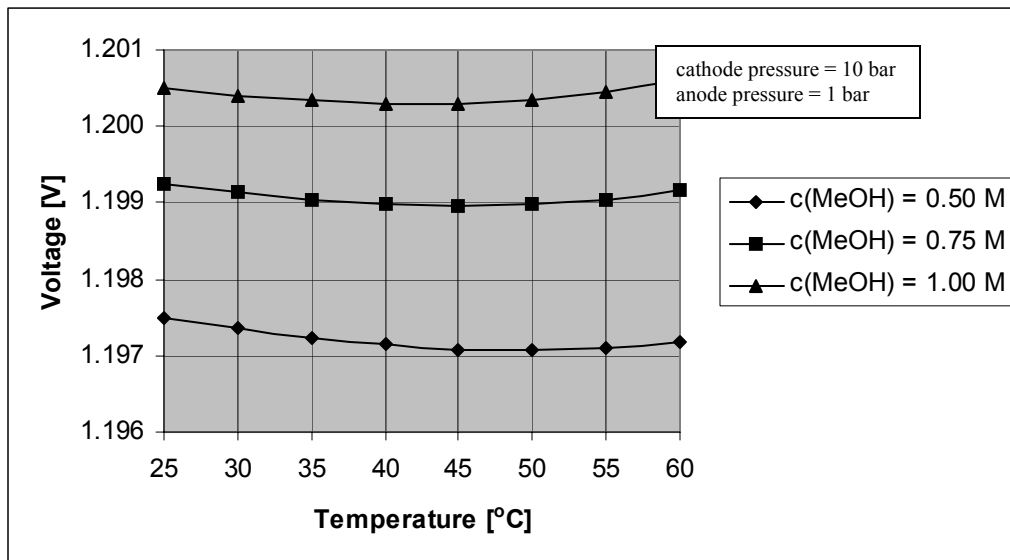


Figure 48. Set 2 - Effect of temperature on the open circuit voltage for the ideal solution and gas behavior (water formation at cathode in vapor phase).

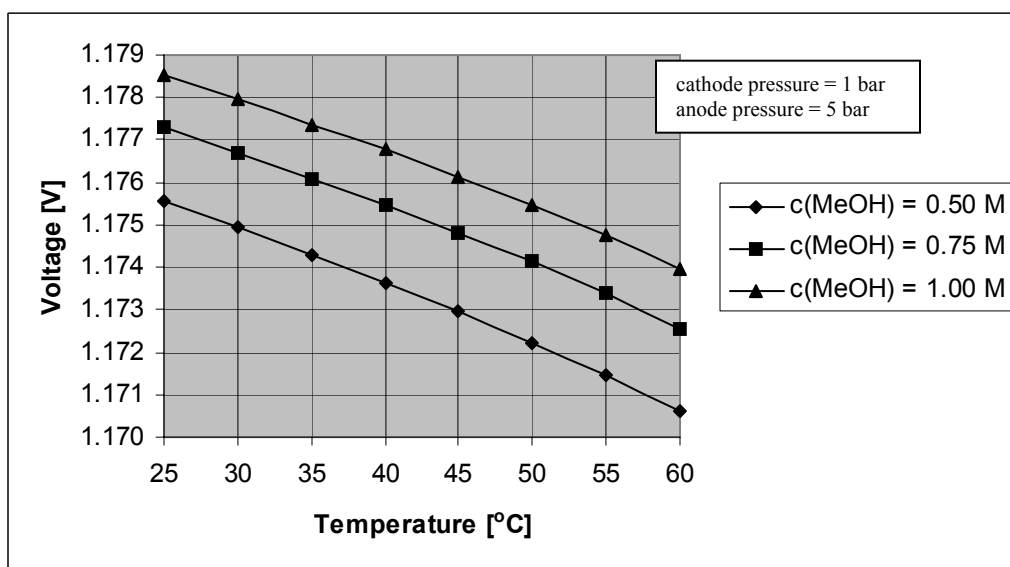


Figure 49. Set 2 - Effect of temperature on the open circuit voltage for the ideal solution and gas behavior (water formation at cathode in vapor phase).

Set 2 – Concentration of methanol range from 0.50 to 1.00 M

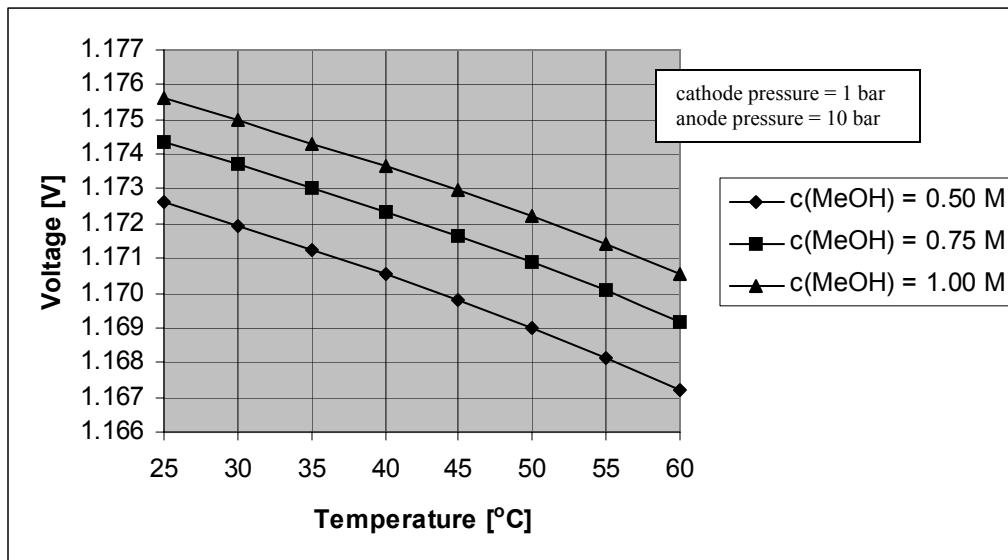


Figure 50. Set 2 - Effect of temperature on the open circuit voltage for the ideal solution and gas behavior (water formation at cathode in vapor phase).

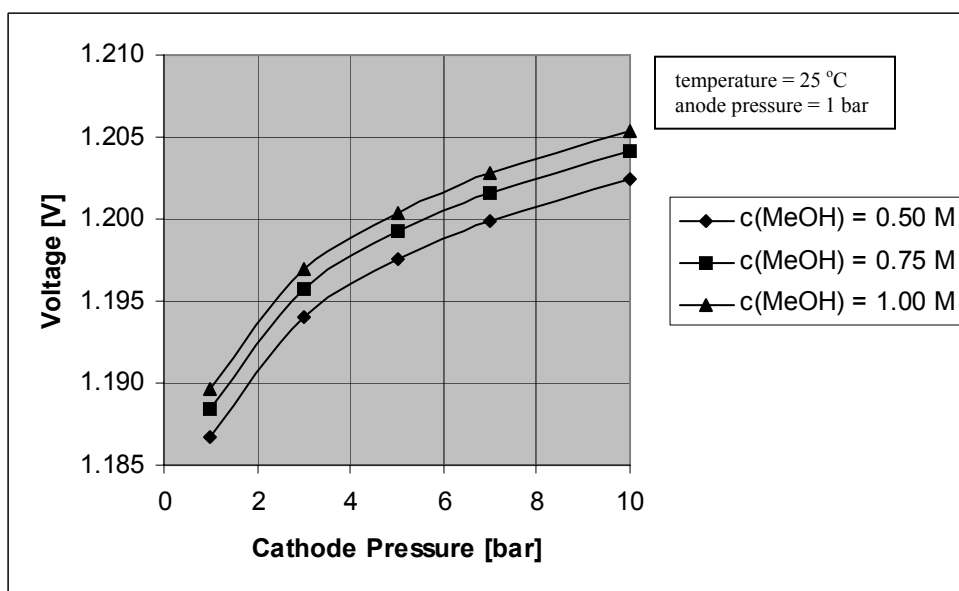


Figure 51. Set 2 - Effect of cathode pressure on the open circuit voltage for the nonideal solution and gas behavior (water formation at cathode in vapor phase).

Set 2 – Concentration of methanol range from 0.50 to 1.00 M

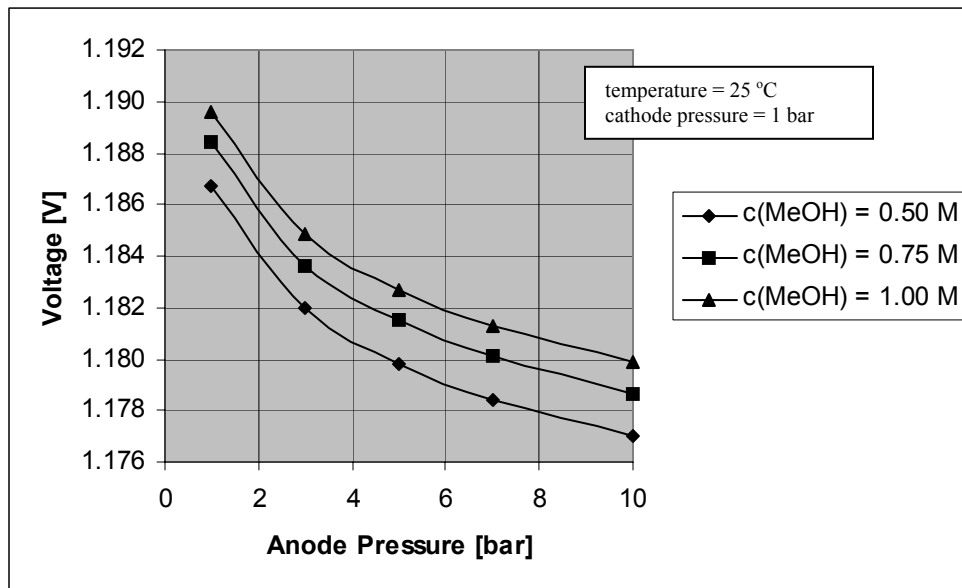


Figure 52. Set 2 - Effect of anode pressure on the open circuit voltage for the nonideal solution and gas behavior (water formation at cathode in vapor phase).

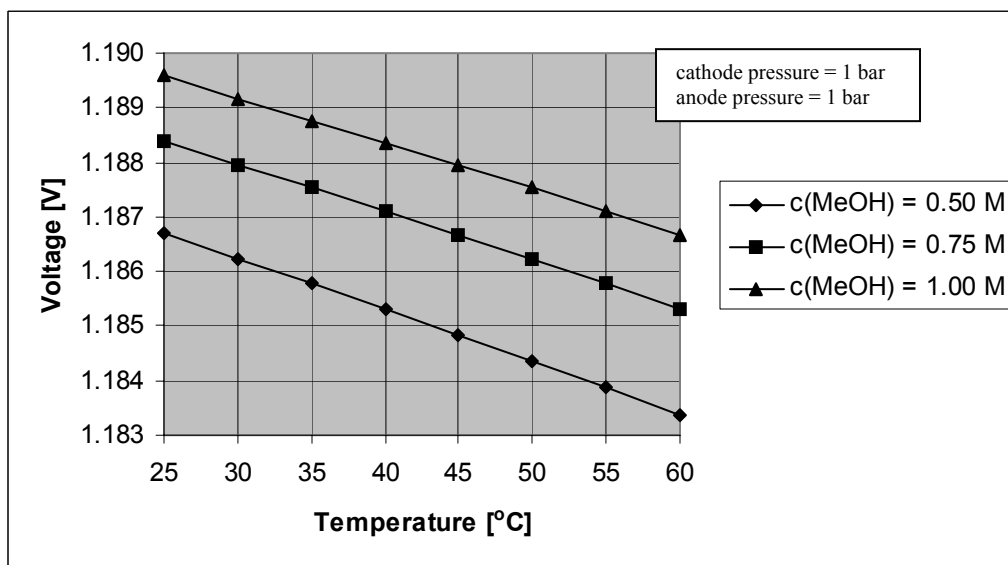


Figure 53. Set 2 - Effect of temperature on the open circuit voltage for the nonideal solution and gas behavior (water formation at cathode in vapor phase).

Set 2 – Concentration of methanol range from 0.50 to 1.00 M

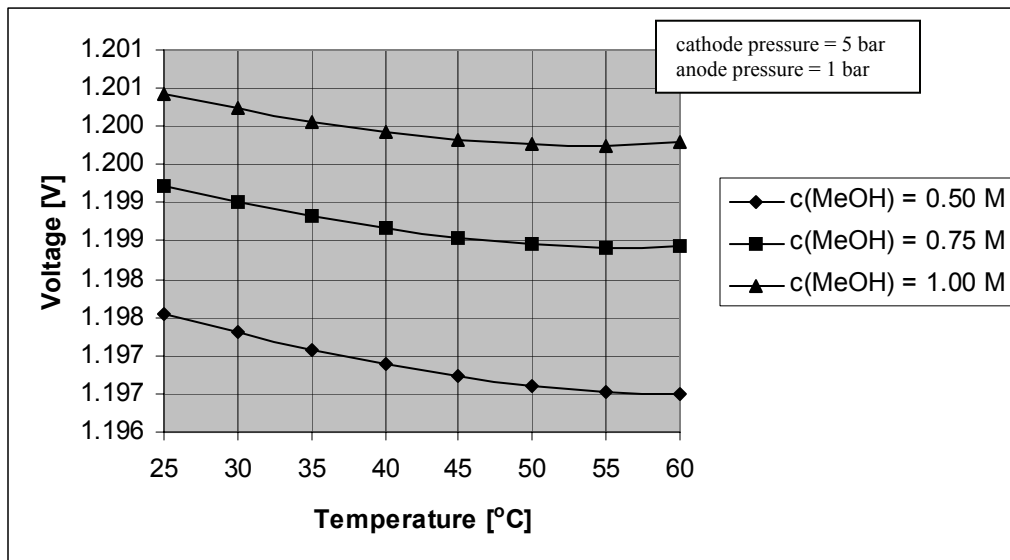


Figure 54. Set 2 - Effect of temperature on the open circuit voltage for the nonideal solution and gas behavior (water formation at cathode in vapor phase).

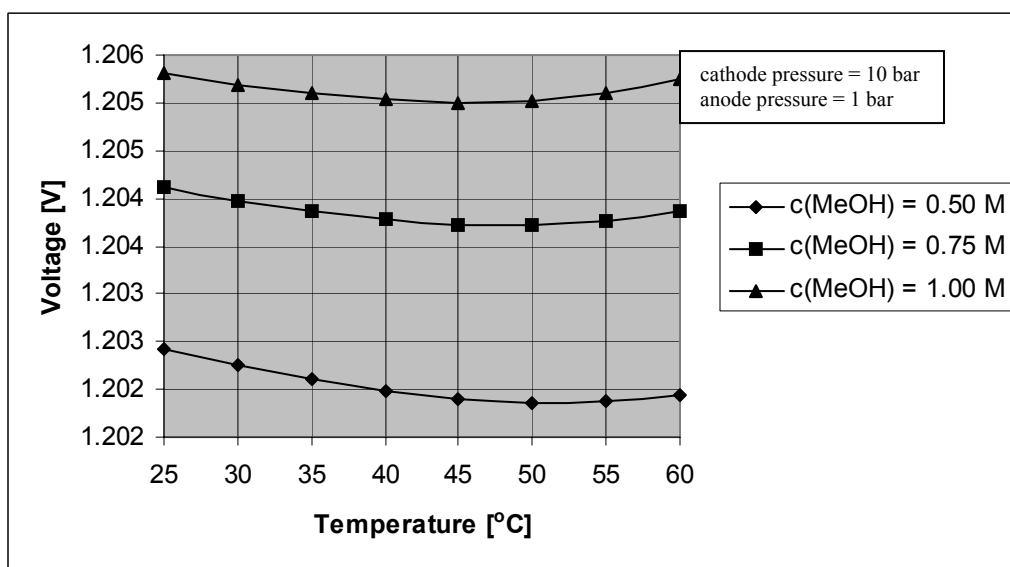


Figure 55. Set 2 - Effect of temperature on the open circuit voltage for the nonideal solution and gas behavior (water formation at cathode in vapor phase).

Set 2 – Concentration of methanol range from 0.50 to 1.00 M

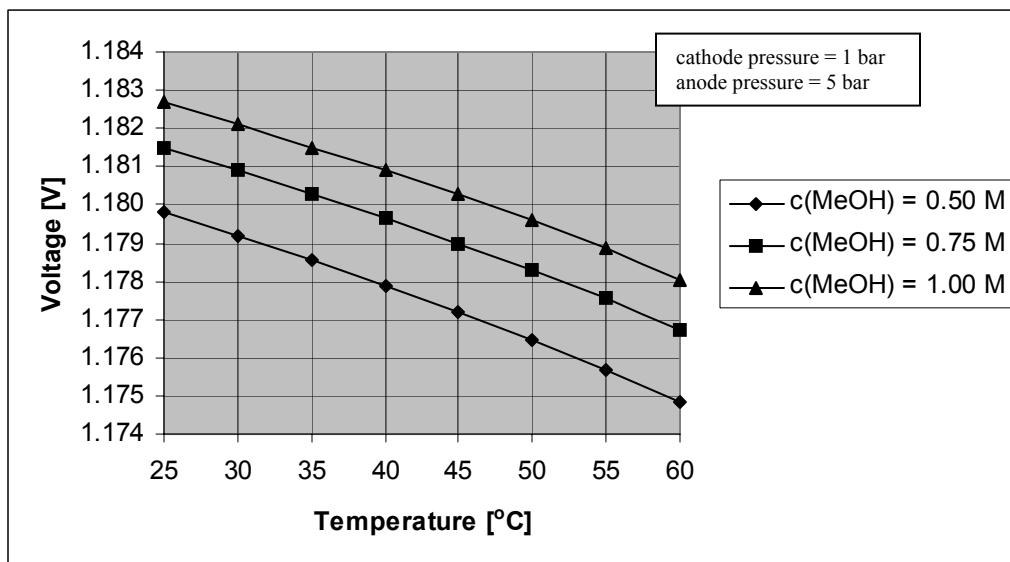


Figure 56. Set 2 - Effect of temperature on the open circuit voltage for the nonideal solution and gas behavior (water formation at cathode in vapor phase).

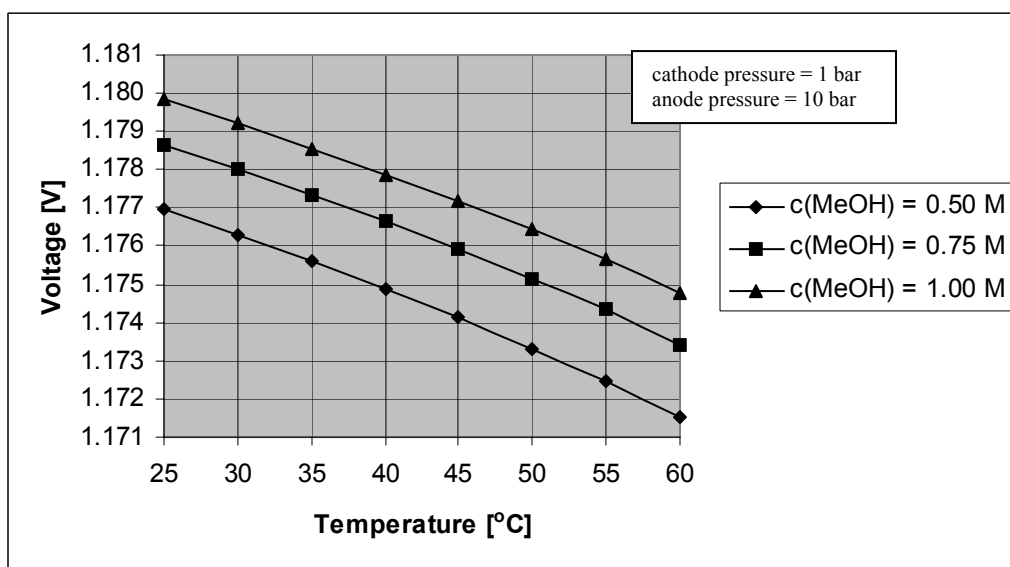


Figure 57. Set 2 - Effect of temperature on the open circuit voltage for the nonideal solution and gas behavior (water formation at cathode in vapor phase).

Set 3 – Concentration of methanol range from 1.00 to 2.00 M

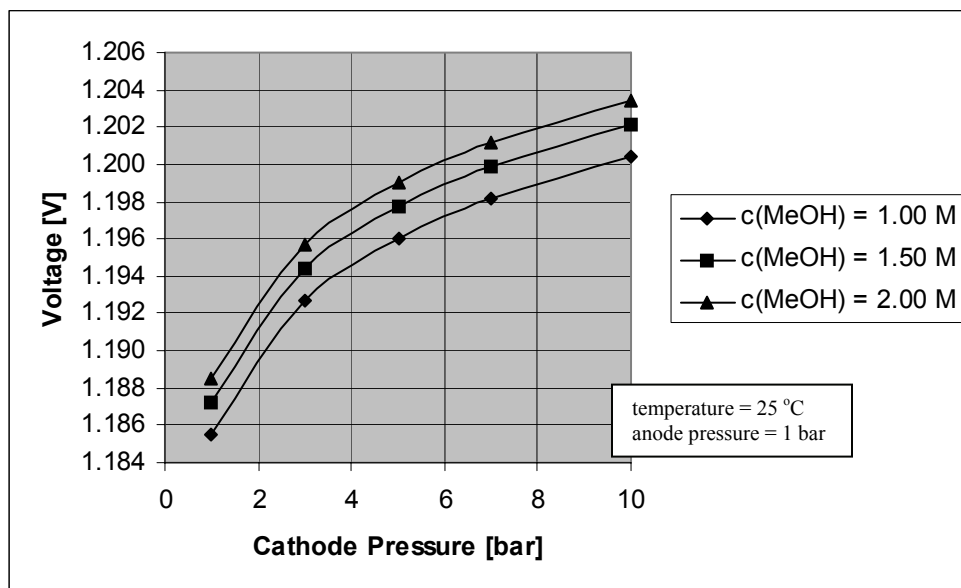


Figure 58. Set 3 - Effect of cathode pressure on the open circuit voltage for the ideal solution and gas behavior (water formation at cathode in liquid phase).

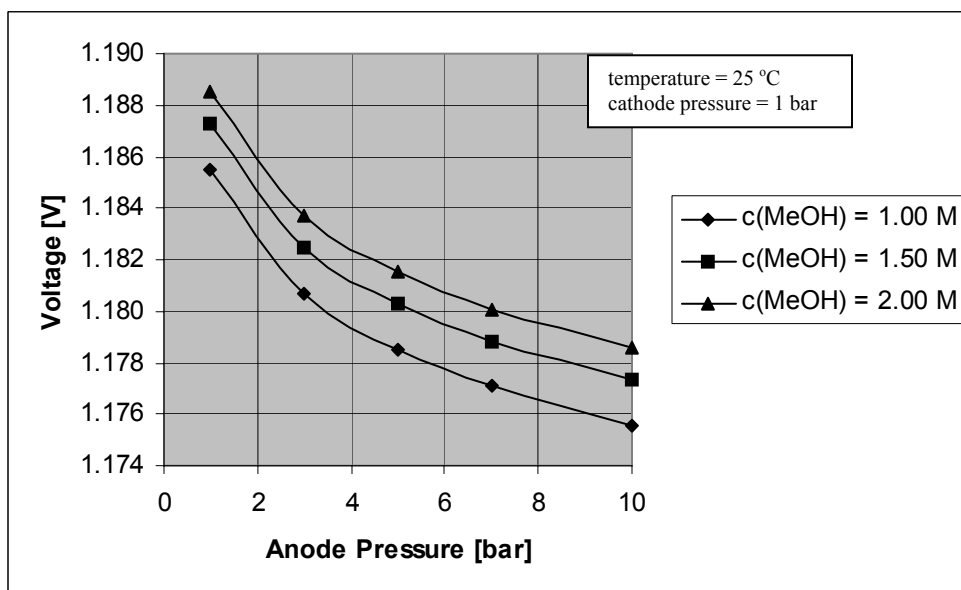


Figure 59. Set 3 - Effect of anode pressure on the open circuit voltage for the ideal solution and gas behavior (water formation at cathode in liquid phase).

Set 3 – Concentration of methanol range from 1.00 to 2.00 M

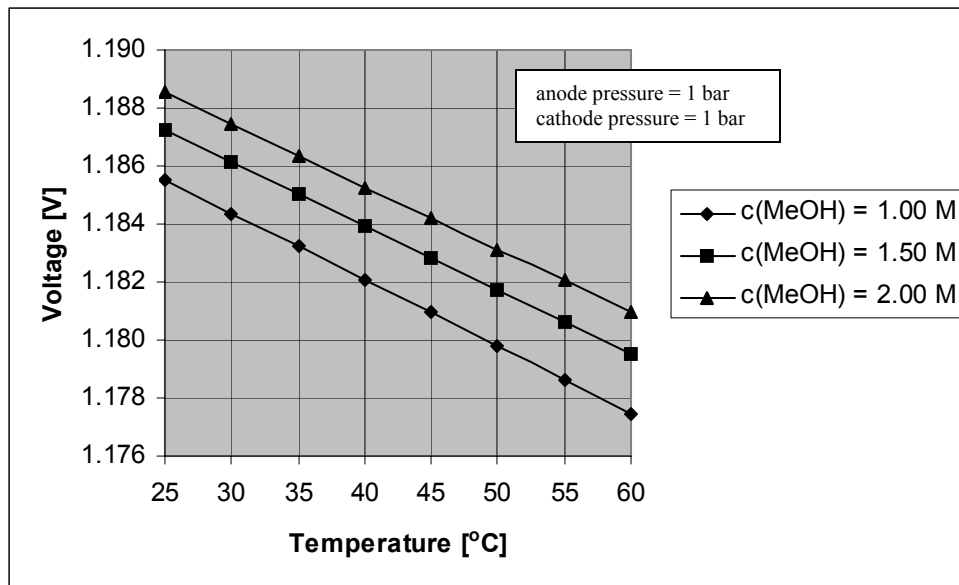


Figure 60. Set 3 - Effect of temperature on the open circuit voltage for the ideal solution and gas behavior (water formation at cathode in liquid phase).

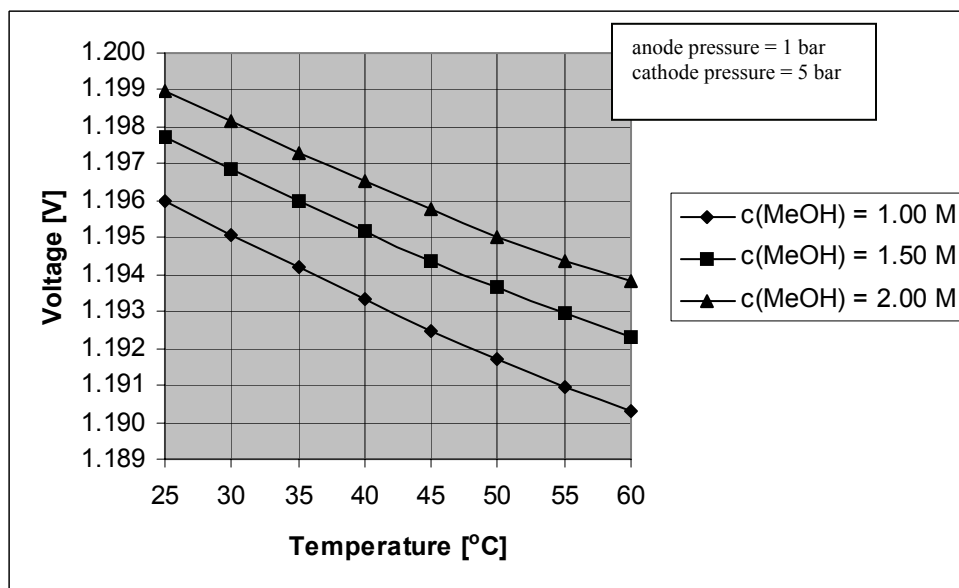


Figure 61. Set 3 - Effect of temperature on the open circuit voltage for the ideal solution and gas behavior (water formation at cathode in liquid phase).

Set 3 – Concentration of methanol range from 1.00 to 2.00 M

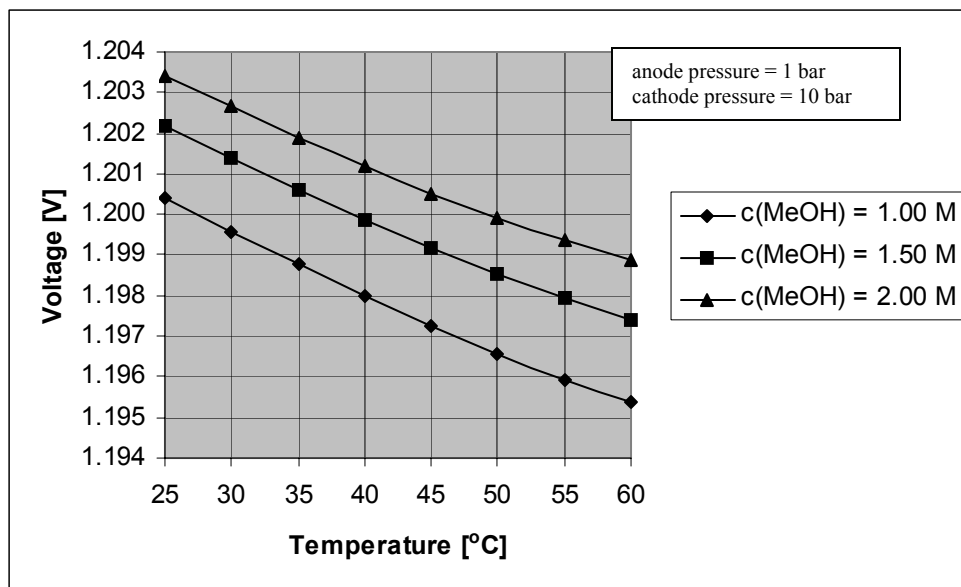


Figure 62. Set 3 - Effect of temperature on the open circuit voltage for the ideal solution and gas behavior (water formation at cathode in liquid phase).

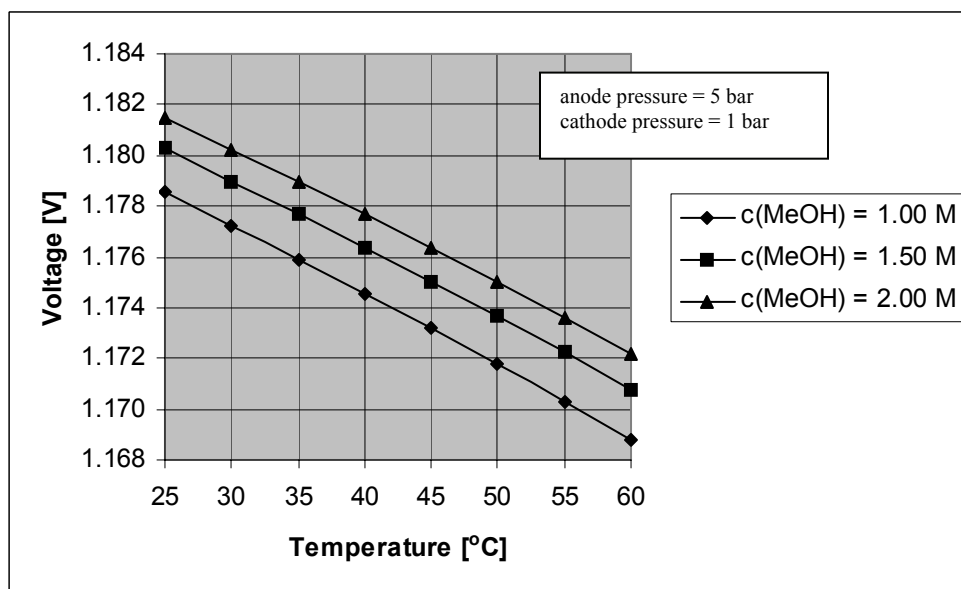


Figure 63. Set 3 - Effect of temperature on the open circuit voltage for the ideal solution and gas behavior (water formation at cathode in liquid phase).

Set 3 – Concentration of methanol range from 1.00 to 2.00 M

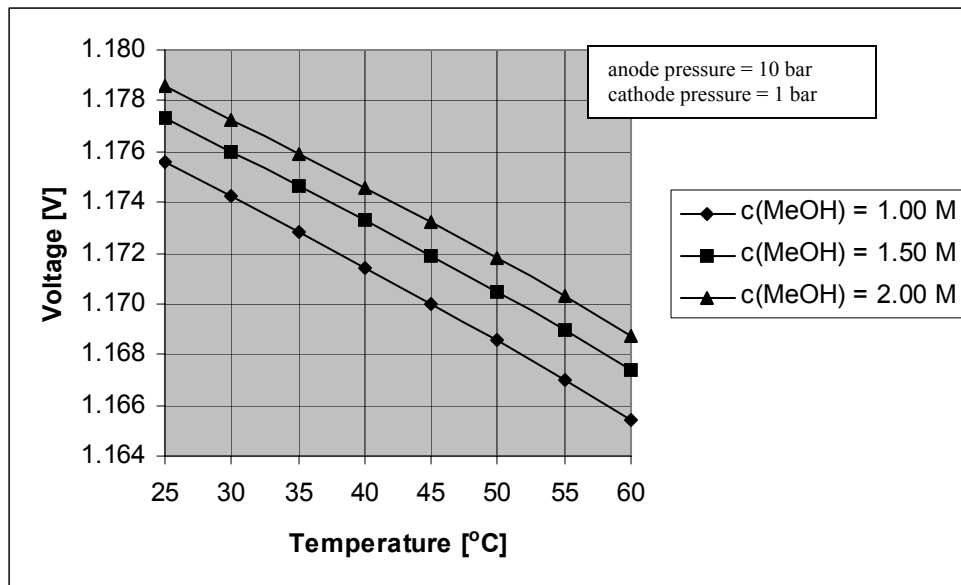


Figure 64. Set 3 - Effect of temperature on the open circuit voltage for the ideal solution and gas behavior (water formation at cathode in liquid phase).

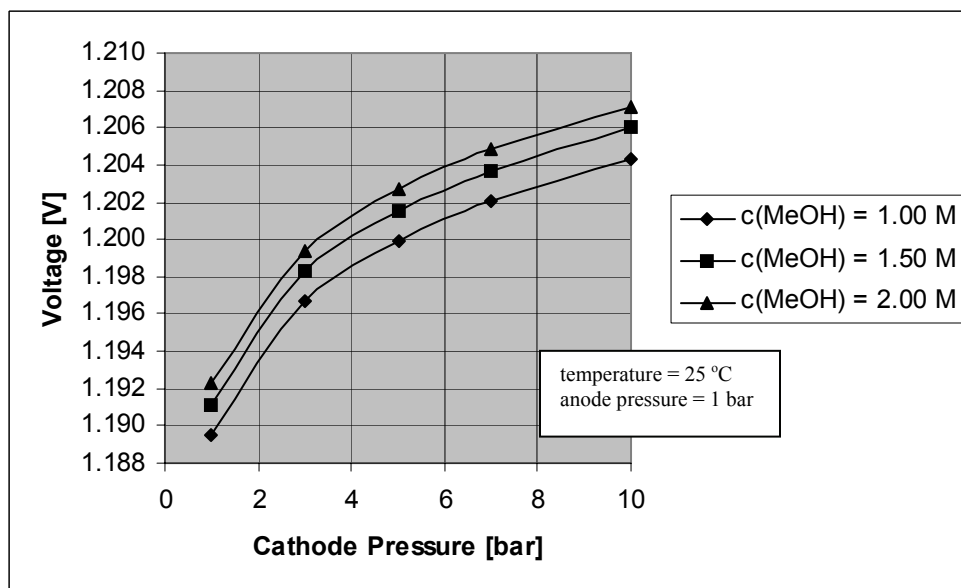


Figure 65. Set 3 - Effect of cathode pressure on the open circuit voltage for the nonideal solution and gas behavior (water formation at cathode in liquid phase).

Set 3 – Concentration of methanol range from 1.00 to 2.00 M

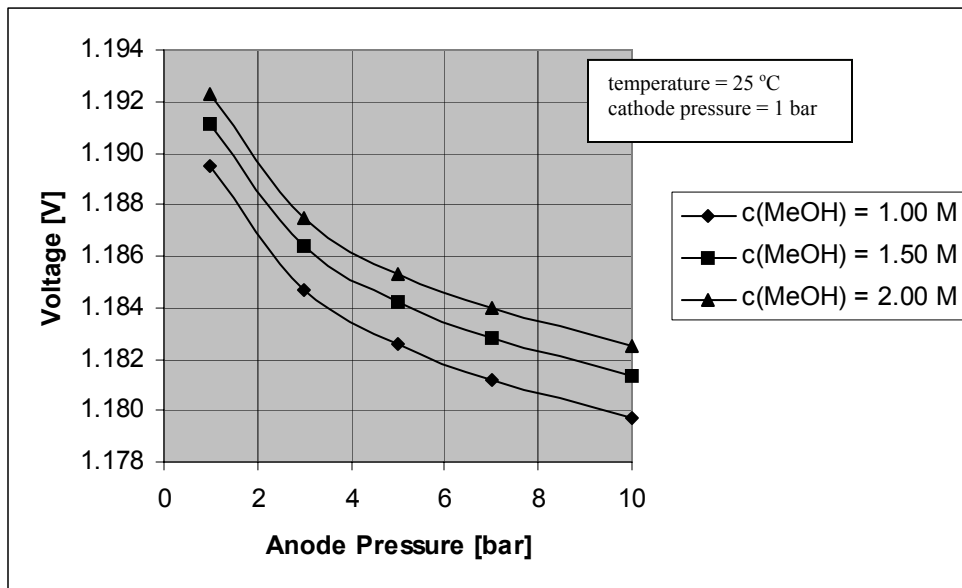


Figure 66. Set 3 - Effect of anode pressure on the open circuit voltage for the nonideal solution and gas behavior (water formation at cathode in liquid phase).

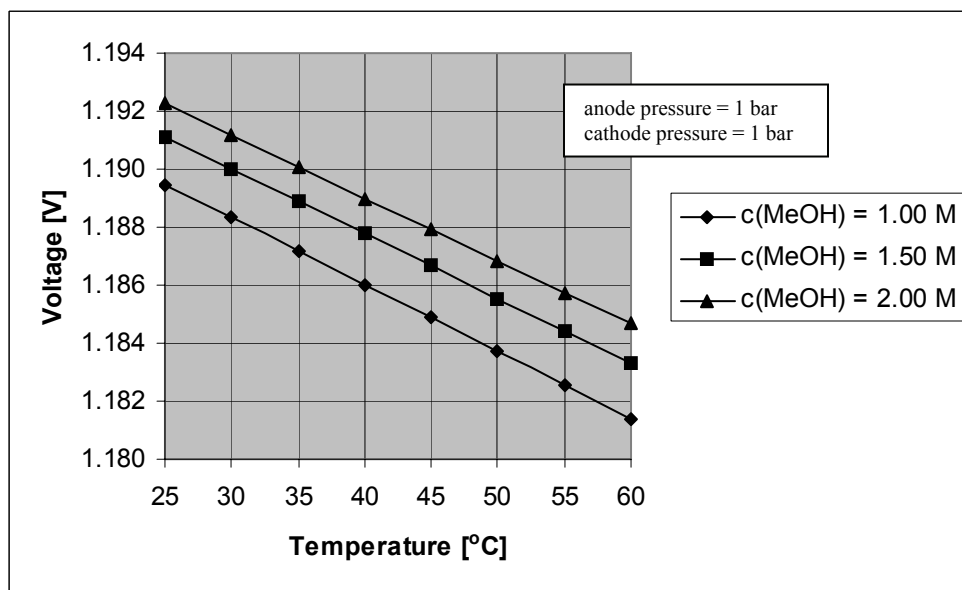


Figure 67. Set 3 - Effect of temperature on the open circuit voltage for the nonideal solution and gas behavior (water formation at cathode in liquid phase).

Set 3 – Concentration of methanol range from 1.00 to 2.00 M

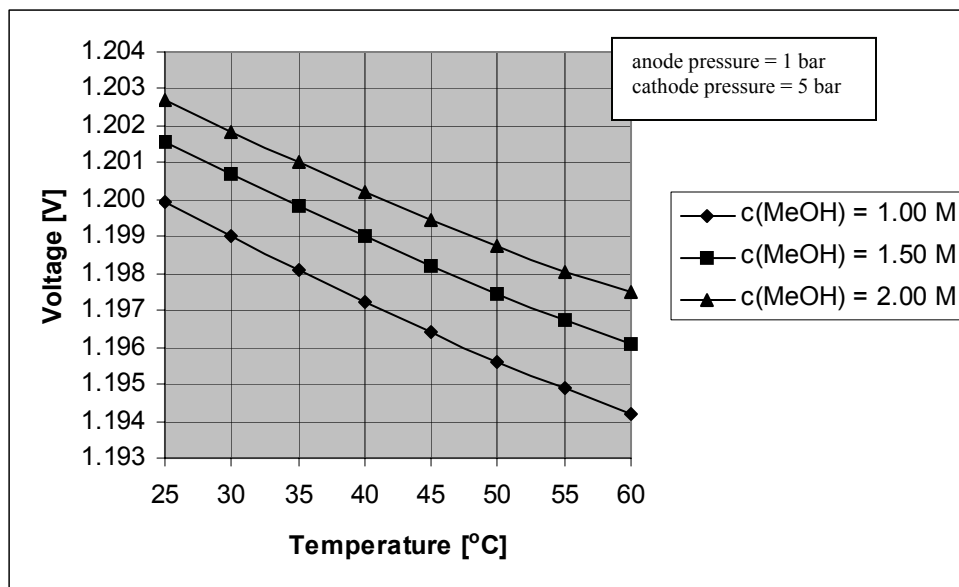


Figure 68. Set 3 - Effect of temperature on the open circuit voltage for the nonideal solution and gas behavior (water formation at cathode in liquid phase).

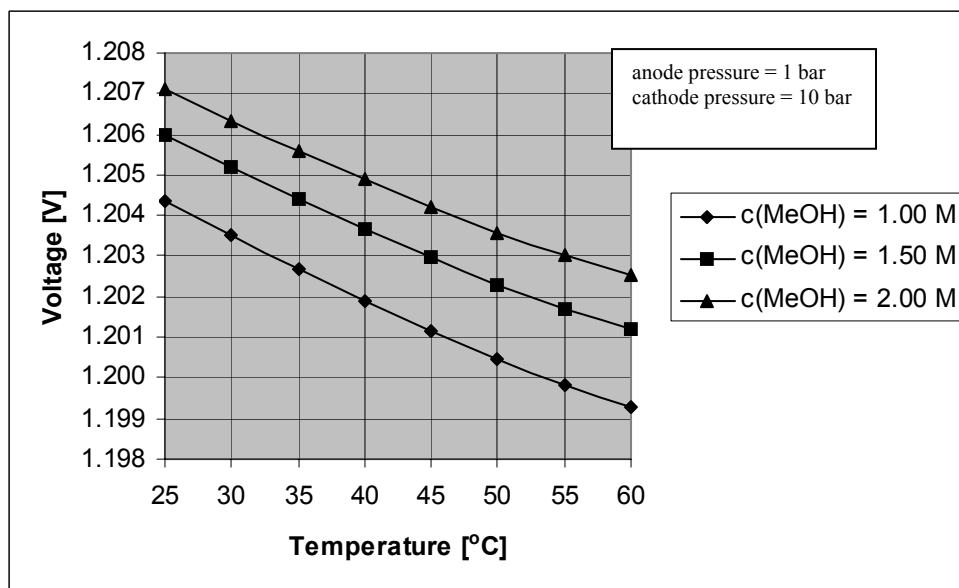


Figure 69. Set 3 - Effect of temperature on the open circuit voltage for the nonideal solution and gas behavior (water formation at cathode in liquid phase).

Set 3 – Concentration of methanol range from 1.00 to 2.00 M

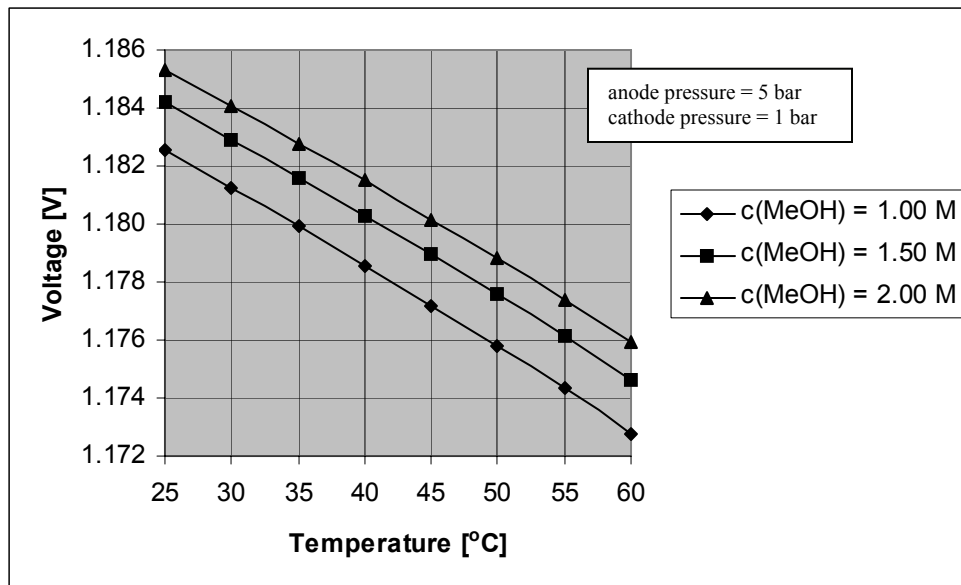


Figure 70. Set 3 - Effect of temperature on the open circuit voltage for the nonideal solution and gas behavior (water formation at cathode in liquid phase).

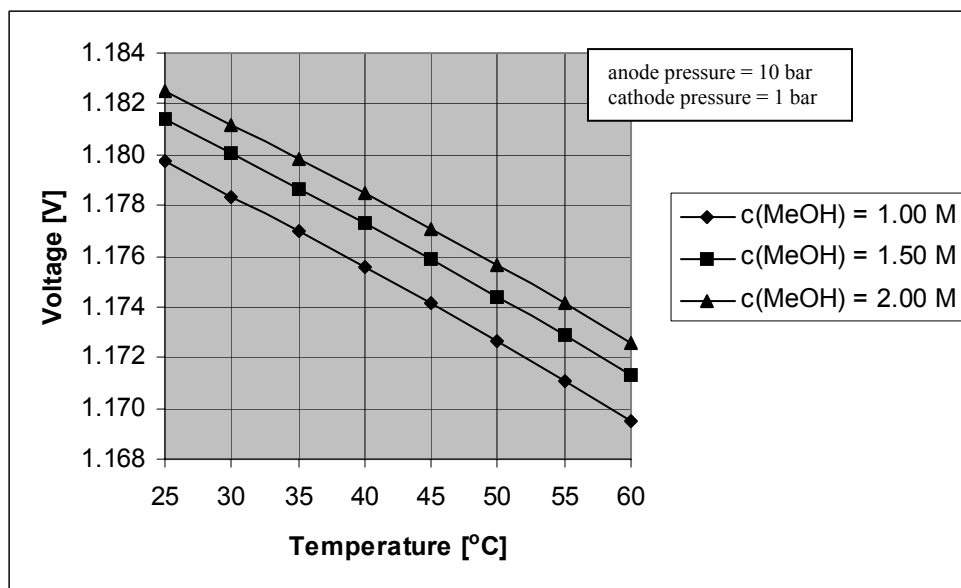


Figure 71. Set 3 - Effect of temperature on the open circuit voltage for the nonideal solution and gas behavior (water formation at cathode in liquid phase).

Set 3 – Concentration of methanol range from 1.00 to 2.00 M

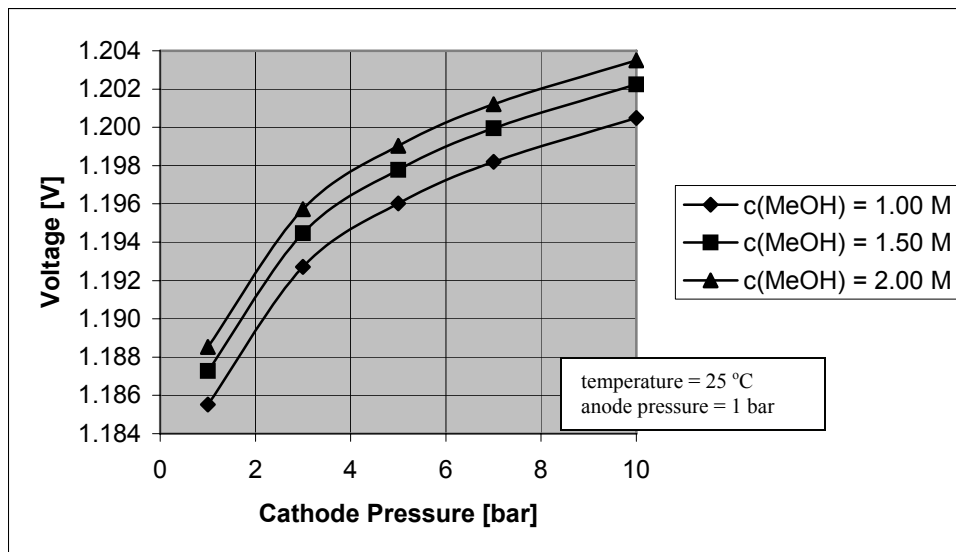


Figure 72. Set 3 - Effect of cathode pressure on the open circuit voltage for the ideal solution and gas behavior (water formation at cathode in vapor phase).

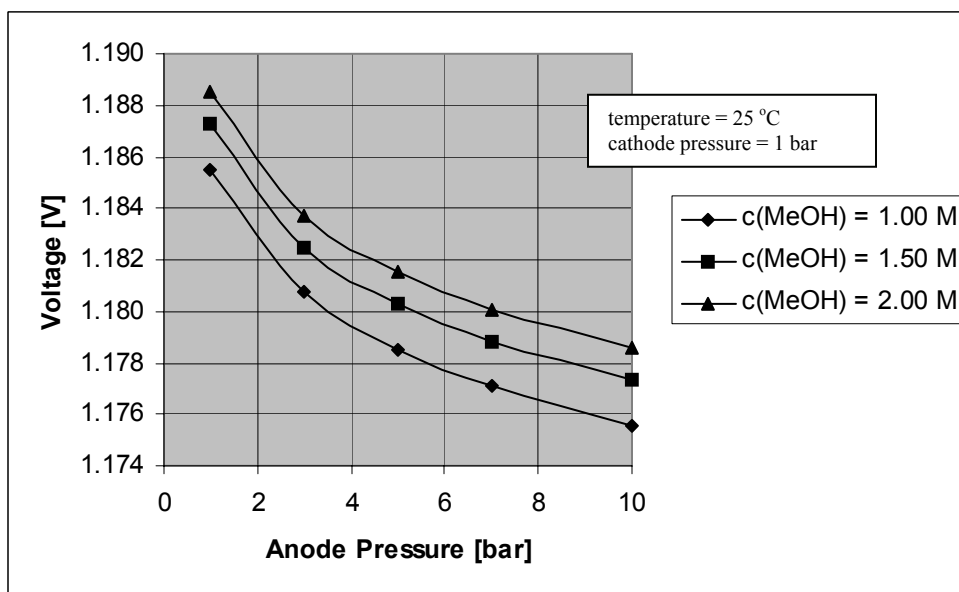


Figure 73. Set 3 - Effect of anode pressure on the open circuit voltage for the ideal solution and gas behavior (water formation at cathode in vapor phase).

Set 3 – Concentration of methanol range from 1.00 to 2.00 M

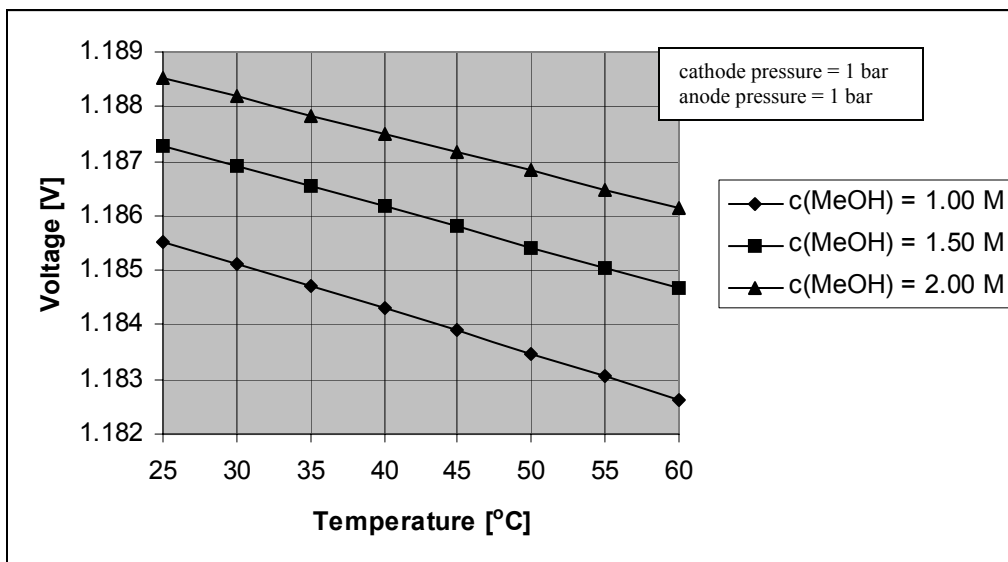


Figure 74. Set 3 - Effect of temperature on the open circuit voltage for the ideal solution and gas behavior (water formation at cathode in vapor phase).

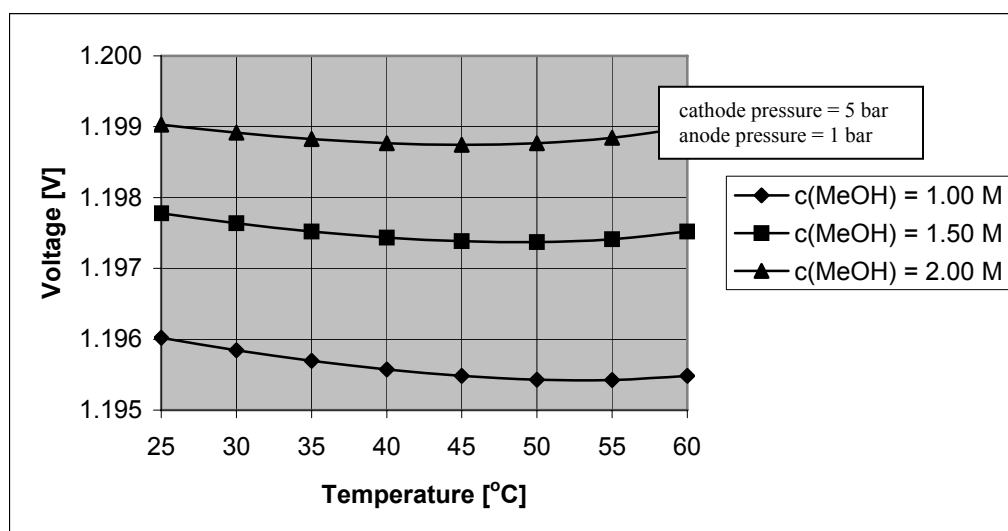


Figure 75. Set 3 - Effect of temperature on the open circuit voltage for the ideal solution and gas behavior (water formation at cathode in vapor phase).

Set 3 – Concentration of methanol range from 1.00 to 2.00 M

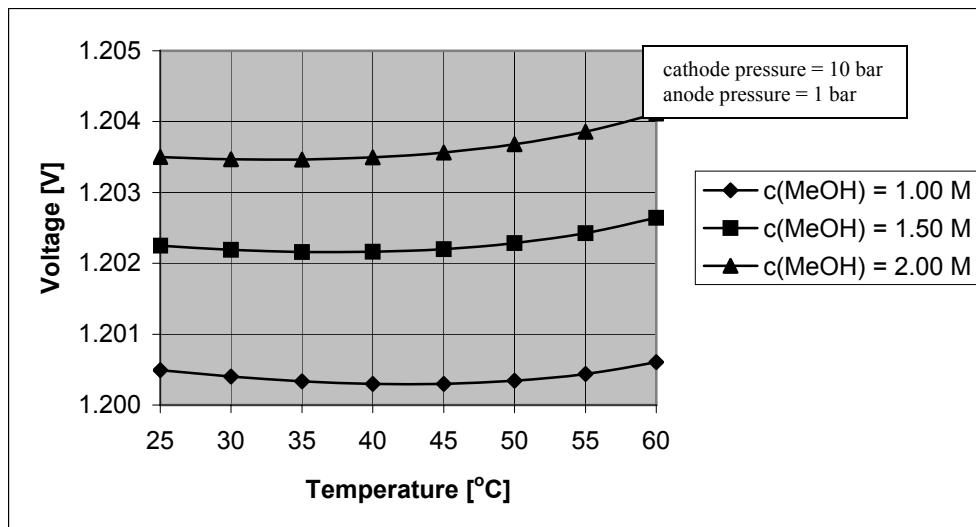


Figure 76. Set 3 - Effect of temperature on the open circuit voltage for the ideal solution and gas behavior (water formation at cathode in vapor phase).

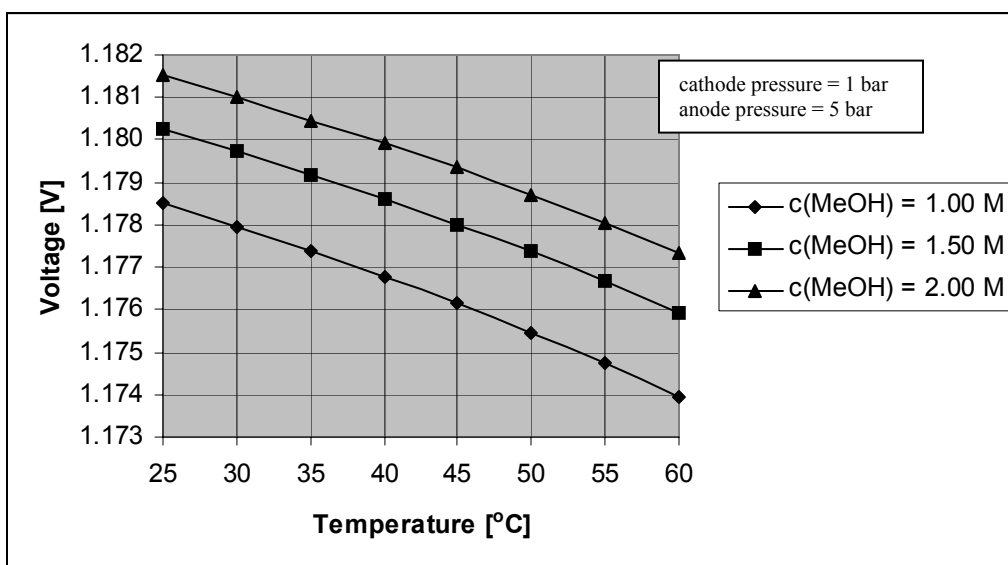


Figure 77. Set 3 - Effect of temperature on the open circuit voltage for the ideal solution and gas behavior (water formation at cathode in vapor phase).

Set 3 – Concentration of methanol range from 1.00 to 2.00 M

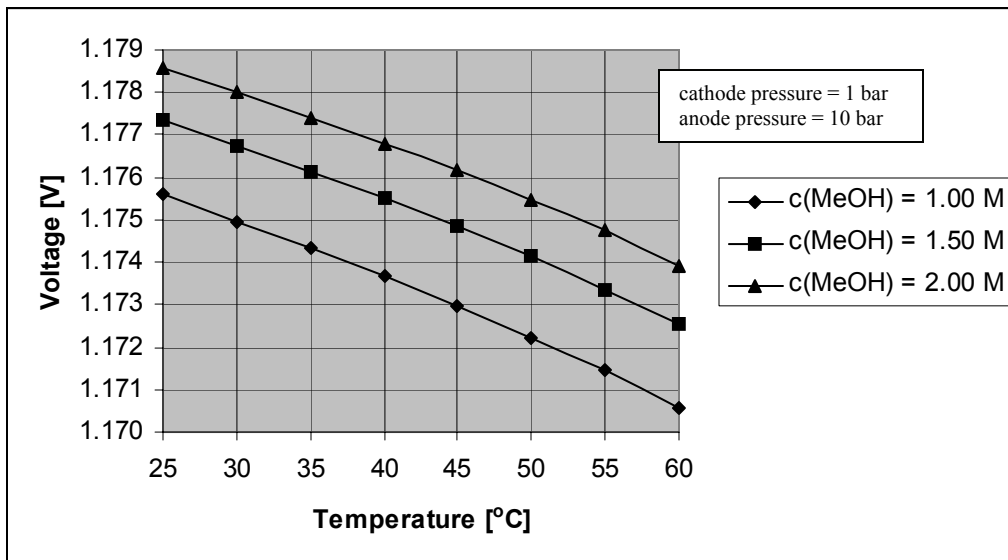


Figure 78. Set 3 - Effect of temperature on the open circuit voltage for the ideal solution and gas behavior (water formation at cathode in vapor phase).

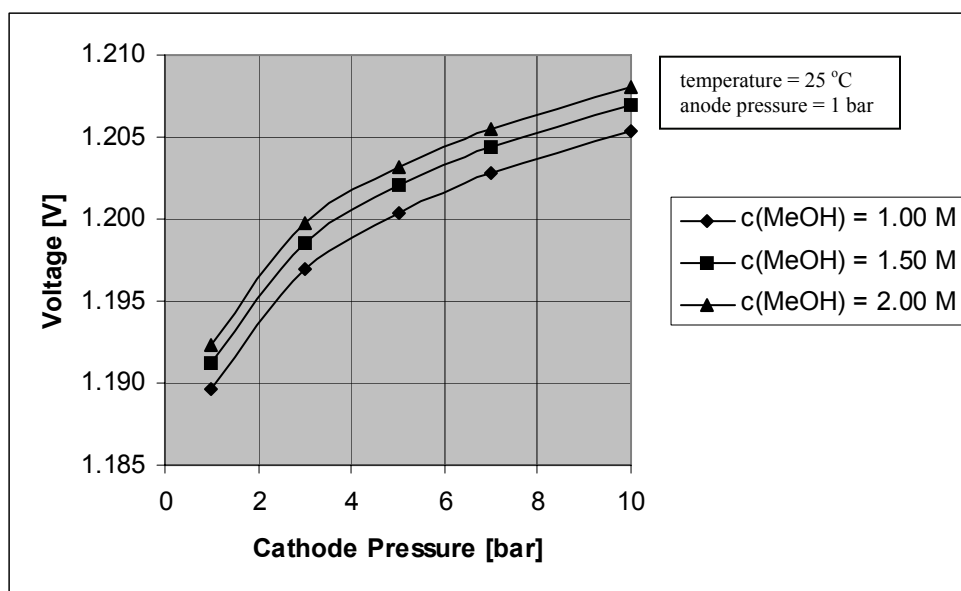


Figure 79. Set 3 - Effect of cathode pressure on the open circuit voltage for the nonideal solution and gas behavior (water formation at cathode in vapor phase).

Set 3 – Concentration of methanol range from 1.00 to 2.00 M

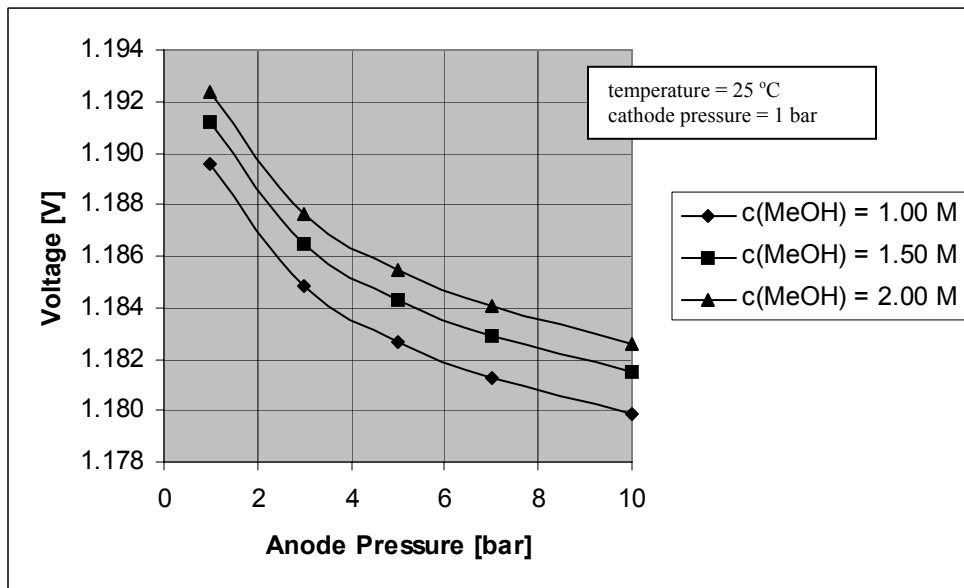


Figure 80. Set 3 - Effect of anode pressure on the open circuit voltage for the nonideal solution and gas behavior (water formation at cathode in vapor phase).

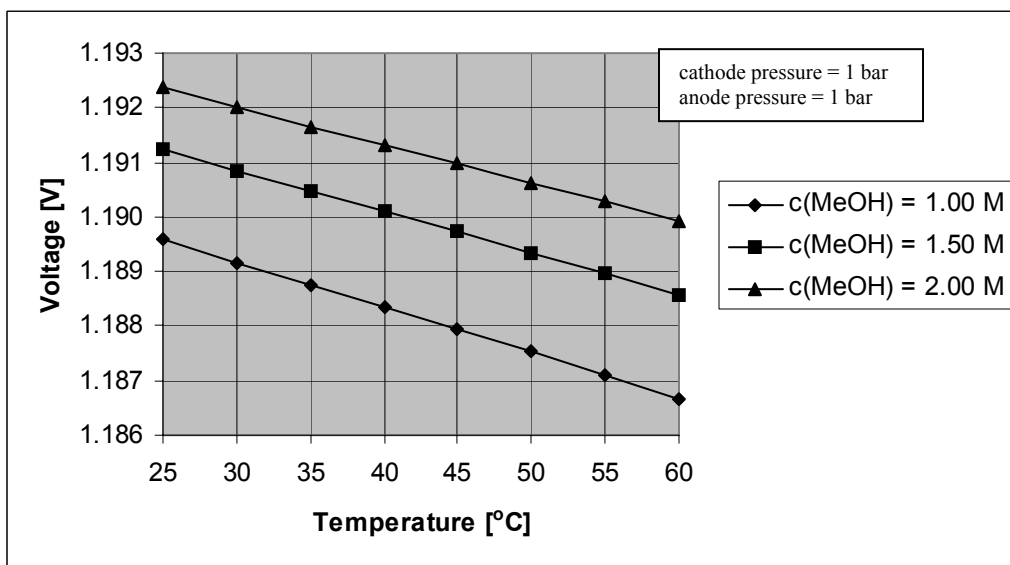


Figure 81. Set 3 - Effect of temperature on the open circuit voltage for the nonideal solution and gas behavior (water formation at cathode in vapor phase).

Set 3 – Concentration of methanol range from 1.00 to 2.00 M

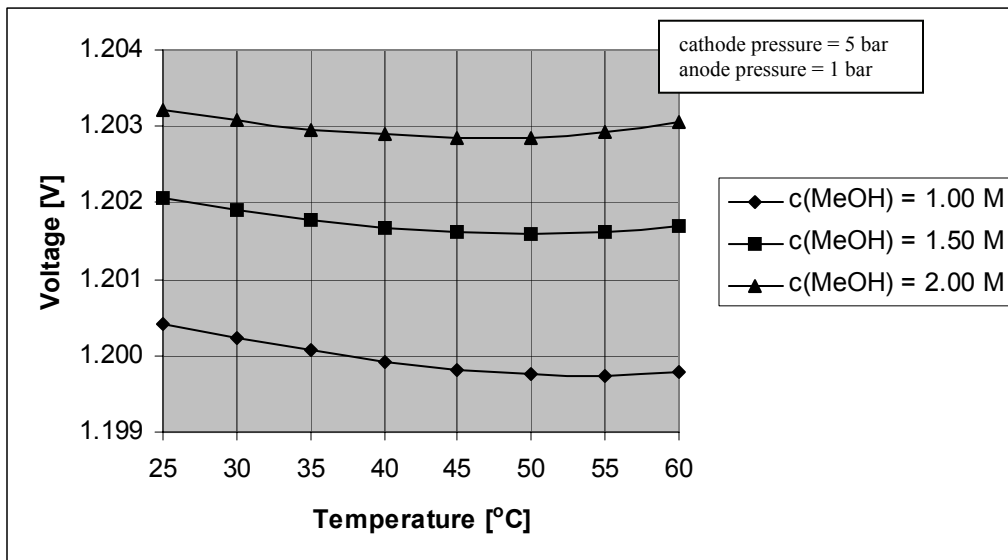


Figure 82. Set 3 - Effect of temperature on the open circuit voltage for the nonideal solution and gas behavior (water formation at cathode in vapor phase).

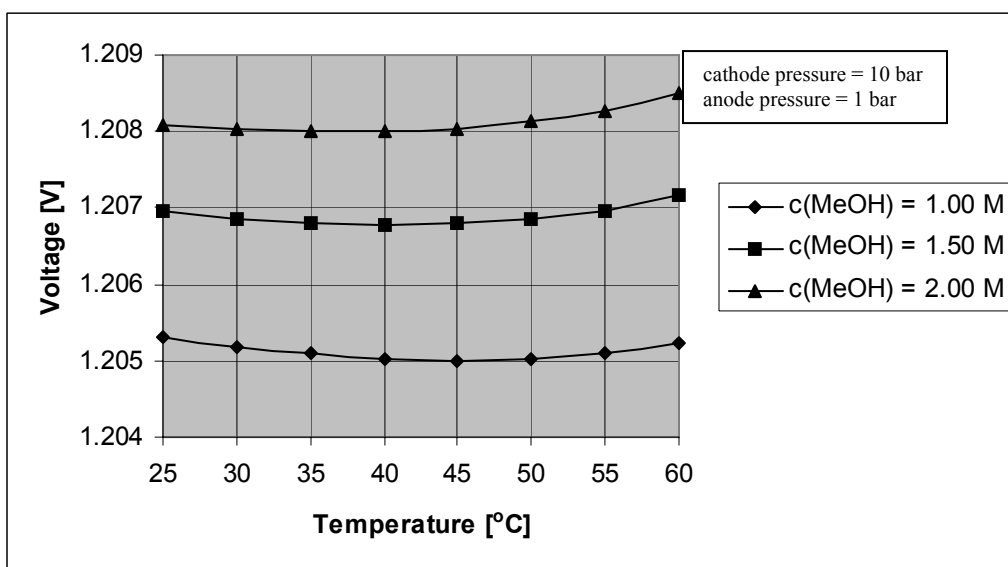


Figure 83. Set 3 - Effect of temperature on the open circuit voltage for the nonideal solution and gas behavior (water formation at cathode in vapor phase).

Set 3 – Concentration of methanol range from 1.00 to 2.00 M

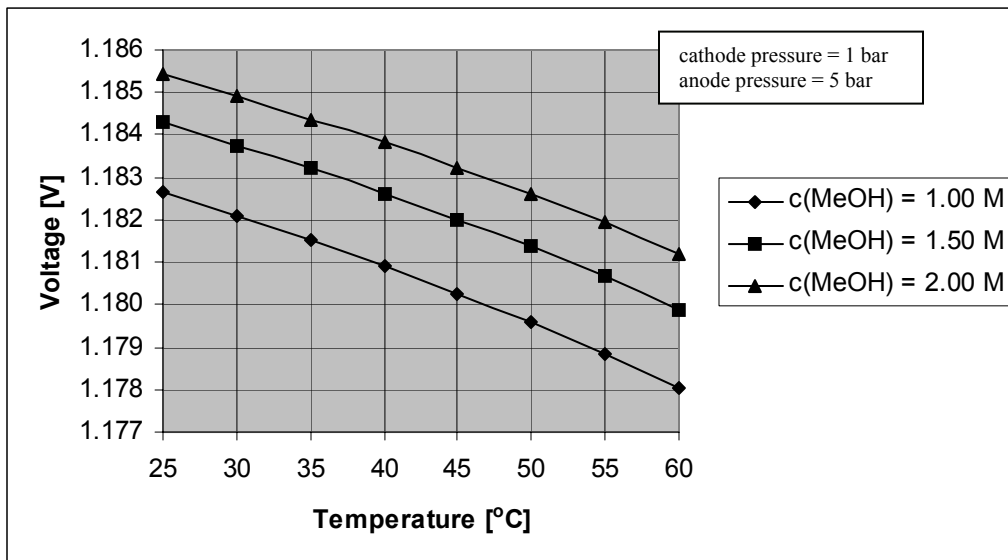


Figure 84. Set 3 - Effect of temperature on the open circuit voltage for the nonideal solution and gas behavior (water formation at cathode in vapor phase).

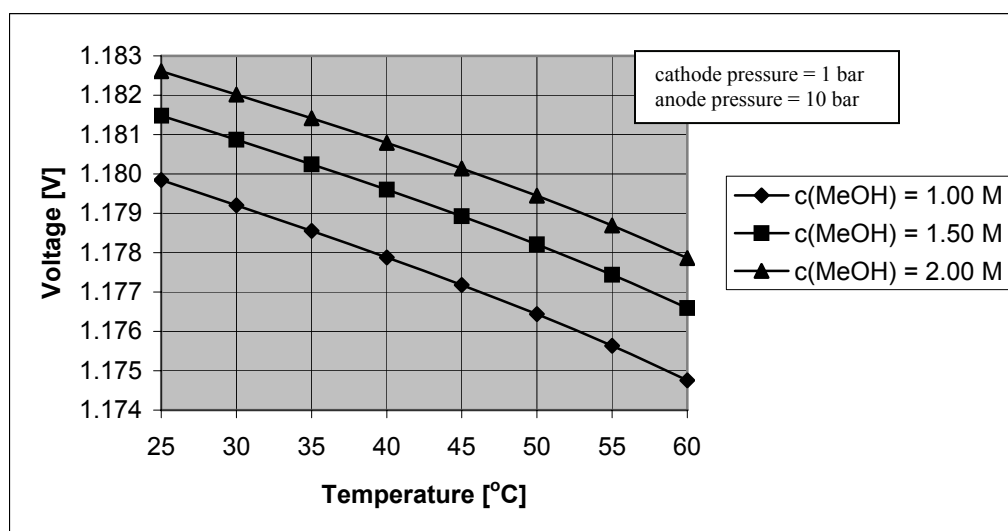


Figure 85. Set 3 - Effect of temperature on the open circuit voltage for the nonideal solution and gas behavior (water formation at cathode in vapor phase).

5 Conclusions

The open-circuit voltage equation for a direct methanol fuel cell was developed to determine the maximum reversible cell voltage obtainable as a function of cell temperature, pressure, and methanol feed concentration. Based on the developed equations and generated figures, the optimal conditions, based on thermodynamics, occur when the cathode pressure is high, the anode pressure is low, the concentration of methanol is high, and the cell temperature is low. Other factors affect the optimal actual fuel cell conditions, but, the effort here delineates the true maximal thermodynamic potential available.